Regulation of Self-Incompatibility by Endocytic Trafficking

Jonathan Schnabel

THÈSE

en vue de l'obtention du grade de

Docteur de l'Université de Lyon, délivré par l'École Normale Supérieure de Lyon

Discipline : Sciences de la vie

Laboratoire Reproduction et développement des plantes UMR5667

École Doctorale Biologie moléculaire intégrative et cellulaire (ED340)

présentée et soutenue publiquement le 29 novembre 2013

par Monsieur Jonathan SCHNABEL

Regulation of Self-Incompatibility by Endocytic Trafficking

Directeur de thèse : M. Thierry GAUDE

Co-encadrant de thèse : Mme Isabelle FOBIS-LOISY

Après l'avis de :

M.Christophe LAMAZE

M.Christophe RITZENTHALER

Devant la commission d'examen formée de :

Mme Isabelle FOBIS-LOISY, co-encadrant

M. Thierry GAUDE, directeur

M. Christophe LAMAZE, rapporteur

M. Benoît LEFEBVRE

M. Christophe RITZENTHALER, rapporteur

M. Gregory VERT

Acknowledgements

For giving me the opportunity to do my PhD in his research team, I would like to express my gratitude to Thierry Gaude.

I am grateful to my supervisor Isabelle Fobis-Loisy for supervising me during the past three and a half years.

For inspiration, advice and support I want to thank Yvon Jaillais and Enric Zelazny.

For accepting to be on the examination committee, I want to express my very great appreciation to Mr. Christophe Lamaze, Mr. Benoît Lefebvre, Mr. Christophe Rietzenthaler and Mr. Gregory Vert. I am truly honored that they have chosen to evaluate my research.

For his insightful answers on questions dealing with microscopy, I want to thank Vincent Bayle, and also for the light-hearted moments we spent together in the office.

For her technical assistance, a difficult and sometimes unrewarding task, I wish to thank Aurélie Chauvet.

For discussions on experiments in immunolocalization, I want to thank Frédérique Rozier.

For their support and precious advice during the PhD meetings, I wish to thank Olivier Hamant and Samantha Vernhettes (a member of the Jean-Pierre Bourgin Institute in Versailles).

Heartfelt thanks are also extended to all the people from the laboratory for their kindness and warm concern.

Special thanks to Hervé for the humorous moment, to Marie-France for the amazing "entremets" and culinary suggestions, to Matthieu for the jam sessions and excellent roast duck breasts with fries, Claudya for her cheerfulness, to Mar for sharing her valuable experience and delicious tapas, and to Jeremy and Thomas for the free typographical advice.

Finally, I wish to thank my parents for their continuous support and encouragement throughout my studies. This research is faithfully dedicated to them.

TABLE OF CONTENTS

LIST OF ABBREVIATIONS

All the abbreviations used in this manuscript are explained in the text or figure legends. In this section, we have included the abbreviations that are the most frequently used.

In the main text, the amino acids are abbreviated according to the international code with a single letter. Proteins are indicated in small capitals (e.g. SRK), genes and nucleotide fragments are indicated in italicized small capitals (e.g. *SRK*) and mutants are indicated in italicized lower case (e.g. *drp1a*).

AFCS *Alexa fluor-467 castasterone*
AP *Adaptor protein complex*
ARC1 *Arm repeat-containing1*
BAK *Brassinosteroid-insensitive1 associated kinase1*
BFA *Brefeldin A*
BIK *Botrytis-induced kinase*
BKI1 *Brassinosteroid-insensitive1 kinase inhibitor1*
BRI1 *Brassinosteroid-insensitive 1*
BSK *Brassinosteroid signaling kinase*
BSU1 *Brassinosteroid-insensitve1 suppressor1*
CLV *Clavata*
DRP *Dynamin-related protein*
EGF *Epidermal growth factor*
EGFR *Epidermal growth factor receptor*
EIX *Ethylene-inducing xylanase*
ESCRT *Endosomal sorting complex required for transport*
FLIM *Fluorescence lifetime imaging microscopy*
FLS2 *Flagellin sensing 2*
FRET *Förster resonance energy transfer*
GAP *GTPase activating protein*
GEF *Guanine nucleotide exchange factor*
GFP *Green fluorescent protein*
GPI *Glycosylphosphatidylinositol*
IRAK *Interleukin-1 receptor associated kinase*
KAPP *Kinase-associated protein phosphatase*
LRR *Leucine-rich repeat*
LTI6B *Low temperature-inducible protein 6b*
LYK3 *Lysine-motif receptor kinase3*
MAPK *Mitogen-activated protein kinase*
MLPK *M-locus protein kinase*
PIN *Pin-formed*
PIP *Plasma membrane intrinsic protein*
PRK *Plant receptor kinase*
RLCK *Receptor like cytoplasmic kinase*
RSK Receptor serine kinase
RTK Receptor tyrosine kinase
SCR *S-locus cysteine-rich*
SERK *Somatic embryogenesis receptor kinase*
SP11 *S-locus protein11*
SRK *S-Locus receptor kinase*
THL1 *Thioredoxin h-like1*
VHAa1 *Vacuolar H+ ATPase subunit a1*

BIBLIOGRAPHICAL ANALYSIS

1. Plant receptor kinases : orchestrators of the cell's partition

Plant genomes encode a large number of proteins phylogenetically related to animal receptor tyrosine kinases (RTK) and receptor serine/threonine kinase (RSK) (**figure 1**), with which they share a similar structure. They are composed of an extracellular domain, a transmembrane helix and a cytosolic kinase domain. Based on this structural similarity, they were labeled receptor-like kinases (RLK) (Walker 1994), but since a ligand was identified for several of these RLK, the term plant receptor kinase (PRK) was introduced (Cock et al. 2002). Throughout this document I will use the abbreviation PRK instead of RLK. Although PRK, RTK and RSK share a similar primary structure, each family of receptor kinases probably evolved independently during evolution. Indeed, PRK, RTK and RSK fall into distinct monophyletic groups. PRK forms a monophyletic clade with Pelle from Drosophila, and Interleukin-1 receptor associated kinase (IRAK) proteins from human (**figure 1**). Moreover, PRK on the one hand, RTK and RSK on the other hand, are found exclusively in plant or animal lineages, respectively (Shiu and Bleecker 2001a). As a result, mechanistic similarities between PRK, RTK and RSK are likely the result of convergent evolution (Shiu and Bleecker 2001a, Cock et al. 2002).

1.1. Functions of plant receptor kinases

PRK regulate many aspects of a cell's life by controlling cell-to-cell communication. A summary of the most studied PRK with their assigned ligand and function is displayed in **table 1**. FERONIA (FER) is involved in male gametophyte (pollen tube, containing male gametes) recognition by the ovule (containing female gametes), perhaps by cell wall sensing (Cheung and Wu, 2011). S-LOCUS RECEPTOR KINASE (SRK) is involved in self-incompatibility (a mechanism preventing self-fertilization) by recognizing S-LOCUS CYSTEINE-RICH (SCR) (see part 3), a protein present at the pollen surface (Ivanov *et al.* 2010). BRASSINOSTEROID-INSENSITIVE1 (BRI1) controls cell elongation through perception of steroid hormones, brassinosteroids (Clouse 2011). FLAGELLIN SENSING2 (FLS2) and ELONGATION FACTOR TU RECEPTOR (EFR) from *Arabidopsis thaliana*, and Xa21 from rice are involved in disease resistance by recognizing the bacterial proteins flagellin (and the flg22 epitope from flagellin), elongation factor Tu (EF-Tu, and the elf18 epitope from EF-Tu), and a tyrosine-sulfated and secreted peptide called $AxY^{S}22$, respectively (Greef *et al.* 2012). CLAVATA1 (CLV1) and its ligand CLAVATA3 (CLV3) are involved in maintenance of the meristems, populations of stem cells that self-replenish and differentiate to produce organs during post-embryonic growth (Katsir *et al.* 2011). HAESA and its ligand INFLORESCENCE DEFICIENT IN ABSCISSION (IDA) regulate organ abscission, the mechanism of organ detachment from the main body of the plant

(Butenko *et al.* 2012). ERECTA and its ligands EPF1/2 regulate the development and distribution of stomata, which are pores delimited by two specialized cells involved in gas exchange between the plant and the environment (Pillitteri and Torii 2012).

1.2. General structure of plant receptor kinases

PRK and RTK share their overall structure and are composed of an N-terminal signal sequence, an extracellular domain followed by a transmembrane segment and an intracellular kinase domain flanked by a juxtamembrane segment and a C-terminal segment (Shiu and Bleecker 2001b) (**figure 2**). The PRK family also contains members that do not possess an extracellular domain and are thus termed receptor-like cytoplasmic kinases (RLCK) but some of these proteins are nevertheless anchored to membranes through transmembrane segments or lipid anchors (Shiu and Bleecker 2001b). Together, PRK and RLCK form a family of more than 600 members in *Arabidopsis thaliana* and twice as many in rice (Shiu *et al.* 2004).

The *Arabidopsis thaliana* genome encodes 417 putative PRK, making PRK one of the largest protein families in this species. The extracellular domains of PRK show extensive variation and contain several identified motifs which define types of extracellular domain. Some of these motifs are shared between animal and plant proteins, while others are plant-specific (Shiu and Bleecker 2001b). More than 15 types of PRK extracellular domains are known, we present three important types.

The most prevalent type of extracellular domain of PRK is the leucine-rich repeat (LRR) type, which is present in BRI1, FLS2, CLV1 and other receptors (Gish and Clark 2011, **table 1**). LRR are 24-amino acid motifs rich in leucine and more generally in hydophobic residues. The number of LRR in a protein domain can vary from two to more than 25. LRR are also found in membrane proteins of animals such as Toll-like receptors, and are involved in ligand binding. An "island domain", a sequence that is unrelated among receptors, is found between the leucine-rich repeats of several receptors. The atomic structure of the LRR domain of BRI1 was determined by X-ray crystallography and shows a helicoidal shape in which the island domain forms the ligand-binding site (Hothorn *et al.* 2011, She *et al.* 2011). The helix formed by the extracellular domain of BRI1 is much different from the horseshoe structure formed by LRR of Toll-like receptors, and may prevent homo-dimerization of BRI1. Recently, the atomic structure of a complex including the LRR of BRI1, its ligand and the LRR domain of the co-receptor SOMATIC EMBRYOGENESIS RECEPTOR KINASE1 (SERK1) was determined by X-ray crystallography (Santiago *et al.* 2013), providing a structural basis for ligand-induced hetero-dimerization of BRI1 and SERK1.

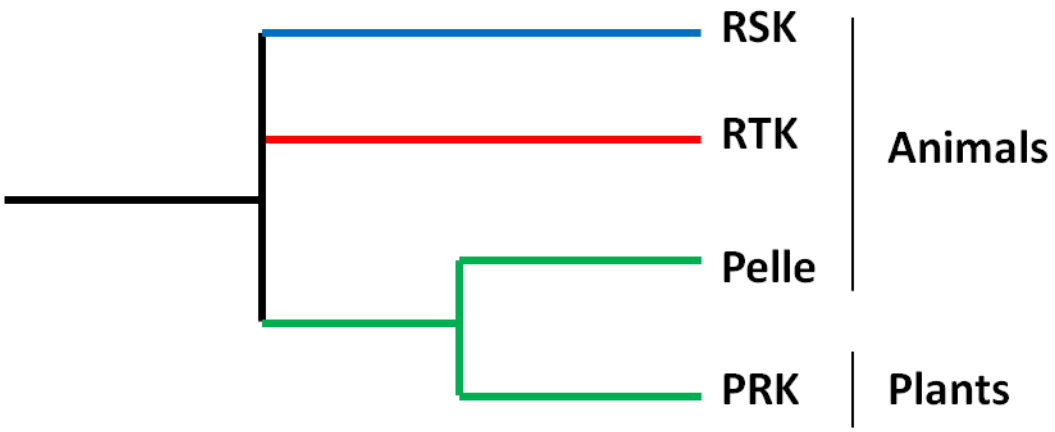

Figure 1: evolutionary relationship between receptor kinases in plant and in animals. According to Shiu and Bleecker 2001a. The phylogeny is based on the protein sequence of kinase domains. RSK = Receptor serine kinase, RTK = Receptor tyrosine kinase, PRK = Plant receptor kinase. Pelle is a cytosolic kinase involved in immune signaling in *Drosophila* and forms a monophyletic clade with PRK.

Table 1: selected PRK with known function and ligand. The name of the species in which the role of the receptor was described is indicated in the column labeled "organism". The "type" column indicates the nature of the extracellular domain of the receptor (see part 1.2). Ligands are all peptides except brassinosteroids which are small molecules from the steroid family, chitin and peptidoglycan are complex sugar polymers.

Receptor	Organism	Type	Function	Ligand	Reference
CERK1	*Arabidopsis*, rice	LysM	recognition of pollen tubes, cell wall sensing	chitin, peptidoglycan	Schwessinger and Ronald 2012
SRK	*Brassica*	S domain	self-incompatibility	SCR	Ivanov *et al.* 2010
BRI1	*Arabidopsis*	LRR	cell growth	brassinosteroids	Clouse 2011
FLS2	*Arabidopsis*	LRR	disease resistance	flg22	Antolín-Llovera *et al.* 2012
CLV1	*Arabidopsis*	LRR	meristem maintenance	CLV3	Katsir *et al.* 2011
Xa21	rice	LRR	disease resistance	$AxY^{S}22$	Schwessinger and Ronald 2012
HAESA	*Arabidopsis*	LRR	delayed floral organ abscission	IDA	Butenko *et al.* 2012
EFR	*Arabidopsis*	LRR	disease resistance	elf18	Greef *et al.* 2012
ERECTA	*Arabidopsis*	LRR	Stomatal development	EPF1/2	Pillitteri and Torii 2012

Lectins are glucid-binding motifs highly represented in the extracellular domains of PRK. For example, the mannose-binding motif agglutinin is present in the S-domain type of extracellular domain. The S-domain is rich in cysteines, contains an Epidermal growth factor (EGF) repeat and a PAN domain. The S-domain is present in several PRK such as SRK (Naithani *et al.* 2007) and S-FAMILY GENE RECEPTOR (SFR) of *Brassica oleracea*, a protein involved in wound signaling and immunity (Pastuglia *et al.* 1997). The structure of the S-domain was partially determined by molecular modeling (Naithani *et al.* 2007). Models for the structure of the agglutinin-like domain and the PAN domain were determined, even though the two models are independent, meaning that their relative position in the 3D structure of the S-domain is not known. In the same study, the PAN domain was demonstrated to be involved in SRK dimerization.

The lysine motif (LysM) is a motif that is conserved between eukaryotes and prokaryotes and recognizes chitin, peptidoglycan and other glucids (Schwessinger and Ronald 2012). It is present in several PRK, such as CHITIN ELICITOR RECEPTOR KINASE1 (CERK1) which is involved in chitin and peptidoglycan recognition (Schwessinger and Ronald 2012) and LYSINE MOTIF RECEPTOR KINASE3 (LYK3) which is involved in establishment of symbiosis between roots and nitrogen-fixing bacteria (Smit *et al.* 2007).

1.3. Atomic-scale structure of the kinase domain of plant receptor kinases

The experimental determination of the structure of the kinase domain of the RLCK Pto (Dong *et al.* 2011) and the PRK BRI1 ASSOCIATED KINASE1 (BAK1, Cheng *et al.* 2011) by X-ray crystallography revealed a similar structure, conserved between RTK, RSK and PRK (**figure 3**, in which the kinase domain of BAK1 is represented). They are composed of an N-terminal lobe (N-ter lobe, orange) and a C-terminal lobe (C-lobe, pink) linked by a hinge region (purple), and an activation loop (blue). The juxtamembrane and C-terminal segments are generally unstructured and thus absent from such structures. The catalytic site, involved in catalyzing the phosphate transfer between ATP and the substrate, is located between the two lobes, and composed of several conserved residues (Johnson *et al.* 1996). Two of these residues are represented as red spheres in **figure 3**. Lysine 317 (the homolog of which are later called *catalytic lysine*) of BAK1 is presumably involved in ATP binding and in the alignment of the phosphate groups for catalysis, while aspartate 416 (the homolog of which are later called *catalytic aspartate*) is presumably involved directly in the transfer of phosphate γ of ATP to the serine or threonine substrate (Cheng *et al.* 2011, Johnson *et al.* 1996). Tyrosine 363 is the "gatekeeper" residue. It is located near the hinge regions, at the bottom of the pocket formed by the catalytic site. This residue is variable among different families of kinases and determines, depending on its size, the access of ATP-

competitive inhibitors to the catalytic site, hence the name gatekeeper (Wang *et al.* 2006). Other residues are important for catalysis and cluster in the catalytic site, but their role will not be discussed here.

The kinase activity of several RTK is self-inhibited by their own activation loop, which switches from an inactive to an active conformation upon phosphorylation of tyrosine residues located in the activation loop (Lemmon and Schlessinger 2010). Several pieces of evidence suggest that similar mechanisms operate in PRK (see part 1.4.2). The activation loop displayed in **figure 3** is away from the catalytic site because it is phosphorylated and in an active conformation (Cheng *et al.* 2011, phosphorylated residues are not represented in **figure 3**). In the inactive conformation, the catalytic loop is oriented towards the catalytic site and blocks ATP and substrate access (Johnson *et al.* 1996).

1.4. Plant receptor kinase activation

In general, receptor kinase activation involves ligand-induced receptor dimerization, which brings together the kinase domains and activates them. Receptors then *trans*-phosphorylate each other on hydroxyl group-containing residues, such as tyrosine, serine and threonine. Phosphorylated residues recruit and activate proteins acting downstream in the signaling pathway (**figure 2**) (Lemmon and Schlessinger 2010). The human genome encodes 58 RTK and 12 RSK (Manning *et al.* 2002). PRK generally phosphorylate serine and threonine residues (Shiu and Bleecker 2001b), although tyrosine phosphorylation has been described, indicating dual substrate specificity (Oh *et al.* 2009, 2010, Jaillais *et al.* 2011).

1.4.1. Pre-existing oligomers of plant receptor kinases

Several PRK form pre-existing oligomers before ligand binding. Förster resonance energy transfer-fluorescence lifetime imaging microscopy (FRET-FLIM) on cowpea protoplasts revealed that BRI1 homodimers are present at the plasma membrane (Russinova *et al.* 2004). BRI1 co-immunoprecipitates itself *in planta* in a brassinosteroid synthesis deficient background, thereby indicating that BRI1 homo-dimerization is at least partly independent on ligand (Wang *et al.* 2005b). The addition of ligand may stabilize the preformed BRI1 homodimer, as it increased the amount of BRI1 that was immunoprecipitated (Wang *et al.* 2005b). The extent of dimerization of BRI1 was quantified by fluorescence correlation spectroscopy and photon counting histogram analysis and showed that 20 % of BRI1 present at the plasma membrane could be found in homodimers while no higher order homo-oligomers were detected (Hink *et al.* 2008).

However, structural studies questioned the concept of pre-existing oligomers of BRI1. The tertiary structure of BRI1 extracellular domain was determined at atomic scale by X-ray crystallography and displays a helicoidal

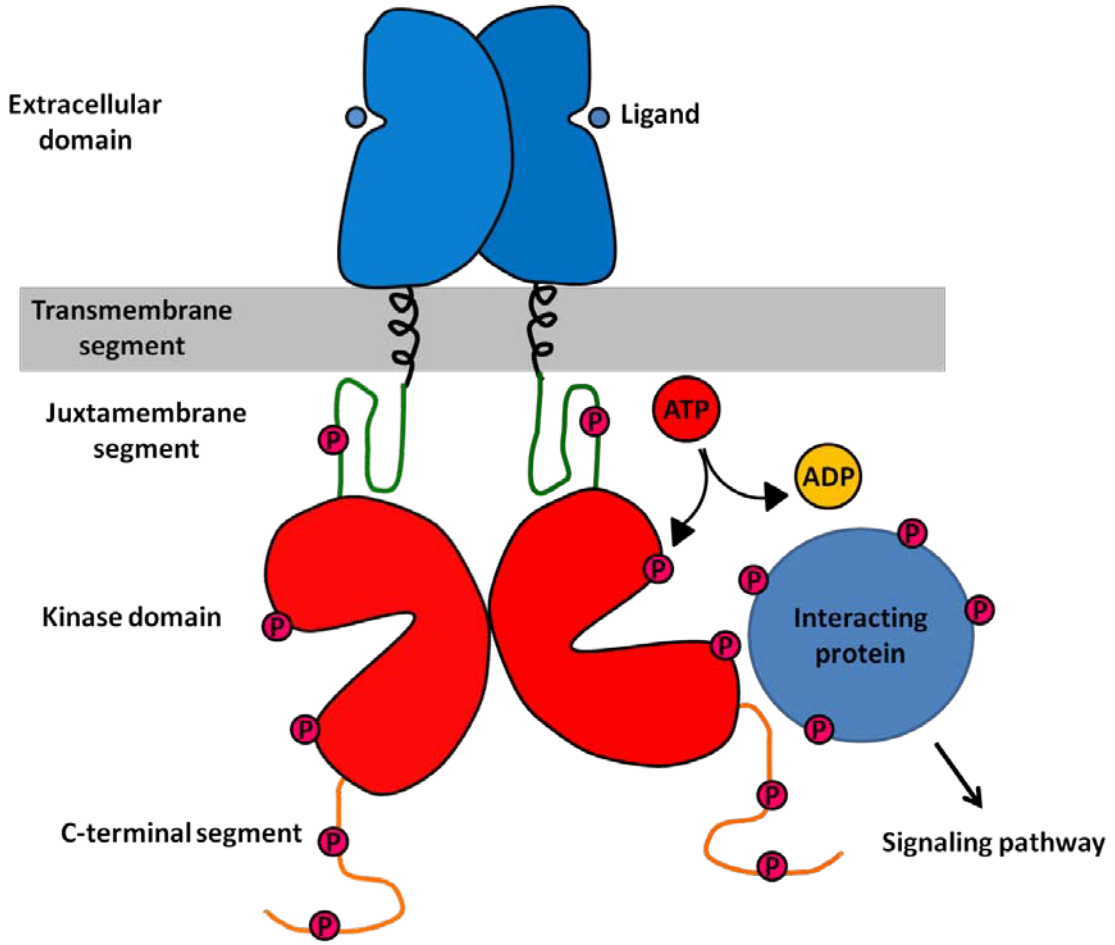

Figure 2: Structure and general mechanisms of PRK function. PRK are composed of an extracellular N-terminal ligand-binding domain (blue), a transmembrane segment (TM, black), a juxtamembrane segment (JM, green), a kinase domain (KD, red) and a C-terminal segment (CT, orange). Ligand binding to the extracellular domain triggers activation of the intracellular kinase domain. PRK molecules then transfer the γ-phosphate of ATP *in trans* to serine and threonine residues located either in the JM, KD or CT, potentiating the activation of the PRK and providing docking sites for interacting proteins (blue) that act downstream in the signaling pathway. Interacting proteins can also be phosphorylated and activated by PRK.

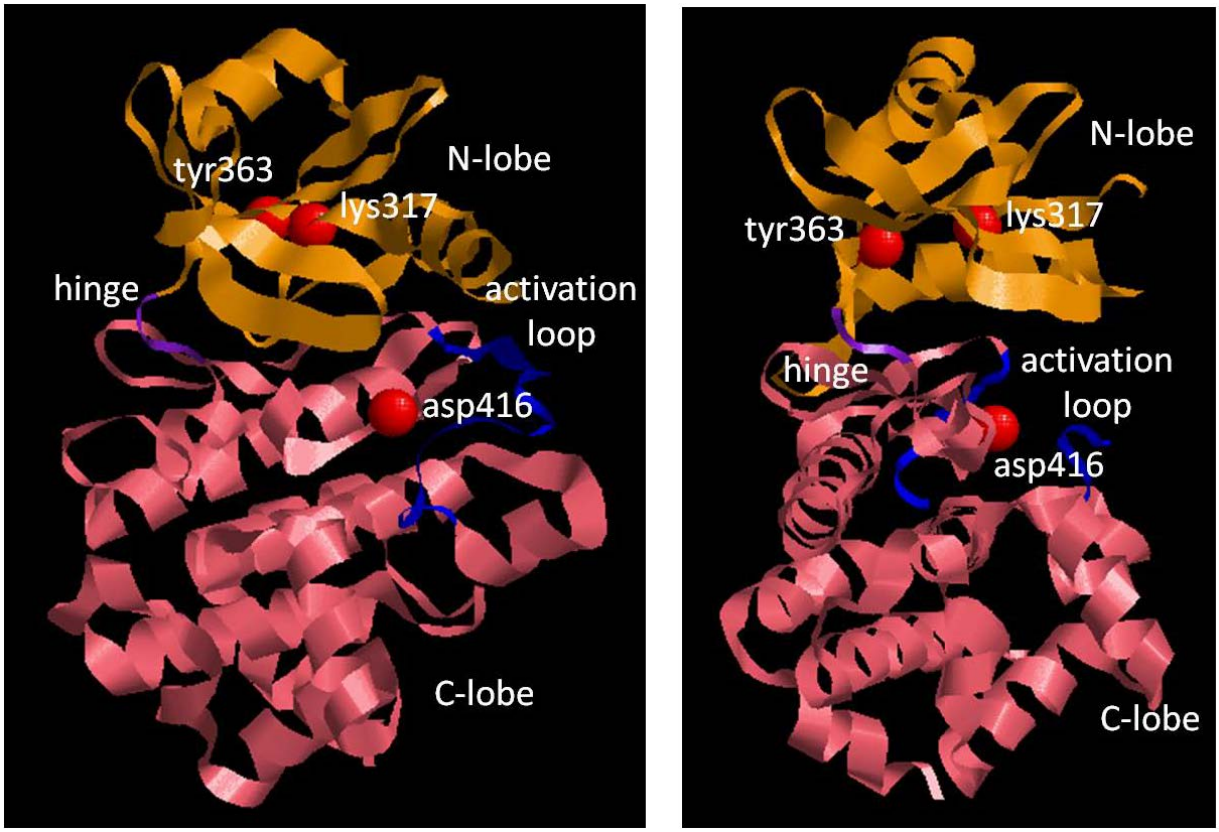

Figure 3: atomic structure of BAK1 kinase domain. The image on the left shows the kinase domain with the catalytic cleft facing us. The image on the right shows a side angle view of the kinase domain. The α helices and β sheets of the protein are displayed in the ribbon representation. The N-terminal lobe (N-lobe) is shown in orange, the C-terminal lobe (C-lobe) is shown in pink, the hinge region is shown in purple, the activation loop is shown in blue, and the lysine 317 and aspartate 416 residues of the catalytic site are shown as red spheres. The gatekeeper tyrosine 363 is shown as a red sphere. The structure of BAK1 kinase domain (PDB ID : 3TL8, Cheng *et al.* 2011) was displayed using Rastop.

shape (Hothorn *et al.* 2011, She *et al.* 2011). The addition of ligand to BRI1 extracellular domain in solution does not induce dimerization, consistent with the existence of BRI1 homo-dimers in absence of ligand. Nonetheless, it was argued that the helicoidal structure prevents homo-dimerization of BRI1 because bringing the C-terminal part of the extracellular domain together (so that the kinase domains can interact) would cause a steric clash. Instead, BRI1 could hetero-dimerize with co-receptors belonging to the SERK family both before and after ligand binding. SERK3 (also known as BAK1) interacts with BRI1 in a brassinosteroid-dependent manner and the two protein *trans*-phosphorylate each other, a required step in BRI1 activation (Wang *et al.* 2005a, 2008). FRET-FLIM (Bücherl *et al.* 2013, Russinova *et al.* 2004), biochemical (Wang *et al.* 2005b) and quantitative analysis of fluorescence from BRI1-fluorescent protein fusions (Hink *et al.* 2008) data indicate that BRI1 and BAK1 form oligomers at both the plasma membrane and endosomes in absence of ligand, and that ligand application stabilizes these oligomers. The atomic structure of a ternary complex composed of BRI1 and SERK1 bridged by the ligand was recently determined and revealed that SERK1 is involved in ligand binding (Santiago *et al.* 2013). To sum up, BRI1 may homo- and also hetero-oligomerize with SERK proteins, but the temporal relationship of such interactions remains an open question.

Co-immunoprecipitation analysis revealed that FLS2 is present as homo-oligomers prior to ligand exposure, and that the association is maintained after ligand addition (Sun *et al.* 2012). A conserved cysteine residue located at the N-terminal side of the extracellular LRR domain is required for FLS2 oligomerization, although it is not involved in a disulfide bond (Sun *et al.* 2012). However, the helicoidal structure of the extracellular domain of BRI1 (an LRR, as for FLS2) and the fact that BAK1 is also involved in FLS2 signaling (see part 1.4.4) questions the function of such homo-oligomers.

Recombinant SRK over-expressed in a heterologous system displays auto-activation and *trans*-phosphorylation, indicating that SRK forms oligomers in absence of ligand (Giranton *et al.* 2000). The presence of oligomers was confirmed *in planta* by cross-linking of stigma extracts followed by SDS-PAGE or by velocity sedimentation on sucrose gradients of native stigma extracts, revealing that SRK homo-dimerizes *in planta* without ligand (Giranton *et al.* 2000). The structural determinants of SRK dimerization are two domains located in the C-terminal part of the extracellular domain of SRK : the PAN and EGF-like domains (Naithani *et al.* 2007).

The existence of pre-existing oligomers of PRK raises the question of how auto-activation is prevented. BRI1 activation is inhibited by the C-terminal tail of the intracellular domain and this inhibition is thought to be released upon ligand binding to BRI1 (Wang *et al.* 2005a). Moreover, BRI1 KINASE INHIBITOR1 (BKI1) interacts with BRI1 at the plasma membrane and inhibits BRI1 signaling (Wang and Chory 2006). The BKI1-BRI1 interaction is relieved upon ligand binding, which

enables BRI1 signaling (Wang and Chory 2006). SRK is mainly localized to endosomal compartments and to a lesser extent at the plasma membrane (Ivanov and Gaude 2009). SRK colocalizes with Thioredoxin h-like1 (THL1) in endosomes, a negative regulator that may prevent auto-activation of SRK in this compartment (Cabrillac *et al.* 2001, Ivanov and Gaude 2010). At the plasma membrane, unknown negative regulators might prevent SRK auto-activation, or ligand binding to SRK may be necessary to stabilize the active conformation of SRK oligomers. This aspect will be further discussed in part 12.1.

1.4.2. Activation of the kinase domain

The molecular mechanisms that occur during RTK activation are described in great detail, and involve structural rearrangements of the kinase domain (Lemmon and Schlessinger 2010). Notably, the activation loop is involved in auto-inhibition of the insulin receptor (InsR) and the fibroblast growth factor receptor (FGFR) (Lemmon and Schlessinger 2010). Phosphorylation and reorientation of the activation loop is necessary to stabilize the active conformation of InsR and FGFR kinase domain. Similarly, the juxtamembrane and C-terminal segments were shown to be involved in auto-inhibition of some RTK or RSK (Lemmon and Schlessinger 2010). Receptor kinases can be divided into "RD kinase" or "non-RD kinase" groups based on the presence or absence of an arginine (R) residue preceding the catalytic aspartate (D) in the kinase domain (Johnson *et al.* 1996). Many RD kinases need to be phosphorylated in the activation loop to be activated, while many non-RD kinases do not (Johnson *et al.* 1996).

BRI1 is an RD PRK. As stated above, inactive BRI1 is complexed to BKI1, which inhibits the interaction between BRI1 and its co-receptor BAK1 (Jaillais *et al.* 2011). Activated BRI1 phosphorylates BKI1 on tyrosine residues, which releases BKI1 from the plasma membrane into the cytosol (Jaillais *et al.* 2011, Wang and Chory 2006). After BRI1-BKI1 dissociation, BAK1 is recruited to BRI1 activated complexes and mutual phosphorylation occurs between BRI1 and BAK1 in the activation loop of each PRK (Wang *et al.* 2005a, 2008). Phosphorylation occurs in the activation loop of BRI1 on serine 1044 and threonine 1049. Mutation of these residues impairs BRI1 kinase activity and BRI1-mediated signaling (Wang *et al.* 2005b). Moreover, the C-terminal segment of BRI1 inhibits BRI1 function and phosphorylation of the C-terminal segment on serine and threonine is required for release of inhibition (Wang *et al.* 2005a). Taken together, these data suggest that activation loop and C-terminal segment auto-inhibition might be at work in BRI1, similar to RTK and RSK, but structural details about BRI1 kinase domain activation are needed to clarify these hypotheses.

FLS2, like most of receptor kinases involved in immunity, is a non-RD PRK. FLS2 phosphorylation in the juxtamembrane segment may be important for signaling, as substitution of threonine 867 by valine abolishes FLS2-mediated signaling (Robatzek *et al.* 2006). In a recent analysis of *in vitro* auto-phosphorylated

residues of FLS2, serine 867 was not identified (Cao *et al.* 2013) but this residue may be phosphorylated by another kinase, or in an *in vivo* context only. Instead, Cao *et al.* identified serine 938 of the kinase domain as a phosphorylated residue *in vitro*. When serine 938 is non-phosphorylable (replaced by alanine), auto-phosphorylation of FLS2, phosphorylation of signaling partners of FLS2 and flg22-induced biologial responses are all impaired (Cao *et al.* 2013). Although serine 938 plays a critical role in FLS2-mediated signaling, its precise role remains unknown.

The rice Xa21, a non-RD PRK, auto-phosphorylates on serine and threonine but not in the activation loop (Liu *et al.* 2002). Xa21 auto-phosphorylates on threonine 705, a residue present in the juxtamembrane segment. Substitution of this residue by alanine or glutamate abolishes auto-phosphorylation of Xa21 and Xa21-mediated immunity (Chen *et al.* 2010b). The precise mechanism by which phosphorylation of threonine 705 positively regulates Xa21 function is presently unknown. A catalytically-impaired Xa21 mutant in which the catalytic lysine was replaced by glutamate maintains partial resistance to pathogenic *Xanthomonas oryzae*, indicating that the kinase activity of Xa21 is not crucial for Xa21-mediated pathogen resistance (Andaya and Ronald 2003).

SRK, an RD PRK, is phosphorylated *in vivo* within 60 minutes after ligand addition in *Brassica* (Cabrillac *et al.* 2001), on serine and threonine residues (Giranton *et al.* 2000). SRK is constitutively active *in vitro*, and THL1 was identified as a protein that prevents auto-activation of SRK *in vivo* (Cabrillac *et al.* 2001). The auto-phosphorylation of SRK occurs *in trans*, meaning that one SRK molecule in the oligomer phosphorylates another neighboring molecule (Giranton *et al.* 2000). SRK is phosphorylated in the C-terminal segment (Giranton *et al.* 2000), but the precise role of this segment in SRK activation is not known, neither is the role of the juxtamembrane segment known, nor that of the activation loop. Perspectives about this topic will be presented in part 12.2.

1.4.3. Atypical plant receptor kinases devoid of kinase activity

It should be noted that around 20 % of PRK lack key catalytic residues like the catalytic lysine or the catalytic aspartate presented in **figure 3**. These PRK are thus probably inactive although the presence of the intracellular domain is required for their function (Castells and Casacuberta 2007). Members of this atypical PRK family include STRUBBELIG (also known as SCRAMBLED) which is involved in floral and root development in *Arabidopsis thaliana* (Bai *et al.* 2013), pangloss1 (PAN1) and PAN2 which are involved in polarized cell division during stomatal development in maize (Zhang *et al.* 2012), maize atypical receptor kinase (MARK) of unknown function (Llompart *et al.* 2003) and *Arabidopsis thaliana* ATCRR1 and ATCRR2 related to maize CRINKLY4 which is involved in endosperm development (Cao *et al.* 2005).

MARK lacks the conserved catalytic aspartate (see **figure 3**) and fails to auto-phosphorylate *in vitro* (Llompart *et al.* 2003). MARK interacts and activates the kinase MIK, probably by inducing a conformational change that relieves MIK auto-inhibition (Llompart *et al.* 2003, Castells *et al.* 2006).

ATCRR2 can be phosphorylated by ACR4, the CRINKLY4 homolog in *Arabidopsis thaliana*, suggesting that ATCRR2 could hetero-dimerize with ACR4 to signal (Cao *et al.* 2005). This is similar to kinase-dead ErbB3 receptors from the epidermal growth factor (EGFR) family in animals. Indeed, ErbB3 hetero-dimerize with kinase-active members of the EGFR family and is phosphorylated by them. The phosphorylated residues of ErbB3 serve as docking sites for downstream signaling proteins (Kim *et al.* 1998, Prigent and Gullick 1994).

The case of ACR4 is intriguing. Although ACR4 is an active kinase *in vitro* (Gifford *et al.* 2003), a kinase-dead ACR4 protein can complement the loss of function *acr4* mutant (Gifford *et al.* 2005), indicating that ACR4 signaling may be independent from its kinase activity. Exactly how ACR4 transduce signaling is currently unknown.

1.4.4. Assembly of signaling complexes

During receptor kinase activation, the phosphorylation of the receptor recruits and activates downstream signaling proteins, which bind to phospho-residues through specific domains (Lemmon and Schlessinger 2010).

After brassinosteroid-induced BRI1 activation and BRI1-BAK1 complex formation, BRI1 but not BAK1 phosphorylates BRASSINOSTEROID-SIGNALING KINASE1 (BSK1) and BSK2, two RLCK anchored to the plasma membrane through myristoylation (Tang *et al.* 2008). Phosphorylated BSK proteins then interact with the phosphatase BRI1 SUPRESSOR1 (BSU1) that relays BRI1 signaling towards the chromatin to control the transcription of genes (Kim *et al.* 2009).

Interestingly enough, BAK1 is also involved in FLS2 signaling (Robatzek and Wirthmuller 2013). Indeed, FLS2 associates with BAK1 upon flagellin binding and BAK1 loss of function abolishes FLS2-mediated responses (Chinchilla *et al.* 2007, Heese *et al.* 2007). While BAK1 kinase activity is not required for FLS2-BAK1 and BRI1-BAK1 association, it is necessary for activation of downstream signaling proteins (Jaillais *et al.* 2011, Shulze *et al.* 2010). FLS2 signaling also involves BOTRYTIS-INDUCED KINASE1 (BIK1), another membrane anchored RLCK (Lu *et al.* 2010). BIK1 interacts *in vivo* with FLS2 and BAK1, is phosphorylated by BAK1 after flagellin treatment and phosphorylates back FLS2 and BAK1, perhaps to further enhance the kinase activity of the complex (Lu *et al.* 2010). The downstream targets of BIK1 remain unknown. FLS2 signaling involves a mitogen activated protein kinases (MAPK) cascade but it appears to be disconnected from BIK1 (Robatzek and Wirthmuller 2013).

Association with membrane-anchored RLCK is a common theme in PRK activation, since SRK signaling involves M-LOCUS PROTEIN KINASE (MLPK), a membrane-anchored protein kinase (Murase *et al.* 2004). MLPK and SRK can both auto-phosphorylate *in vitro* (Murase *et al.* 2004, Giranton *et al.* 2000), and SRK phosphorylates MLPK (Kakita *et al.* 2007b). Bimolecular fluorescence complementation (BIFC) in tobacco protoplasts showed that MLPK interacts with SRK in a ligand-independent manner (Kakita *et al.* 2007a). However, yeast two hybrid and split ubiquitin experiments failed to show interaction between MLPK and SRK, suggesting a transient interaction between these two proteins (Kakita *et al.* 2007b). The SRK-MLPK complex recruits ARM REPEAT-CONTAINING1 (ARC1), an E3 ubiquitin ligase that binds to the phosphorylated domain of SRK (Gu *et al.* 1998). ARC1 is phosphorylated by SRK and MLPK and in turn ubiquitinates multiple substrates, promoting their degradation (Stone *et al.* 2003, Samuel *et al.* 2009). However, the exact nature and function of the proteins ubiquitinated by ARC1 remains to be determined.

2. Signaling and endocytic trafficking : intimate relationships

In addition to its function in phosphorylating BRI1 and FLS2 signaling complexes, there is evidence that BAK1 is involved in endocytic trafficking of both PRK (Russinova *et al.* 2004, Chinchilla *et al.* 2007). Co-expression of BRI1 and BAK1 in cowpea protoplasts results in increased endosomal localization of both proteins, compared to expression of each protein alone, and FRET-FLIM analysis showed that BRI1 and BAK1 form dimers in endosomes (Russinova *et al.* 2004). Ligand-induced endocytosis of FLS2 is reduced in a *bak1* knock-out background (Chinchilla *et al.* 2007). Given the role of BAK1 in BRI1 and FLS2 signaling, these data suggest a connection between signaling and endocytosis of BRI1 and FLS2. In support of this hypothesis, threonine 867 substitution by valine in the juxtamembrane segment of FLS2 abolishes both FLS2-mediated responses and ligand-induced endocytosis, although the mutated receptor was addressed at the plasma membrane (Robatzek *et al.* 2006). Such a connection between PRK signaling and endocytosis is not unexpected and is widely documented in research studying animal cells (Gonnord *et al.* 2012, Murphy *et al.* 2009, Polo and Di Fiore 2006, Sorkin and von Zastrow 2009).

2.1. Endocytic trafficking routes in plant cells

Endocytosis consists in the internalization of plasma membrane and the formation of intracellular compartments called endosomes. During endocytosis, plasma membrane lipids and proteins, and extracellular fluid are internalized (Doherty and MacMahon 2010). The use of the endocytic tracer FM4-64 (a hydrophobic dye which inserts into membranes and which is internalized with the

plasma membrane, Bolte *et al.* 2004) and drugs that inhibit specific steps of endocytic trafficking (**table 2**, Irani and Russinova *et al.* 2009) enabled mapping of the different endosomal compartments of plants and their temporal relationship during endocytic trafficking (**figure 4**, Contento and Bassham 2012). In animals, endosomes are traditionally classified as early endosomes, late endosomes and recycling endosomes. Early endosomes are the compartments where internalized material arrives first. From there, internalized material can be either recycled back to the plasma membrane through recycling endosomes, or routed to late endosomes and then to lysosomes for degradation (McMahon and Boucrot 2012). In plants, the *trans*-Golgi network appears to be an early endosome. Indeed, FM4-64 colocalizes with the a1 subunit of VACUOLAR H^+ ATPase (VHAa1), which is localized to the *trans*-Golgi network, as soon as two minutes after FM4-64 addition (Dettmer *et al.* 2006).

The identity of the recycling endosome is less clear. According to some authors, the *trans*-Golgi network can fulfill the recycling function (Reyes *et al.* 2011). However, it could be a separate organelle labeled by the guanine nucleotide exchange factor (GEF) GNOM (Contento and Bassham 2012, Geldner *et al.* 2003, Geldner *et al.* 2009). Indeed, the GNOM-labeled compartment is distinct from the *trans*-Golgi network since it does not colocalize quickly with FM4-64 and it is more sensitive to brefeldin A (BFA) treatment (Geldner *et al.* 2003, Geldner *et al.* 2009). Late endosomes appear as multivesicular bodies (Tse *et al.* 2004), in which inward budding of the endosomal membrane generates intraluminal vesicles that contain proteins destined to be degraded (Contento and Bassham 2012). Intraluminal vesicles are generated by the activity of five multiproteic complexes called endosomal sorting complex required for transport (ESCRT). ESCRT complexes recognize on the endocytosed cargo a post-translational modification called ubiquitination. ESCRT complexes then drive membrane deformation, constriction and finally scission to generate intraluminal vesicles that contain the cargo destined to be degraded (Reyes *et al.* 2011). The traditional view of *trans*-Golgi network to multivesicular bodies transport involves formation of vesicles at the *trans*-Golgi network in a clathrin-mediated process, and the fusion of these vesicles with the multivesicular bodies. However, it has been demonstrated that interference with clathrin function does not perturb trafficking to the vacuole (Scheuring *et al.* 2011). The same authors show that concanamycin A treatment, which inhibits VHA proteins and perturbs trafficking from the *trans*-Golgi network to the vacuole, reduces the number of multivesicular bodies and increases the colocalization of otherwise distinct *trans*-Golgi network and multivesicular body markers. Moreover, by using electron microscopy, they report that intraluminal vesicles are present in structures resembling the *trans*-Golgi network, and that multivesicular body markers are present in such structures (Scheuring *et al.* 2011). Taken collectively, these data suggest that multivesicular bodies arise through maturation of *trans*-Golgi networks. It is therefore likely that this process resembles the maturation of early endosomes to late endosomes that has been

Table 2: principal inhibitors of endocytic trafficking in plants. AP2 = adaptor protein complex 2. DRP = dynamin related protein. ARF-GEF = adenosine ribosylation factor-guanine nucleotide exchange factor. VHA = vacuolar H^+ ATPases. EE/TGN = early endosome/trans-Golgi network. PI3 kinase = phosphatidylinositol-3 kinase. LE/MVB = late endosome/multivesicular body.

Drug	Target	Effect	References
Tyrphostin A23	Cargo recognition by the μ subunit of the AP2 complex	Blocks clathrin-mediated endocytosis	Ortiz-Zapater *et al.* 2006, Robinson *et al.* 2008
Dynasore	GTPase activity of DRP	Blocks DRP-mediated endocytosis	Kirchausen *et al.* 2008, Sharfman *et al.* 2011
1-butanol	Phospholipase D	Blocks endocytosis	Boucrot *et al.* 2006, Sharfman *et al.* 2011
Ikarugamycin	Unknown	Blocks clathrin-mediated endocytosis	Moscatelli *et al.* 2007
Brefeldin A	ARF-GEFs	Blocks exocytosis, endosomal recycling and vacuole addressing	Robinson *et al.* 2008
Endosidin1	Unknown	Blocks trafficking at the EE/TGN	Robert *et al.* 2008
Concanamycin A	Endosome acidification by VHA	Blocks trafficking at the EE/TGN	Robinson *et al.* 2008
Wortmannin	PI3 kinase (VPS34)	Blocks trafficking at the LE/MVB	Robinson *et al.* 2008
LY294002	PI3 kinase (VPS34)	Blocks trafficking at the LE/MVB	Lee *et al.* 2008

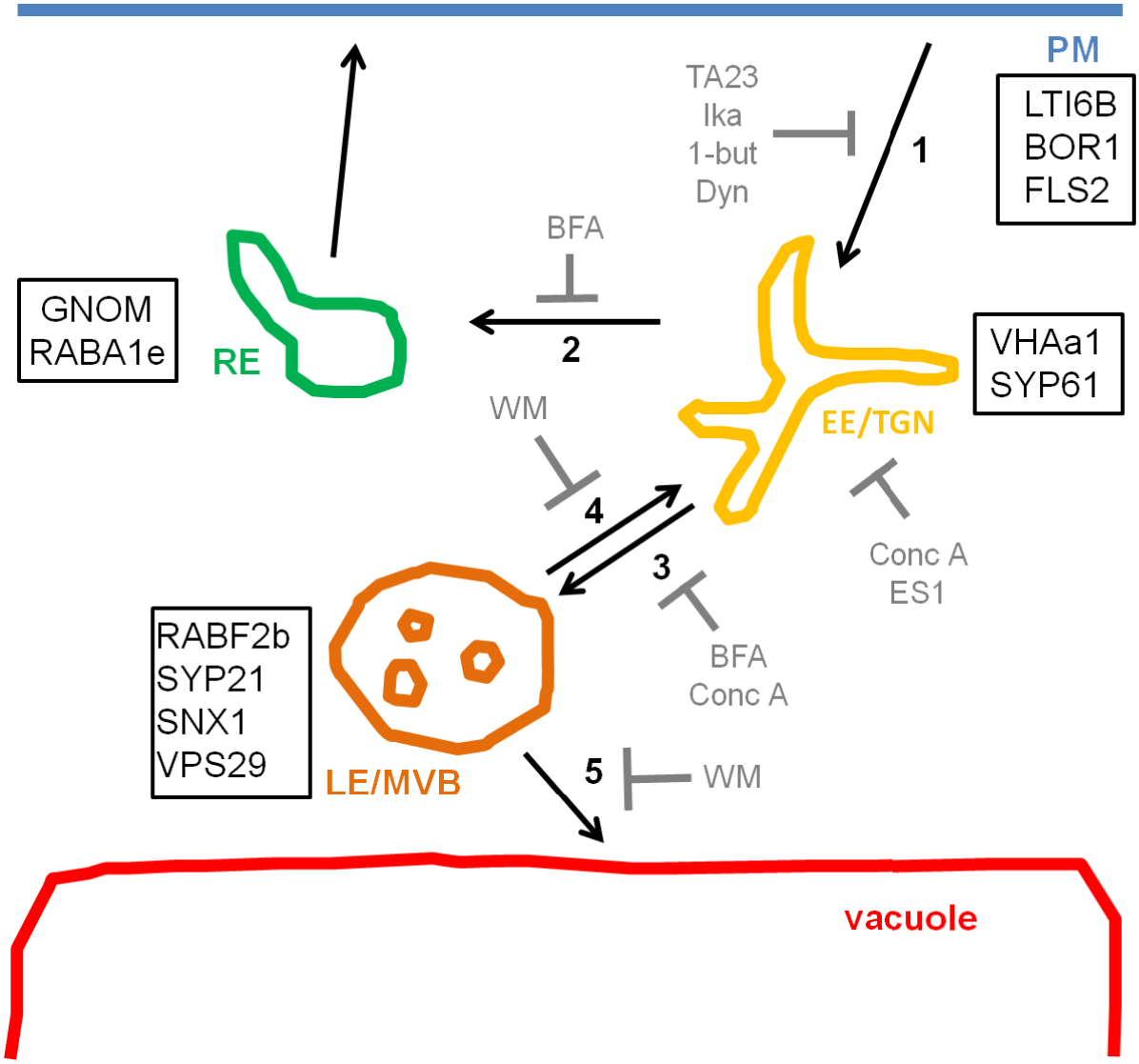

Figure 4: simplified map of the endocytic compartments in plants. Each endocytic compartment is represented in the diagram with a different color and trafficking between compartments is symbolized with a black numbered arrow. Proteins considered as markers of each compartment are shown in black boxes. Endocytosed material leaves the plasma membrane (PM, blue) and reaches first the *trans*-Golgi network (TGN, yellow), which is functionally the early endosome (EE) (arrow 1). At the EE/TGN, endocytosed material can enter a recycling pathway and transit through recycling endosomes (RE, green) to be redirected to the plasma membrane (arrow 2). Endocytosed material can also enter a degradation pathway and reach the late endosome (LE, orange), which is also called the multivesicular body (MVB) (arrow 3). Retrograde trafficking from the LE to the TGN is indicated by arrow 4. LE can fuse with the vacuole (red) and release material destined to be degraded in the vacuolar lumen (arrow 5). Drugs perturbing endocytic trafficking are indicated in grey (see table 2, TA23 = tyrphostin A23, Ika = ikarugamycin, 1-but = 1-butanol, Dyn = dynasore, Conc A = concanamycin A, ES1 = endosidin 1, BFA = brefeldin A, WM = wortmannin).

observed in animal cells. Endocytosed material is finally degraded in the vacuole, which is the functional equivalent of the lysosome of animal cells. The intraluminal vesicles of multivesicular bodies are released through direct membrane fusion between multivesicular bodies and the vacuole (Contento and Bassham 2012).

2.2. Endocytosis in plants : welcome to the inside of plant cells

2.2.1. Clathrin and plant endocytosis

The most studied endocytic pathway is clathrin-mediated endocytosis. It is characterized by the involvement of a hexameric complex called clathrin, composed of three heavy chains and three light chains together making a triskelion-shaped complex. Clathrin molecules assemble and coat endocytic pits and vesicles during their formation to stabilize membrane curvature. The clathrin coat is later removed after vesicle release in the cytoplasm (**figure 5**) (Chen *et al.* 2011, MacMahon and Boucrot 2011). Clathrin-mediated endocytosis was investigated through interference with the function of clathrin by over-expression of the "clathrin-hub". The clathrin-hub is a dominant-negative form of clathrin composed of the C-terminal part of clathrin heavy chain, which binds clathrin light chains. Over-expression of the clathrin-hub captures light chains and prevents their association with endogenous heavy chains (Liu *et al.* 1995, 1998). Clathrin-hub over-expression reduces endocytosis of FM4-64 (Dhonukshe *et al.* 2007). Loss of function of clathrin heavy chains gave similar results (Kitakura *et al.* 2011). Quantitative data obtained in *Arabidopsis thaliana* protoplasts revealed that clathrin-hub over-expression reduced endocytosis by 57 % (Scheuring *et al.* 2012). These data suggest that clathrin-mediated endocytosis is a major route of endocytosis in *Arabidopsis thaliana*. Clathrin-hub also prevents endocytosis of PIN-FORMED1 (PIN1) and PIN2 (which are integral transmembrane proteins functioning as efflux carriers of the plant hormone auxin, Dhonukshe *et al.* 2007), and H^+ plasma membrane ATPase (Kitakura *et al.* 2011), indicating that they are cargos for clathrin-mediated endocytosis. The endocytosis of BRI1 bound to its ligand was investigated using a fluorescent analog of brassinosteroids called Alexa fluor-467 castasterone (AFCS). Over-expression of the clathrin-hub blocks internalization of BRI1-AFCS, indicating activated BRI1 follows clathrin-mediated endocytosis (Irani *et al.* 2012).

2.2.2. Endocytic motifs and adaptor complexes

Cargo proteins are sorted for endocytosis through specific linear motifs present in the intracellular part of the protein and recognized by the endocytic machinery (Chen *et al.* 2011). One such motif is the YXXΦ motif, where Y represents a tyrosine residue, X any amino acid residue, and Φ a hydrophobic residue. The YXXΦ motif binds to μ2, the μ subunit of the adaptor protein complex 2 (AP2) (Kurten 2003), and AP2 then recruits clathrin at the plasma membrane for endocytosis (McMahon and Boucrot 2011).

Genetic evidence underlines the involvement of AP2 during endocytosis in plant cells. Loss of function of the AP2 subunit μ2 reduces endocytosis of FM4-64 and cellulose synthase complexes (Bashline *et al.* 2013). In the same study, the authors show that μ2 and clathrin light chains are both localized to transient foci at the plasma membrane. μ2 dynamics parallels the one observed for clathrin, with μ2 being recruited a few seconds before clathrin, as expected (Bashline *et al.* 2013). Consistently, loss of function of the AP2 subunit σ impairs FM4-64 and PIN1 endocytosis, leading to PIN1 polarity defects and altered development (Fan *et al.* 2013). A thorough analysis of AP2 structure and function in *Arabidopsis thaliana* was recently published. The composition of the AP2 complex, previously inferred from sequence analysis, was confirmed by biochemical data and is composed of one α (among two isoforms), one β (among two isoforms), one μ and one σ subunits (Rubbo *et al.* 2013, Yamaoka *et al.* 2013). Loss of function of the gene encoding the μ2 subunit leads to defects in endocytosis of FM4-64 and PIN proteins (Kim *et al.* 2013, Yamaoka *et al.* 2013). Knock-down of subunit α1 by siRNA or by over-expression of a dominant negative form impaired BRI1 endocytosis (Rubbo *et al.* 2013).

PIN proteins are polarly localized at the plasma membrane, thanks to mechanisms involving endocytosis at the boundaries of the polar domain (Kleine-Vehn *et al.* 2011). A YXXΦ motif is conserved in all *Arabidopsis thaliana* PIN proteins. Mutation of this motif increases localization of PIN2 outside the polar domain, indicating that it might be involved in endocytosis of PIN2 (Kleine-Vehn 2011). In agreement with this, tyrphostin A23—a drug that blocks clathrin-mediated endocytosis by binding AP2 at the same site as the tyrosine of the YXXΦ motif (Robinson *et al.* 2008)—blocks endocytosis of PIN1 and PIN2 (Dhonukshe *et al.* 2007, Robert *et al.* 2010). Tyrphostin A23 also perturbs endocytosis of H^+ plasma membrane ATPase (Dhonukshe *et al.* 2007), LOW TEMPERATURE-INDUCIBLE PROTEIN 6B (LTI6B) (Dhonukshe *et al.* 2007), the water channel PLASMA MEMBRANE INTRINSIC PROTEIN2 (PIP2) (Dhonukshe *et al.* 2007), the iron transporter IRT1 (Barberon *et al.* 2011), ligand-bounded BRI1 (Irani *et al.* 2012) and activated FLS2 (Beck *et al.* 2012), suggesting or confirming that these proteins are cargoes for clathrin-mediated endocytosis.

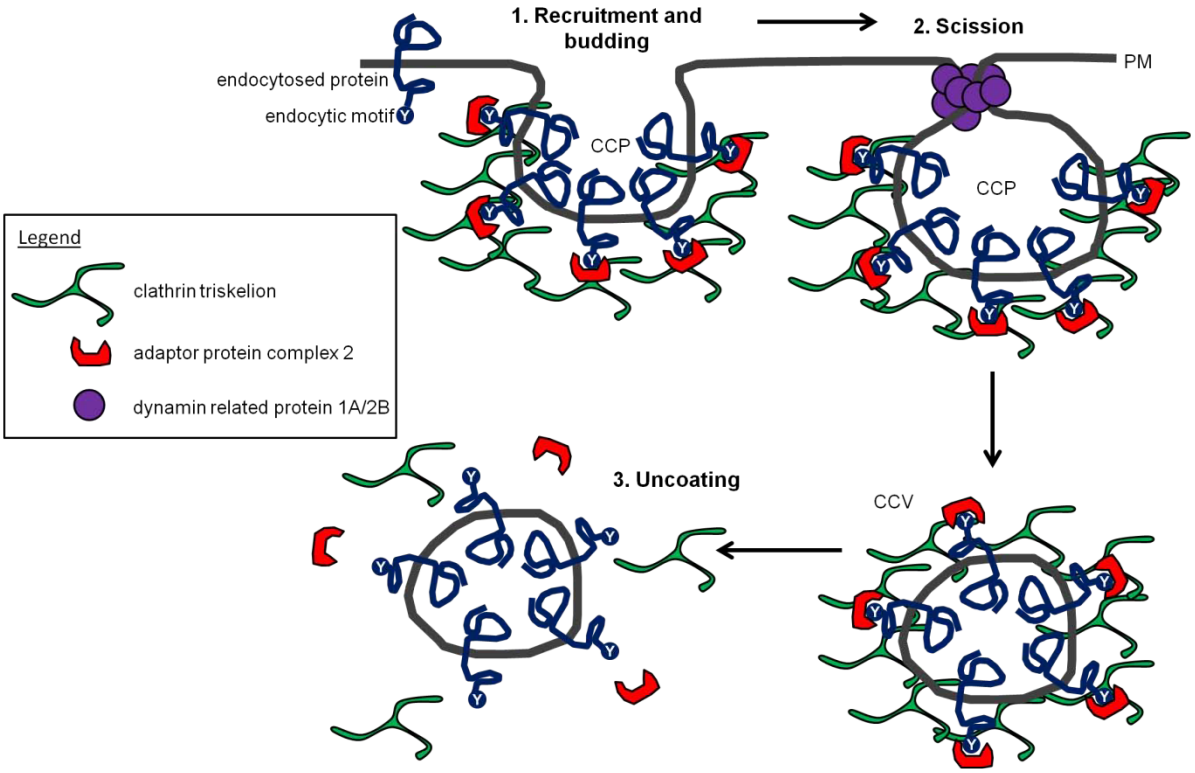

Figure 5: schematic representation of clathrin-mediated endocytosis in plants. Step 1 : a plasma membrane (PM) protein bearing an endocytic motif (represented as Y) is recognized by the adaptor protein complex 2 (AP2). AP2 recruits clathrin triskelions, which stabilize the budding of the PM to form a clathrin-coated pit (CCP). Step 2 : dynamin related proteins 1A and 2B polymerize at the neck of the CCP to drive scission of the CCP and lead to the formation of a clathrin-coated vesicle (CCV). Step 3 : the CCV is uncoated and fuses with the trans-Golgi network (TGN, which is functionally the early endosome).

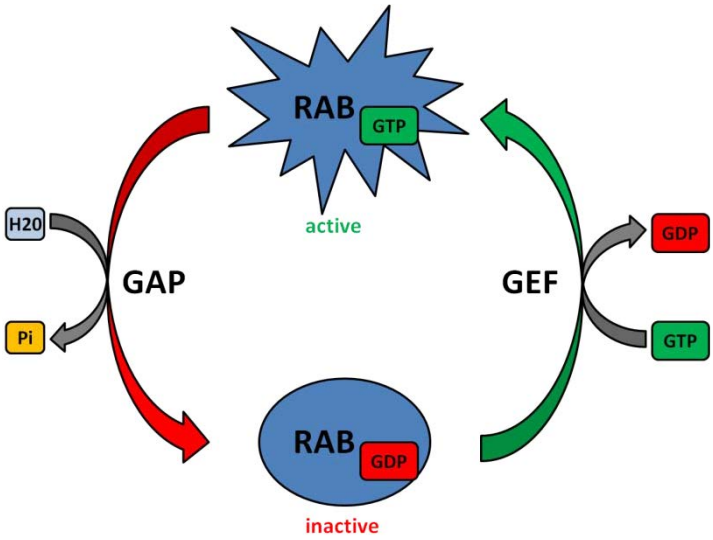

Figure 6: the RAB GTPase activity cycle. RAB GTPases cycle between GTP-bound active and GDP-bound inactive states. Activation occurs through GDP/GTP exchange, a process catalyzed by a guanine nucleotide exchange factor (GEF), while inactivation occurs through hydrolysis of GTP to form GDP, a process catalyzed by a GTPase activating protein (GAP).

BOR1, a boron transporter, contains three YXXΦ motifs. Under high boron conditions, BOR1 is internalized before being degraded in the vacuole. While mutation of the first motif does not produce a visible effect, mutation of at least one of the two other motifs impairs BOR1 vacuolar trafficking in response to high boron concentrations and stabilizes BOR1 at the plasma membrane (Takano *et al.* 2010). LeEIX2 is a transmembrane protein that recognizes the fungal protein ethylene-inducing xylanase (EIX) and signals to induce defense responses. LeEIX2 contains a YXXΦ motif in its cytoplasmic tail and mutation of this motif abolishes ligand-induced endocytosis of LeEIX2 (Bar and Avni 2009).

2.2.3. Dynamin-related proteins

Arabidopsis thaliana dynamin-related proteins (DRP) are GTPases, homologs of animal dynamins. Based on protein sequence identity, 6 families of DRP are identified. While DRP3 to DRP6 families are involved in mitochondrial, chloroplast and peroxisome fission/biogenesis, DRP1 and DRP2 families are involved in endocytosis. DRP polymerize at the neck of clathrin-coated pits to allow vesicle detachment from the plasma membrane through hydrolysis of GTP (Bednarek and Backues 2010, Fujimoto and Ueda 2012).

Loss of function of proteins of the DRP1 family leads to defective cell expansion and plasma membrane abnormalities (Bednarek and Backues 2010). Notably, DRP1A loss-of-function leads to defects in cell expansion, abnormal cell wall and plasma membrane morphology and reduced internalization of FM4-64, consistent with impaired endocytosis (Collings *et al.* 2008). DRP2B and DRP1A proteins colocalize at the plasma membrane in dynamic spots and each protein also colocalizes with clathrin light chain. DRP2B and DRP1A are recruited to the plasma membrane slightly after clathrin, in agreement with a role in clathrin-coated vesicle detachment from the plasma membrane (see **figure 5**, Fujimoto *et al.* 2010). Tyrphostin A23 treatment perturbs the distribution and dynamics of different DRP1 proteins at the plasma membrane (Fujimoto *et al.* 2010, Konopka *et al.* 2008). DRP2A and DRP2B are the closest homologs of animal Dynamin1, the canonical dynamin involved in endocytosis. They are composed of a GTPase domain, a GTPase effector domain involved in dynamin polymer assembly. They also contain a pleckstrin-homology domain and a proline-rich domain involved in membrane lipid binding and protein-protein interaction, respectively. The pleckstrin-homology domain of DRP2B binds phosphatidylinositol (4,5)-bisphosphate (PtdIns(4,5)P*2*) and PtdIns(4)P *in vitro* (Lam *et al.* 2002), which are phospholipids found at the plasma membrane (Kost *et al.* 1999, Vermeer *et al.* 2009). By contrast, proteins of the DRP1A subfamily do not possess proline-rich nor pleckstrin-homology domains, but show higher GTPase domain sequence identity with Dynamin1 than DRP2 proteins (Bednarek and Backues 2010). Based on these results, it believed that DRP1A and DRP2B function together to mediate endocytosis at the plasma membrane, with each protein fulfilling a different

function of animal dynamin : membrane targeting by DRP2B and catalytic activity by DRP1A (Fujimoto *et al.* 2010). Consistent with this, DRP2B has a low GTPase activity compared to DRP1A (Yan *et al.* 2011).

2.2.4. Rab GTPases

RAB GTPases constitute a conserved proteins family composed of 57 members in *Arabidopsis thaliana*. This family is divided into 8 classes, from RAB-A to RAB-H (Wollard and Moore 2008). RAB GTPases specify membrane identity and regulate docking and fusion of vesicles with target membranes by cycling between active and inactive states, depending on the nucleotide that is bound by the RAB (**figure 6**). When bound to GDP, the RAB is inactive. Exchange of GDP for GTP, catalyzed by a GEF, activates the RAB. Hydrolysis of GTP to form GDP, catalyzed by a GTPase-activating protein (GAP), returns the RAB to the inactive state (Nielsen *et al.* 2008). Dominant-negative and dominant-positive variants of RAB GTPases (locked in GDP-bound and GTP-bound states, respectively) are instrumental in the study of their roles.

The RAB-F class, homolog to the animal RAB5, contains three proteins : RAB-F1/ARA6, RAB-F2a/RHA1 and RAB-F2b/ARA7. All proteins localize to the multivesicular bodies (Haas *et al.* 2007, Kotzer *et al.* 2004, Lee *et al.* 2004), although they show partially overlapping distribution (Ueda *et al.* 2004). This may reflect different populations of multivesicular bodies depending on their maturing state. ARA6 is plant-specific and mediates trafficking from multivesicular bodies to the plasma membrane (Ebine *et al.* 2011), while conventional ARA7 and RHA1 are involved in trafficking to the vacuole. ARA7^{S24N} and RHA1^{S24N} (in which serine 24 was replaced with asparagine) is putatively locked in the GDP-bound form and thus has a dominant-negative effect by trapping the GEF and making it unavailable to activate endogenous proteins. Over-expression of ARA7^{S24N} or RHA1^{S24N} redirects vacuolar proteins to the secretion pathway (Kotzer *et al.* 2004, Sohn *et al.* 2003). ARA7^{S24N} also perturbed endocytosis of FM4-64 and several plasma membrane proteins (Dhonukshe *et al.* 2006, Dhonukshe *et al.* 2008), suggesting that ARA7 also regulates endocytosis.

2.2.1. Ubiquitin in endocytosis regulation

Ubiquitin moieties attached to plasma membrane proteins can serve as a signal for their endocytosis and subsequent sorting into intraluminal vesicles for degradation (Sorkin and von Zastrow 2009). In animals, active EGFR signals through Grb2, which binds to phospho-tyrosine residues of EGFR and recruits c-Cbl, an E3 ubiquitin ligase that ubiquitinates EGFR (Jiang *et al.* 2003). EGFR then binds ubiquitin-interacting motifs of Epsin1, an adaptor protein interacting with AP2, clathrin and phospholipids. RNAi-mediated knockdown of Epsin1 perturbs EGFR endocytosis, suggesting a link between ubiquitination of EGFR and endocytosis

(Kazazic *et al.* 2009). However, mutation of the ubiquinated residues of EGFR results in impaired ubiquitination and endosomal sorting but leaves internalization rates unaffected (Huang *et al.* 2007). Attachment of ubiquitin on ubiquitin itself generates poly-ubiquitin chains. Lysine 48-linked chains preferentially serve as signals for proteasome degradation (Komander and Rape 2012), while lysine 63-linked chains are recognized by the signaling and endocytic machineries (Haglund and Dikic 2012). Recent proteomic studies demonstrate that EGFR is ubiquitinated by one or two short (two to three ubiquitins) lysine 63-linked chains or mono-ubiquitinated at a single lysine (Huang *et al.* 2013). In the same study, it is demonstrated that removal of poly-ubiquitin chains by fusion of EGFR with the de-ubiquitinating enzyme AMSH decreases ligand-induced endosomal sorting and degradation. Moreover, the presence of c-Cbl in endosomes suggests that ubiquitination of active EGFR continues in endosomes (Umebayashi *et al.* 2008). Together, these data show that ubiquitination is not crucial for endocytosis but only participates in the redundant molecular network established during clathrin-coated vesicle formation. Instead, sustained ubiquitination of active EGFR in endosomes is necessary for routing to the degradation pathway.

The ubiquitination of several plant plasma membrane proteins, including PIN proteins (Abas *et al.* 2006), BOR1 (Kasai *et al.* 2011), IRT1 (Barberon *et al.* 2011) and FLS2 (Lu *et al.* 2011) plays a role in their endocytic trafficking. IRT1 cycles between the plasma membrane and the *trans*-Golgi network, where it accumulates at steady state, and part of endocytosed IRT1 is routed to the vacuole in a constitutive manner. IRT1 is mono-ubiquitinated *in vivo* at several residues, and mutation of these residues stabilizes IRT1 at the plasma membrane and leads to plant lethality. This indicates that mono-ubiquitination regulates trafficking of IRT1 and keeps plasma membrane levels of IRT1 low, preventing excess and toxic uptake of iron (Barberon *et al.* 2011).

The boron transporter BOR1 is ubiquitinated and degraded in the vacuole in high boron conditions to avoid toxic accumulation of boron in plants. Mutation of lysine 590 of BOR1 into alanine ($BOR1^{K590A}$) abolishes high boron-induced ubiquitination and degradation but not endocytosis of the transporter. Apparently, trafficking of $BOR1^{K590A}$ from the *trans*-Golgi network to the multivesicular bodies is impaired. Indeed, BFA treatment results in accumulation of $BOR1^{K590A}$-GFP (green fluorescent protein) in BFA bodies, indicating that endocytosis of $BOR1^{K590A}$-GFP is not affected. On the other hand, wortmannin treatment did not result in accumulation of $BOR1^{K590A}$-GFP into wortmannin-induced enlarged multivesicular bodies, contrary to wild-type BOR1-GFP which, indicating that trafficking of $BOR1^{K590A}$-GFP to multivesicular bodies is impaired (Kasai *et al.* 2011). These data demonstrate that ubiquitination of BOR1 at lysine 590 is not required for endocytosis but is important for endosomal sorting and degradation.

FLS2 activation triggers within seconds BAK1-dependent recruitment and phosphorylation of PUB12 and PUB13, two E3 ubiquitin ligases that ubiquitinate

FLS2. In PUB12 and PUB13 loss-of-function mutants, ligand-induced degradation of FLS2 is reduced, supporting a role of ubiquitination in FLS2 endocytic sorting towards a vacuolar pathway (Lu *et al.* 2011).

In conclusion, ubiquitination of endocytosed proteins in plants plays a role in endocytic events at the plasma membrane and during subsequent sorting of the internalized proteins to target them to the vacuole.

2.2.2. Clathrin-independent endocytosis in plants

Although many different types of clathrin-independent endocytosis, were described in animals (Doherty and McMahon 2009), clathrin-independent is only starting to be characterized in plants, and the machinery involved is still unknown.

Growing pollen tubes treated with ikarugamycin, a drug that specifically affects clathrin-mediated endocytosis (**table 2**) show a 80 % reduction in endocytosed FM4-64, thereby suggesting that if inhibition is complete, the remaining 20 % of endocytosis follow a clathrin-independent route (Moscatelli *et al.* 2007). Using positively or negatively charged nanometric gold beads, the same authors identify different trafficking pathways. Positively charged gold is endocytosed and either recycled in the secretory pathway through the Golgi apparatus or enter the degradation pathway as attested by labeling of the vacuole. Negatively charged gold mostly enters the degradation pathway. Ikarugamycin greatly reduces Golgi apparatus labeling by positively charged gold and vacuole labeling by negatively charged gold, indicating that these trafficking routes depend on clathrin-dependent endocytosis. It is interesting to not that ikarugamycin does not affect accumulation of positively charged gold in the vacuole, indicating that clathrin-independent endocytosis may be at work in pollen tubes to direct negatively charged plasma membrane regions (which presumably bind positive gold) to the degradation pathway (Moscatelli *et al.* 2007, Onelli *et al.* 2008).

Fluid-phase endocytosis is the endocytosis of solutes captured in endocytic vesicles (Doherty and McMahon 2009). 2-NBDG, a fluorescent derivative of sucrose is endocytosed through fluid-phase endocytosis and colocalizes with the *trans*-Golgi network marker SYP61 in tobacco protoplasts (Bandmann and Homann 2012). Ikarugamycin treatment or clathrin-hub over-expression did not prevent 2-NBDG internalization, indicating that fluid-phase endocytosis of glucose is clathrin-independent (Bandmann and Homann 2012), as similarly occurs in animal cells for various metabolites (Doherty and McMahon 2009). The fact that 2-NBDG localizes to the *trans*-Golgi network after internalization also suggests that clathrin-mediated and clathrin-independent-endocytosis share the same intracellular route, at least during the initial steps of endocytic trafficking.

In animal cells, caveolae are flask-shaped invaginations of the plasma membrane devoid of any obvious coat and participate in several aspects of membrane function, including mechanosensing, membrane organization and

endocytosis (Parton and del Pozo 2013). Cargos endocytosed through caveolae include glycosylphosphatidylinositol (GPI)-linked proteins, cholera toxin and simian virus 40 (Parton and Simons 2007). The main proteins of caveolae are caveolins, which oligomerize to form caveolae, are palmitoylated at the C-terminus, have a putative hairpin transmembrane segment and bind cholesterol (Parton and Simons 2007). Cells devoid of caveolins are also devoid of caveolae, and over-expression of caveolins induces formation of caveolae, indicating that caveolins are a necessary component of caveolae (Doherty and McMahon 2009). Cavins are other proteins necessary for caveolae function, perhaps by stabilizing caveolin oligomers (Parton and del Pozo 2013). Caveolae have a specific lipid composition, being enriched in cholesterol and sphingolipids in comparison to the whole plasma membrane, so that caveolae can be seen as lipid rafts with a specific morphology and stabilized by caveolins (Parton and Simons 2007). Other proteins present in lipid rafts, called flotillins, are palmitoylated and may form a hairpin structure similar to caveolins but they oligomerize in plasma membrane regions distinct from caveolae (Doherty and McMahon 2009). Flotillins are involved in endocytosis of some GPI-linked proteins, cholera toxin and proteoglycans (Doherty and McMahon 2009).

Genes encoding caveolins are absent from plant genomes (Šamaj *et al.* 2004) but the involvement of flotillins in endocytosis was recently investigated in *Arabidopsis thaliana* (Li *et al.* 2012). GFP-FLOTILLIN1 is present in intracellular spots that colocalize with FM4-64, and at the plasma membrane in discrete and dynamic spots distinct from clathrin light chain-mOrange labeling. The diffusion coefficient of GFP-FLOTILLIN1 and clathrin light chain-mOrange spots was quantified in the presence of tyrphostin A23 and methyl-β-cyclodextrin, a cholesterol depleting agent. Tyrphostin A23 treatment little perturbs the dynamics of GFP-FLOTILLIN1 spots, contrary to clathrin light chain-mOrange spots. Moreover, methyl-β-cyclodextrin significantly decreases the diffusion coefficient of GFP-FLOTILLIN1 spots by 100 fold while it little affects clathrin light chain-mOrange spots, in line with GFP-FLOTILLIN1 being involved in an endocytic pathway independent of clathrin and dependent on sterols. However, cargos of flotillin-dependent endocytosis remain to be identified.

2.3. Relationships between endocytosis and receptor signaling

2.3.1. Endocytosis attenuates signaling from the plasma membrane

Historically, endocytosis was first demonstrated to downregulate RTK. EGFR is internalized and degraded in lysosomes after EGF binding (Stoscheck and Carpenter 1984, Beguinot *et al.* 1984). In addition, a mutant EGFR with a truncated C-terminal tail (which contains endocytic motifs) fails to be internalized and shows enhanced EGF-induced responses (Wells *et al.* 1990). These early studies indicated that endocytosis and degradation of activated receptors serve the purpose of preventing excess receptor signaling. In line with this model, a low dose of EGF preferentially directs EGFR towards clathrin-mediated endocytosis and recycling, while a high dose of EGF directs EGFR towards an additional clathrin-independent endocytic pathway which leads to receptor degradation (Sigismund *et al.* 2008).

EGFR signaling involves PtdIns(4,5)P2 hydrolysis by phospholipase Cγ (PLCγ) and phosphorylation of PtdIns(4,5)P2 into PtdIns(3,4,5)P3 by PI 3-kinases. While activated EGFR are endocytosed, PtdIns(4,5)P2 remain at the plasma membrane. Moreover, PtdIns(3,4,5)P3 are also absent from endosomes containing activated EGFR, indicating that PI 3-kinase-mediated signaling happens only at the plasma membrane. These data indicate that EGFR signaling through PLCγ is downregulated by endocytosis because the substrate of this pathway, PtdIns(4,5)P2, is absent from endosomes (Haugh and Meyer 2002).

FLS2^{T876V}, which is mutated at a putatively phosphorylated residue of the juxtamembrane segment, has abolished signaling and ligand-induced endocytosis (Robatzek *et al.* 2006). In the same way, wortmannin treatment impairs ligand-induced endocytosis of FLS2 (Robatzek *et al.* 2006) and reduces MAPK activation upon ligand stimulation (Chinchilla *et al.* 2007), drawing a link between endocytosis and signaling. In a screen to identify small molecules that affect pathogen-induced responses, cantharidin was identified as a perturbator of FLS2 trafficking and signaling (Serrano *et al.* 2007). Cantharidin treatment diminishes ligand-induced FLS2 endocytosis and increases persistence of reactive oxygen species, which are produced early during FLS2 signaling. Interestingly, cantharidin is an inhibitor of type 2A phosphatases such as KINASE-ASSOCIATED PROTEIN PHOSPHATASE (KAPP), which interacts with the activated kinase domain of several PRK, including FLS2 (Gomez-Gomez *et al.* 2001). Moreover, KAPP over-expression enhances endocytosis of SERK1, suggesting that KAPP positively regulates endocytosis of SERK1 (Shah *et al.* 2002). It is possible that cantharidin, through inhibition of the phosphatase activity of KAPP, perturbs the phosphorylation and activation status of FLS2—thereby impairing its endocytosis. In conclusion, the

persistence of activated FLS2 at the plasma membrane could be responsible for the increased reactive oxygen species production following catharidin treatment, indicating that endocytosis of FLS2 contributes to signal termination at the plasma membrane (**figure 7**, arrow 1).

2.3.2. Endocytosis enables sustained signaling in endosomes

The first clue of endosomal signaling came from subcellular fractionation approaches demonstrating that phosphorylated EGFR is present in endosomes along with constituents of EGFR signaling pathway (Guglielmo *et al.* 1994). Many studies then investigated the effect of perturbation of endocytic trafficking on receptor signaling. In a seminal article, interference with endocytosis by using a GTPase-defective dominant-negative mutant of Dynamin in which lysine 44 was replaced with alanine (Dyn^{K44A}) was used to study EGFR signaling in HeLa cells (Vieira *et al.* 1996). Over-expression of Dyn^{K44A} results in suppression MAPK signaling. In contrast, other proteins participating in EGFR signaling are hyper-activated in cells over-expressing Dyn^{K44A}. In conclusion, Dynamin-dependent endocytosis of EGFR is required for the full extent of signaling and controls specific signaling pathways (Vieira *et al.* 1996). In another study, siRNA-mediated knockdown of clathrin heavy chain, of the α or μ subunit of the AP2 complex were used in HeLa cells (Sigismund *et al.* 2008). The authors demonstrate that not the peak but rather the decay phase of EGFR signaling through MAPK is diminished in clathrin heavy chain or AP2 knockdown cells, while the activation of another signaling pathway is not altered. This indicates that plasma membrane signaling is responsible for the peak of EGFR signaling and clathrin-mediated endocytosis allows sustained signaling from endosomes and recycling to the plasma membrane where additional rounds of signaling can be initiated (Sigismund *et al.* 2008).

However, several studies provided evidence in conflict with the results discussed above (Galperin and Sorkin 2008, Johannessen *et al.* 2000). It is not easy to reconcile the conflicting evidence regarding EGFR endosomal signaling, but experimental conditions, in particular the concentration of EGF used to stimulate cells, the time of analysis and the cell types could influence the speed of EGFR recycling or degradation and help to explain these discrepancies.

As endosomes are motile compartments, the signals they convey can reach considerable distances. For example, the neurotrophins receptors Trk bind their ligand in the axon terminus and then move towards the cell body to elicit nuclear responses, a transport that requires microtubules (Watson *et al.* 1999) and the molecular motor complex dynein (Wu *et al.* 2007). In support of this model, Trk-ligand complexes along with activated proteins of the MAPK signaling pathway are found in clathrin-coated vesicles following ligand treatment (Howe *et al.* 2001).

In *Arabidopsis thaliana*, BRI1 is localized at the plasma membrane, at the *trans*-Golgi network and at multivesicular bodies, based on colocalization with FM4-64, VHAa1 and SNX1 (Jaillais *et al.* 2008, Geldner *et al.* 2007) and on electron microscopy experiments (Viotti *et al.* 2010). This distribution is constitutive, since it is independent of the presence of the ligand (Geldner *et al.* 2007). It must be noted that part of this localization could represent BRI1 biosynthesis and secretion, so the trafficking of putatively ligand-bound and active BRI1 was studied using a fluorescent ligand, AFCS (Irani *et al.* 2012). BRI1 and AFCS colocalize at *trans*-Golgi networks and multivesicular bodies. AFCS is finally found at the vacuole, in agreement with previous studies (Geldner *et al.* 2007, Viotti *et al.* 2010). AFCS and BRI1 endocytosis are impaired following tyrphostin A23 treatment, clathrin-hub over-expression or ARA7^{S24N} over-expression (Irani *et al.* 2012). The same treatments result in dephosphorylation of BES1, a readout of BRI1 signaling, indicating that BRI1 signaling occurs at the plasma membrane (Irani *et al.* 2012). BRI1 was also proposed to signal from endosomes (Geldner *et al.* 2007). Indeed, BFA treatment aggregates BRI1 into BFA-bodies and also increases the endosomal pool of BRI1 while it decreases the plasma membrane pool. BRI1 signaling appears to be triggered by BFA treatment alone, since BES1 is then dephosphorylated and *DWF4* expression levels are decreased, two markers of BRI1 signaling (Geldner *et al.* 2007).

However, Irani *et al.* (2012) argued that BFA may perturb endocytosis and increase the pool of active BRI1 at the plasma membrane, since the target of BFA, GNOM, and the functionally redundant and BFA-insensitive GNOM-LIKE1 (GNL1) play a role in endocytosis (Teh and Moore 2007, Naramoto *et al.* 2010). Irani *et al.* (2012) report that *GNL1* loss of function results in less frequent BRI1-positive endosomes, and additional BFA treatment shows BFA-bodies with reduced BRI1-GFP fluorescence compared to the wild-type—this is consistent with reduced internalization of BRI1 (Irani *et al.* 2012). In addition, *GNL1* loss of function plus BFA treatment, as well as tyrphostin A23 treatment, results in increased sensitivity of BRI1 to ligand addition, confirming plasma membrane signaling of BRI1 (Irani *et al.* 2012). Finally, concanamycin A treatment retains BRI1-AFCS complexes in the *trans*-Golgi network, but this does not result in increased BRI1 signaling (Irani *et al.* 2012).

The localization of BRI1 signaling partners is also informative. BAK1 colocalizes with BRI1 at the plasma membrane and in endosomes (Bücherl *et al.* 2013, Russinova *et al.* 2004), and colocalization is enhanced in both compartments upon ligand application (Bücherl *et al.* 2013). FRET-FLIM (Bücherl *et al.* 2013, Russinova *et al.* 2004), biochemical (Wang *et al.* 2005b) and quantitative analysis of fluorescence from BRI1-fluorescent protein fusions (Hink *et al.* 2008, see part 1.4.1) indicate that BRI1 and BAK1 form oligomers at both the plasma membrane and in endosomes in absence of ligand, and that ligand application stabilizes these oligomers. Nevertheless, BSK kinases, which are phosphorylated by activated BRI1,

are localized to the plasma membrane where they interact with BRI1 (Tang *et al.* 2008). BSK kinases then interact with the phosphatase BSU1, which dephosphorylates the BIN2 kinase. BIN2 is localized at the plasma membrane, cytosol and nucleus and is involved in inactivation of brassinosteroid-regulated transcription factor (Vert and Chory 2006). Brassinosteroid signaling could benefit from the presence of activated BRI1 in motile endosomes for two reasons: firstly, it would inform the whole cell and prevent BIN2 dephosphorylation and reactivation, which would terminate signaling; secondly, it would effectively transmit signaling to the chromatin by directing endosomes to the nucleus through cytoskeleton-based motility, since the sole diffusion of signaling molecules to the nucleus is not efficient (Howe 2005). Taken together, these data are consistent with a model in which BRI1 primarily signals from the plasma membrane before being internalized in endosomes where sustained signaling could occur (**figure 7**, arrow 2).

2.3.3. Specific signaling from endosomes

In the budding yeast, the pheromone receptor Ste2 traffics to endosomes where it activates signaling molecules that are specific to this compartment. Ste2 is a G protein-coupled receptor (GPCR) that associates with a trimeric G protein composed of α, β and γ subunits. Ste2 activation results in activation of the G protein, dissociation of Gα from the Gβ-Gγ dimer, Gβ-Gγ-mediated MAPK signaling at the plasma membrane and endocytosis of Gα. In endosomes, activated Gα stimulates production of PtdIns(3)P by the PI 3-kinase, resulting in recruitment of the PtdIns(3)P-binding protein Bem1 to the endosome, which is thought to propagate downstream signaling (Slessareva *et al.* 2006).

Signaling by the G-protein coupled receptor Regulation of G-protein Signaling 1 (RGS1) in *Arabidopsis thaliana* provides an example for the requirement of endocytosis in signaling, but in an indirect way. Indeed, *Arabidopsis thaliana* Gα protein auto-activates because it exchanges GDP for GTP much faster than it hydrolyzes GTP. Gα is kept inactive by binding to RGS1, which stimulates the GTPase activity of Gα. Upon ligand binding, RGS1 is endocytosed, which releases the downregulation of Gα by RGS1 and allows Gα signaling (Urano *et al.* 2012).

A localization-specific signaling is seen with regulation of neuron survival by Trk signaling. A specific signaling pathway is elicited by retrograde endosomes carrying activated Trk. Indeed, Trk activation at the axon terminus promotes neuron survival through an ERK5-dependent signaling pathway, while Trk activation in the cell body activates both ERK1/2 and ERK5 signaling pathway but does not promote neuron survival (Murphy *et al.* 2009, see references therein).

In *Arabidopsis thaliana*, LeEIX2 is endocytosed upon ligand stimulation and subsequently colocalizes with the PtdIns(3)P-containing endosomes (Bar and Avni 2009). Inhibition of the PI 3-kinase with wortmannin or LY294002 results in

abolished endocytosis of LeEIX2 (Bar and Avni 2009) and reduced LeEIX2-mediated cellular response (Sharfman *et al.* 2011). LeEIX2 contains a YXXΦ motif in its intracellular region, and mutation of this motif abolished both LeEIX2 endocytosis (Bar and Avni 2009) and LeEIX2-mediated cellular response (Ron and Avni 2004). Together these data indicate that LeEIX2 cannot signal from the plasma membrane and must be internalized in endosomes to do so, where it may meet signaling partners that are absent from the plasma membrane (**figure 7**, arrow 4).

As previously discussed, wortmannin treatment impairs ligand-induced endocytosis of FLS2 (Robatzek *et al.* 2006) and reduced downstream MAPK activation but not the immediate reactive oxygen species production (Chinchilla *et al.* 2007). Although wortmannin has broad effects on cellular physiology and does not inhibit endocytosis only, it is tempting to speculate that specific signaling pathways might be activated depending on the subcellular localization of FLS2, i.e. reactive oxygen species production at the plasma membrane and MAPK activation from endosomal compartments (**figure 7**).

2.3.4. Endosomal sorting regulates signaling

Sorting of activated receptors in intraluminal vesicles of multivesicular bodies isolates the receptor from cytosolic signaling partners and routes receptors for degradation (Sorkin and von Zastrow 2009). Ubiquitination of receptor induces their sorting into intraluminal vesicles through the ESCRT complex, which recognizes ubiquitin moieties on the receptor and induce inward budding of the endosomal membrane to form intraluminal vesicles (see parts 2.1 and 2.2.1).

Early studies demonstrated that EGFR interacts with the ESCRT-0 component Hrs (Sigismund *et al.* 2005) and that loss of function of Hrs results in perturbed multivesicular body formation, leading to increased EGFR signaling and perturbed development (Lloyd *et al.* 2002). In Hela cells, siRNA knock-down of Tsg101 from ESCRT-I and hVps24 from ESCRT-III both impair EGFR degradation and transport to lysosomes, but only Tsg101 knockdown results in sustained EGFR signaling (Bache *et al.* 2006), indicating that EGFR down-regulation in endosomes happens before ESCRT-III activity and likely before degradation. As stated in part 2.2.1, endosomal sorting and degradation of activated EGFR requires poly-ubiquitination through lysine 63-linked chains both at the plasma membrane and in endosomes. The role of EGFR ubiquitination in signaling was investigated by expression of a fusion between EGFR and AMSH, a de-ubiquitinating enzyme specific for lysine 63 linkages (Huang *et al.* 2013). EGFR-AMSH is less poly-ubiquitinated, displays a delayed lysosomal targeting and degradation, which results in sustained activation. However, it should be noted that different concentrations of ligand are used to quantify each of these parameters. Since different ligand concentrations trigger different endocytic trafficking rates and activate different trafficking pathways, it is unclear whether sustained signaling

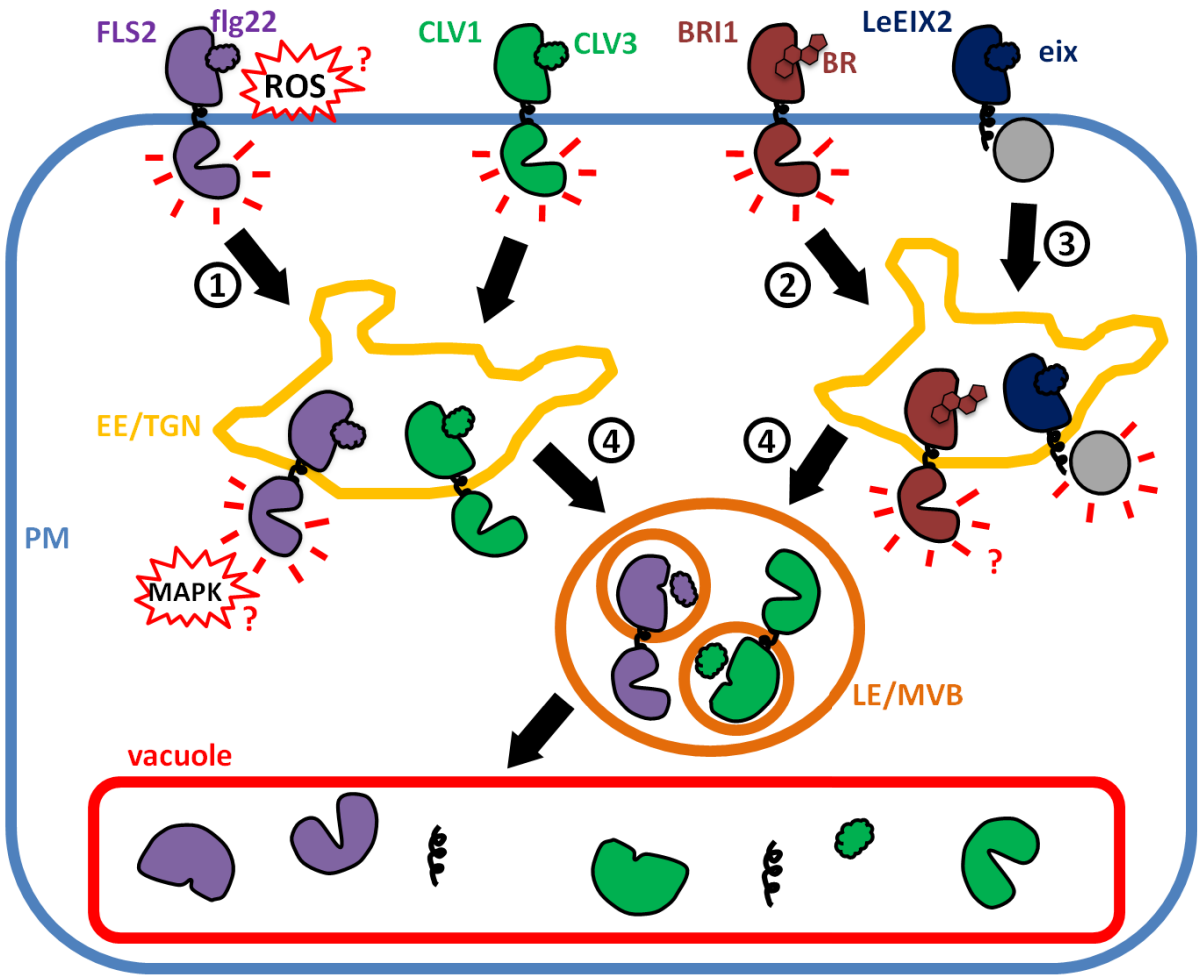

Figure 7: relationships between trafficking and signaling of plant receptors. The plasma membrane (PM) is shown in light blue, the early endosome/*trans*-Golgi network (EE/TGN) is shown in yellow, the late endosome/multivesicular body (LE/MVB) is shown in orange and the vacuole is shown in red. The trafficking (black arrows) and signaling (short red lines) of the plant receptor kinases FLS2 (purple), CLV1 (green), BRI1 (brown) and the receptor-like protein LeEIX2 (blue) are represented in a schematic plant cell. Since LeEIX2 is devoid of a kinase domain, it may signal by association with signaling partners (gray discs). Endocytosis can be a way to stop signaling at the PM (ROS = reactive oxygen species production) (arrow 1), and may be followed by an endosomal-specific signaling (MAPK = mitogen activated protein kinases signaling). Signaling at the PM may be followed by endocytosis and sustained signaling in endosomes (arrow 2). Signaling by LeEIX2 requires internalization into endosomes, where it could meet signaling partners that are absent from the plasma membrane (arrow 3). Finally, endocytosis of active receptors can be followed by sorting to LE/MVB for degradation in the vacuole (arrow 4).

following perturbed endosomal sorting comes from EGFR localized in endosomes or in other compartments.

Evidence for a role of ubiquitin-mediated endosomal sorting in PRK signal termination comes from studies on FLS2. FLS2 recycles between endosomes and the plasma membrane in absence of ligand (Beck *et al.* 2012, Robatzek *et al.* 2006), but ligand binding triggers transient accumulation of FLS2 in multivesicular bodies (Beck *et al.* 2012) and prolonged ligand stimulation induces disappearance of FLS2-GFP (Robatzek *et al.* 2006), thereby suggesting that endocytosis of activated FLS2 leads to sorting for degradation. A PEST-like motif, putatively involved in ubiquitin-triggered endocytosis, is present in the C-terminal segment of FLS2 and mutation of this motif impairs ligand-induced endocytosis of FLS2 (Robatzek *et al.* 2006). Moreover, FLS2 is ubiquitinated by the PUB12 and PUB13 ubiquitin ligases (Lu *et al.* 2011). In PUB12 and PUB13 loss-of-function mutants, ligand-induced degradation of FLS2 is reduced while FLS2-mediated cellular responses are enhanced. However, mutation of the PEST-like motif does not affect ubiquitination of FLS2 by PUB12 and PUB13, suggesting that ubiquitination is uncoupled from endocytosis (Lu *et al.* 2011). Altogether, these data are in line with ubiquitin-mediated degradation of FLS2 in the vacuole after activation as a means to terminate signaling (**figure 7**, arrow 4).

There is some evidence of CLV1 endosomal sorting. CLV1 is detected in the vacuole in a *CLV3* (ligand) wild-type background but is seen at the plasma membrane in a *CLV3* null mutant background, indicating that ligand binding induces receptor endocytic sorting for degradation (Nimchuk *et al.* 2011) (**figure 7**, arrow 4). According to these authors, down-regulation of CLV1 by CLV3 could explain the buffering of CLV1 signaling, since a similar phenotype is observed over a 10-fold range of CLV3 expression levels (Müller *et al.* 2006).

2.3.5. Proposed roles of endosomal signaling

Signaling from endosomes takes advantage of several properties that distinguish them from the plasma membrane. These properties include, among others, a closed space that enables a sustained ligand-receptor interaction (by "trapping" the ligand), the motility of endosomes that spreads signals to remote parts of the cell and the presence of specific molecules that recruit signaling effectors (Sorkin and von Zastrow 2009).

In plants, although such considerations can apply, it has also been affirmed that endosomal signaling could be a necessary adaptation for two reasons (Geldner and Robatzek 2008). Firstly, endosomal signaling occurrences are sparse in unicellular organisms, and the apparition of multicellularity was accompanied by a large increase in the PRK/plasma membrane surface ratio (1 in *Chlamydomonas* to 102 in *Arabidopsis*). Thus, endosomal signaling could be a means to increase the membrane surface that is available for PRK signaling. Secondly, the increase in

cytoplasm volume in multicellular organisms could make diffusion-based propagation of signaling insufficient to inform the whole cell. Since endosomes are generally motile compartments, endosomal signaling could spread the signals sent by active receptors.

THESIS RESEARCH FRAMEWORK

3. Self-incompatibility in the *Brassicaceae*

In flowering plants, including *Arabidopsis thaliana*, the reproductive organ is the flower. *Arabidopsis thaliana* is a hermaphrodite, meaning that it bears flowers with both male (stamens) and female (gynœcium) organs (**figure 8**). Pollen grains carry the male gametes. Pollen grains are emitted when anthers (the structures that produce pollen and located at the tip of stamens) open, a stage of development called anthesis and which approximately corresponds to the time of opening of the flower bud. Pollen grains are then brought to the stigma, located at the extremity of the gynœcium (the female organ), and make contact with stigmatic epidermal cells called papillae. When this contact occurs, the pollen grain can emit a pollen tube that will make its path down the gynœcium to reach an ovule, which contains the female gametes. Once the pollen tube reaches an ovule, male gametes are released and they fertilize the female gametes, ultimately generating a seed.

In self-incompatible species, the pollen undergoes a genetic check-up called self-incompatibility before it is permitted to emit a pollen tube. Self-incompatibility is a genetic barrier by which a plant recognizes and rejects its own pollen while allowing pollen from more distantly related individuals to germinate. It is present in around half of all flowering plant species distributed in dozens of plant families including *Rosaceae*, *Papaveraceae*, *Solanaceae* and *Brassicaceae* and displays different mechanisms of activation depending on the family (Gaude *et al.* 2006). In the *Brassicacea*, it is controlled by a highly polymorphic locus called the *S*-locus, which contains the male and female determinants of self-incompatibility. There are more than 90 locus variants called haplotypes described in *Brassica*. The female determinant is S-LOCUS RECEPTOR KINASE (SRK), a PRK expressed in the stigma. The male determinant is S-LOCUS CYSTEINE-RICH (SCR)/S-LOCUS PROTEIN11 (SP11) and is present at the pollen surface. During pollination, SCR is transported to the papillae plasma membrane. If SRK and SCR are from the same haplotype of the *S*-locus, their interaction triggers activation of SRK and a downstream signaling pathway leading to self-pollen rejection. If SRK and SCR are from different haplotypes, SRK is not activated and pollen germination can follow, resulting in the fertilization of the ovules (**figure 9**) (Ivanov *et al.* 2010).

4. SRK endosomal localization in *Brassica oleracea*

SRK subcellular localization was investigated in *Brassica oleracea S3* (haplotype 3 of the *S*-locus) stigmatic papillae using anti-SRK3 antibodies (Ivanov and Gaude 2009). It revealed a striking picture—most of SRK is localized in endosomes and to a lesser extent at the plasma membrane. Although ligand stimulation increases SRK turnover, this subcellular distribution is constitutive, since it remains unchanged by the presence or absence of the ligand. Although several PRK and other receptors can be present in endosomal compartments in a constitutive (BRI1) or ligand-dependent manner (FLS2, LeEIX2), plasma membrane localization

is usually predominant—this makes SRK localization unique. In addition, the anti-SRK3 antibody used by Ivanov and Gaude can activate SRK and thus substitute for a ligand. This antibody binds SRK3 at the plasma membrane and is then endocytosed and colocalizes with SRK3 in endosomes, raising the possibility that SRK remains active in endosomes. It was also shown that SRK colocalizes in endosomes with THL1 (Ivanov and Gaude 2009), a negative regulator of self-incompatibility (Cabrillac *et al.* 2001). Moreover, SRK3 is internalized and degraded after ligand engagement (Ivanov and Gaude 2009), indicating that endocytosis of SRK downregulates signaling by endosomal silencing through THL1 and subsequent degradation of SRK. However, such an enrichment of SRK in endosomal compartments raises the question of whether some endosomal populations can sustain SRK signaling.

5. *Arabidopsis thaliana* as a model to study self-incompatibility

Our knowledge of how self-incompatibility works at the molecular level comes from biochemical and genetic studies on *Brassica sp.* (Ivanov *et al.* 2010). However, exploring the hypothesis of endosomal signaling of SRK requires cell biology and genetic tools that are far more developed in *Arabidopsis thaliana* (which belongs to the same botanical family as *Brassica sp.*) than in *Brassica sp.* Indeed, *Arabidopsis thaliana* transgenesis is easy (Logemann *et al.* 2006) and a wide collection markers of endosomal compartments (Geldner *et al.* 2009) and mutants (O'Malley and Ecker 2010) are also available.

Arabidopsis thaliana is a self-compatible species, and no evidence of self-incompatibility in any of the hundreds of ecotypes collected from various geographical locations has been reported. *Arabidopsis thaliana* lost the ancestral self-incompatible phenotype due to null mutations in different genes required for self-incompatibility. For example, the Col-0 ecotype lost self-incompatibility through a change in a splice site that introduced a stop codon in the beginning of the sequence encoding SRK's kinase domain, generating a truncated protein. Nevertheless, the promoter of Col-0 *pseudo-SRK* remains functional and drives spatio-temporal expression similar to what is reported for SRK in *Brassica* (Kusaba *et al.* 2001). In Col-0, there are three SCR pseudogenes that encode truncated ORF (Kusaba *et al.* 2001). It has been demonstrated that self-incompatibility can be re-introduced in *Arabidopsis thaliana* by expression of functional *SRK* and *SCR* genes from a related and self-incompatible species called *Arabidopsis lyrata*, from which *Arabidopsis thaliana* diverged about five million years ago (Nasrallah *et al.* 2002).

Following the same approach as Nasrallah *et al.* (2002), we generated transgenic self-incompatible *Arabidopsis thaliana* by isolating *SRK14* from *Arabidopsis lyrata* and expressing it in *Arabidopsis thaliana* (**figure 10**). We drive expression of *SRK* using two different promoters : the Col-0 *pseudo-SRK* promoter

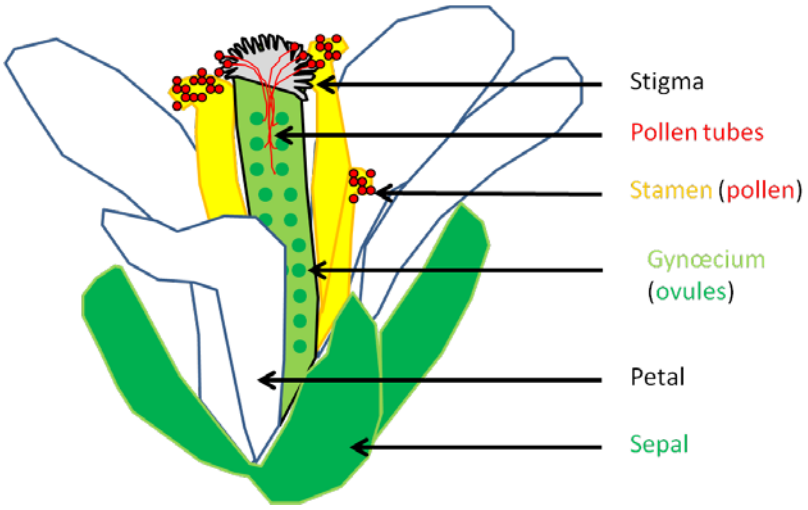

Figure 8: schematic representation of an *Arabidopsis thaliana* open flower illustrates sexual reproduction in flowering plants. The flower is composed of 4 sepals, 4 petals, 6 stamens that produce pollen grains and 1 gynœcium, which contains the ovules, capped by the stigma. Pollen grains released from the stamen are brought into contact with the stigmatic papillae, the elongated cells that cover the stigma. Upon this contact, the pollen grain can emit a pollen tube that penetrates the gynœcium to reach and fecundate an ovule, ultimately generating a seed.

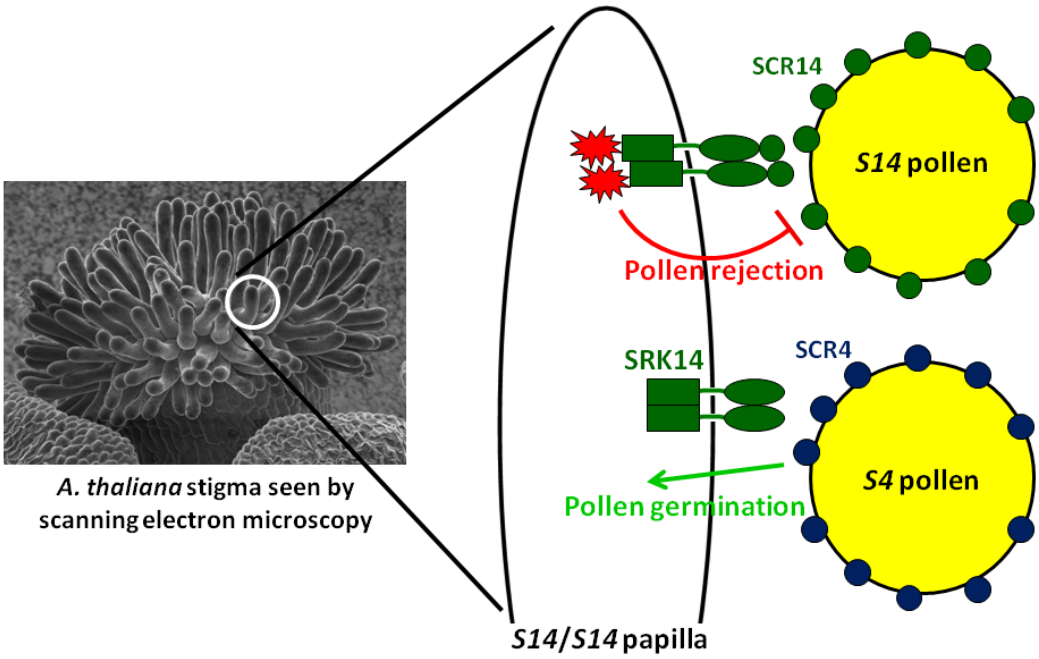

Figure 9: self-incompatibility in the *Brassicaceae*. Self-pollen recognition is mediated by the interaction between the stigmatic S-LOCUS RECEPTOR KINASE (SRK) and the pollen-borne S-LOCUS CYSTEINE RICH (SCR) proteins. A papilla from a plant homozygous for the haplotype 14 of the *S*- locus (shown in green) is represented. If a pollen grain bearing SCR14 lands on the *S14/S14* stigma, the interaction between SRK14 and SCR14 activates SRK and a signaling pathway leading to pollen rejection. If SCR4 (shown in blue) arrives on the *S14/S14* stigma, SRK is not activated and pollen germinates on the stigma surface, generating a pollen tube that will fecundate an ovule.

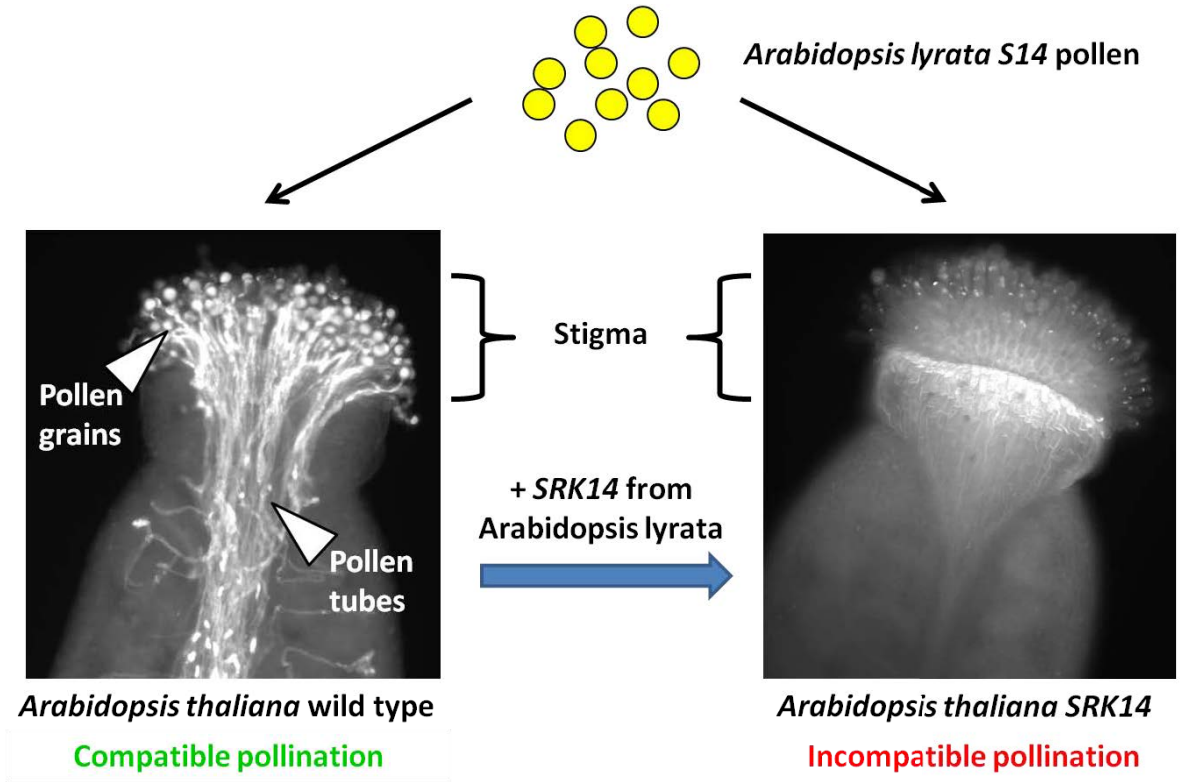

Figure 10: a transgenic self-incompatible *Arabidopsis thaliana* to study self-incompatibility. The naturally self-compatible *Arabidopsis thaliana* can be rendered self-incompatible by expression of a functional *SRK* from a related and self-incompatible species, *Arabidopsis lyrata*. As seen by analine blue staining of stigmas, which reveals pollen grains and tubes, *S14* pollen from *Arabidopsis lyrata* is fully accepted by wild-type *Arabidopsis thaliana*, while it is fully rejected by transgenic *Arabidopsis thaliana* expressing *SRK14*.

(*pSRK*), which is still functional as noted above (Kusaba *et al.* 2001), and the *SLR1* promoter from *Brassica oleracea* (*pSLR1*), which regulates expression with a similar spatio-temporal pattern as *pSRK* promoter and drives higher levels of expression than *pSRK* (Fobis-Loisy *et* al. 2007, Hackett *et al.* 1996).

We were not able to isolate the sequence encoding *SCR14* so we did not introduce *SCR14* in the genome of *Arabidopsis thaliana*. Consequently, the incompatible pollination is performed with *Arabidopsis lyrata S14* pollen. Wild-type *Arabidopsis thaliana* fully accepts pollen grains from *Arabidopsis lyrata S14* while *Arabidopsis thaliana* expressing *SRK14* from *Arabidopsis lyrata* is self-incompatible and able to reject pollen from *Arabidopsis lyrata S14*. It should be noted that when we talk about self-incompatible *Arabidopsis thaliana*, the male "self" component is actually exogenous and is brought by the pollen of *Arabidopsis lyrata* instead of being brought by the pollen of *Arabidopsis thaliana*.

6. Is SRK signaling from endosomal compartments?

Given the prevalent localization of SRK in endosomal in comparison to the plasma membrane, we hypothesized that SRK could be signaling from endosomal compartments. My thesis research framework was built on two complementary axes.

We first intended to locate SRK at the subcellular level in *Arabidopsis thaliana* stigmatic papillae to confirm the results obtained in *Brassica oleracea* (Ivanov and Gaude 2009) and lay the groundwork for future investigation of the link between the subcellular localization of SRK and self-incompatibility. We generated fluorescent protein fusions for live-cell imaging, and epitope-tagged proteins for immunolocalization experiments. We explored various sites of insertion of the tag in SRK sequence, and also used several different fluorescent proteins and epitopes.

Secondly, we aimed at perturbing SRK endocytic trafficking and steady state subcellular localization using several approaches. We targeted the function of the following proteins and protein complexes :

- Clathrin, using the clathrin-hub, a dominant negative variant
- The dynamin DRP1A, using dominant negative variants or a loss-of-function mutant
- The RAB GTPase ARA7, using dominant-negative and dominant positive variants

We also aimed at targeting more specifically the endocytic trafficking of SRK by mutation of a tyrosine-based motif putatively involved in binding the μ subunit of AP-2 during clathrin-mediated endocytosis. We expected to shift the steady state localization of SRK from a predominant endosomal localization to a predominant plasma membrane localization using the approaches listed above.

Our goal was to correlate changes in the localization of SRK to changes in the self-incompatible phenotype. If SRK must be localized in endosomal compartments to be activated, or at least to sustain an activation initiated at the plasma membrane to properly activate its signaling pathway, we should see a reversion of the self-incompatible phenotype into a self-compatible phenotype. If, on the other hand, endocytosis is rather involved in the down-regulation of SRK signaling by stopping signaling at the plasma membrane, and/or later sorting SRK for degradation, we should see a maintained self-incompatible phenotype.

EXPERIMENTAL RESULTS

7. SRK tagging

The primary structure of PRK allowed the prediction of structural domains by sequence identity. It appeared that SRK has the typical structure of a PRK with an N-terminal signal sequence followed by an extracellular ligand-binding domain, a single transmembrane segment and an intracellular kinase domain flanked by a juxtamembrane segment and a C-terminal tail (Stein *et al.* 1991, Naithani *et al.* 2007).

7.1. SRK C-terminal fusion with GFP

Before I started my PhD, fusion-proteins in which GFP was located at the C-terminus of SRK14 were generated and analyzed (C-ter, **figure 11**). This construct, called SRK14-GFP was expressed in *Arabidopsis thaliana* stigmatic papillae under the control of the *SLR1* promoter (*pSLR1*). The subcellular localization of SRK14-GFP was analyzed by confocal laser scanning microscopy (**figure 12**). The pictures in **figure 12** display the typical appearance of papillae seen by confocal microscopy. The focal plane cuts through the middle of the cell, which is constituted in most part by a large vacuole, compressing a thin (1–2μm) sheath of cytoplasm against the plasma membrane. Because they contain photosynthetic pigments, chloroplasts absorb the incident light and fluoresce in the whole light spectrum, including the emission wavelength of GFP. Chloroplast fluorescence can be discriminated from GFP fluorescence because they also fluoresce in the red part of the light spectrum, where GFP does not. A strong GFP fluorescence was seen, indicating that SRK14-GFP was expressed. However, the subcellular localization of SRK14-GFP was inconsistent with the predominant endosomal localization seen in *Brassica oleracea* papillae (**figure 12**, right-hand image, Ivanov & Gaude 2009). Indeed, the signal was mainly found at the periphery of the cell and in a thin region surrounding the vacuole, suggesting a plasma membrane and cytosolic distribution (**figure 12**, left-hand image, large arrowhead), with few endosomes visible (**figure 12**, small arrowhead). The localization of LTI6B-GFP, which labels the plasma membrane and endosomes, is indicated for comparison (**figure 12**, center image).

The self-incompatible phenotype of plants expressing SRK14-GFP was then investigated. We pollinated recently opened flowers (stage 13 according to Smyth *et al.* 1990), when expression of *SRK14* is at its maximum, of second generation transgenic plants with pollen from *Arabidopsis lyrata* expressing the *S14* haplotype of the *S*-locus. We harvested stigmas 18 hours after pollination and colored pollen grains and pollen tubes with aniline blue, a dye that stains callose (a cell wall component). During aniline blue staining, rejected and thus ungerminated pollen grains are detached from the stigma while accepted and germinated pollen grains remain on the stigma and accumulate aniline blue. Pollen grains and pollen tubes that accumulated aniline blue are then visualized by fluorescence microscopy. We

counted the number of pollen grains that germinated on the stigma and plotted the mean number of germinated pollen grains per stigma. We distinguish three categories of self-incompatibility degree. Plants are categorized as self-incompatible when they display less than 5 germinated pollen grains per stigma, on the average. Plants are categorized as partially self-incompatible when they display more than 5 but less than 30 germinated pollen grains per stigma. Finally, plants with more than 30 germinated pollen grains per stigma fit in the self-compatible category. Out of 14 first generation transgenic plants analyzed, all displayed a self-compatible phenotype. By contrast, analysis of 14 first generation transgenic plants expressing untagged SRK14 gave the following results: only one was self-compatible while the others displayed phenotypes ranging from partially self-incompatible to self-incompatible. It is worth noting that *Arabidopsis thaliana* displayed both a subcellular localization of SRK14 and self-compatible phenotype opposite of what is seen in *Brassica oleracea*. This suggests that the self-compatible phenotype we observed results from mis-localization of SRK.

7.2. SRK C-terminal fusion with epitopes

We then reasoned that a smaller tag would be less likely to perturb the function of SRK than GFP, which is around 27 kDa. We thus generated C-terminal fusions with FLAG (DYKDDDDK) or hemagglutinin (abbreviated HA, YPYDVPDYA) epitope tags. These tags are expected to minimally perturb the activity of SRK14 since their molecular masses are 10 Da and 11 Da, respectively. SRK14-FLAG and SRK14-HA were expressed in stigmatic papillae under the control of *pSLR1*.

The self-incompatibility phenotype of plants expressing SRK14-HA and SRK14-FLAG is presented in **figure 13**. Each plant represents an independent single insertion of the transgene. Col-0, the wild-type, is the compatible control. When pollinated with *Arabidopsis lyrata S14* pollen, Col-0 stigmas typically accept a high number of pollen grains, around 75. Col-0 plants expressing untagged SRK14 under the control of *pSLR1* are the self-incompatible control. These plants typically allow germination of less than 5 pollen grains per stigma, on average (**figure 13**, red line). Although plants expressing SRK14-HA or SRK14-FLAG allowed less incompatible pollen to germinate than Col-0, they accepted more than 30 incompatible pollen grains on the average (**figure 13**, orange line), which ranks as a self-compatible phenotype. This indicates that even a small polypeptide added to the C-terminus of SRK is sufficient to perturb self-incompatibility, suggesting that the C-terminus of SRK contains critical structures or motifs for function.

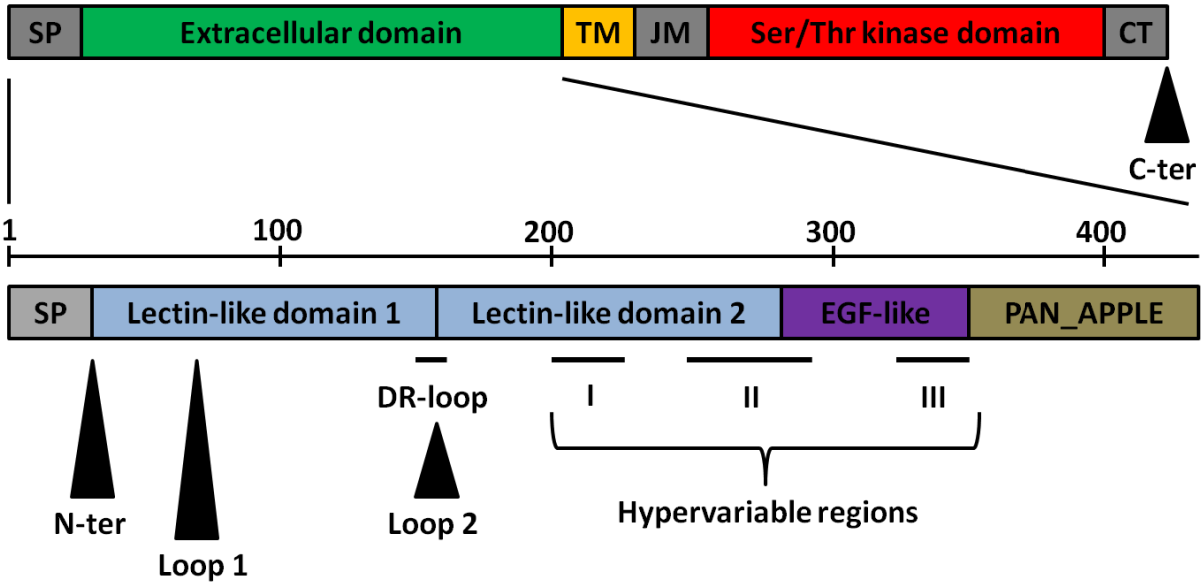

Figure 11: location of the tags introduced in fusion with SRK sequence. The above diagram represents the structural and functional domains of SRK. SP = signal peptide, TM = transmembrane segment, JM = juxtamembrane segment, CT = C-terminal tail. The location of the C-terminal tag is represented by a black triangle. Below is shown a schematic representation of the extracellular domain of SRK describing the different structural domains according to Naithani *et al.* (2007). The numbers represent the positions of the amino acids. DR-loop = deletable region loop. The three hypervariable regions involved in SCR binding are shown. The location of the different N-terminal tags are represented by black triangles.

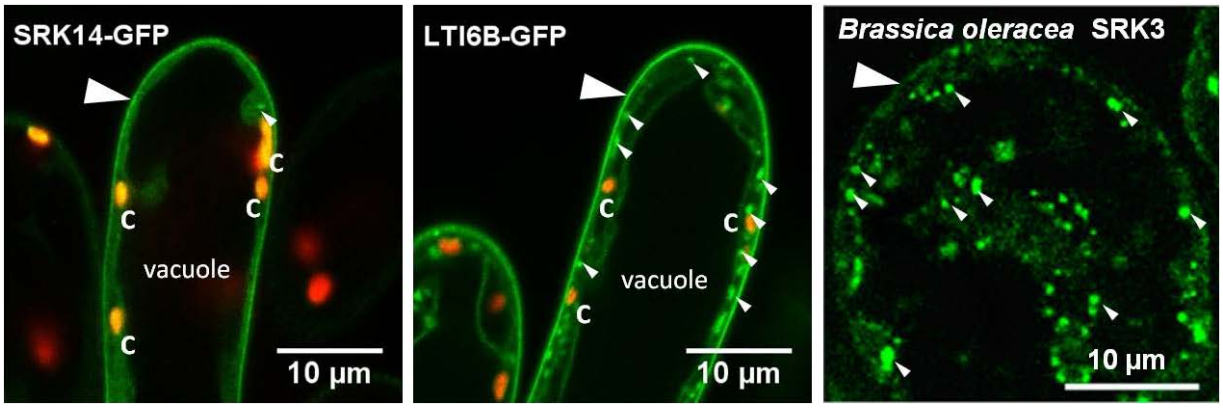

Figure 12: subcellular localization of SRK14-GFP in papillae. SRK14-GFP-expressing papillae were observed by confocal microscopy (left-hand image). A papilla expressing LTI6B-GFP is represented in the center image. GFP channel is displayed in green and chloroplast fluorescence is displayed in red, hence giving a yellow color by superposition of chloroplast fluorescence in green and red channels. C = chloroplasts. The plasma membrane is indicated by a large arrowhead, endosomes are indicated by small arrowheads. The right-hand image is the result of immunolocalization of SRK3 in *Brassica oleracea* (Ivanov and Gaude 2009).

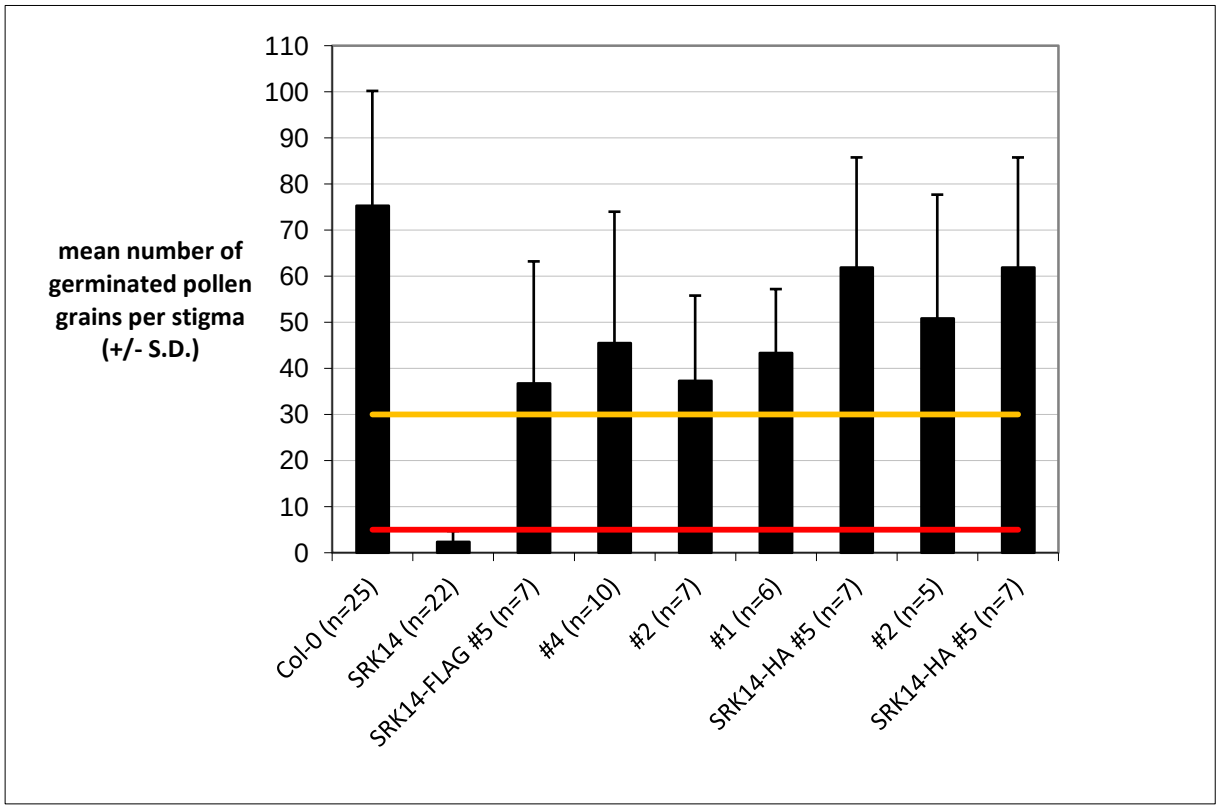

Figure 13: the self-incompatible phenotype of second generation transgenic plants expressing SRK14-FLAG/HA. Second generation transgenic plants that represent independent single transgene insertions were pollinated with incompatible pollen and the number of germinated pollen grains found on the stigma were counted. Untagged SRK14 is used as an incompatible control and wild-type Col-0 as a compatible control. The number n of stigmas examined is noted for each genotype. S.D. = standard deviation. The red line marks the upper boundary for a self-incompatible phenotype and the orange line marks the upper boundary for the partial self-incompatible phenotype. Above the orange line plants display a self-compatible phenotype.

7.3. Fluorescent proteins inserted in loops of the extracellular domain of SRK

As a third approach, we created fusion proteins in which the fluorescent protein is located inside the extracellular domain of SRK14. We selected two locations inside the SRK14 sequence, designated loop1 and loop2 (**figure 11**), predicted to form loops in the 3D structure of the protein. The ProteinCCD server (Mooij *et al.* 2009) was used to predict disordered regions which were then compared between different SRK alleles to look for amino acids insertions or deletions, an additional clue about the presence of a loop. Loop2 actually corresponds to the "deletable region", which is identified as a region of varying length in sequence alignments of SRK variants. The deletable region forms a loop in the 3D structure of SRK determined by homology modeling (Naithani *et al.* 2007), validating our approach. We introduced a *PstI* restriction site by PCR-mediated mutagenesis at loop1 and loop2 to insert a fluorescent protein coding sequence flanked by the same restriction sites.

The fluorescence intensity of fluorescent proteins depends on pH and GFP fluorescence intensity drops below a pH of 5.9 (Chudakov *et al.* 2010). The pH of the cell wall is between 5 and 6 (Fasano *et al.* 2001). The pH of *trans*-Golgi networks and multivesicular bodies are 6.2 and 6.3 respectively (Shen *et al.* 2013). In loop1/2-SRK14 constructs, the GFP would be inserted in the extracellular domain, which is located either in the cell wall if the protein is at the plasma membrane, or in the lumen of endosomes if the protein is endocytosed, raising the possibility that GFP fluorescence would not be detected because of an acidic environment. Several fluorescent proteins retain substantial fluorescence at acidic pH (reviewed in Chudakov *et al.* 2010). TagBFP2 is a blue fluorescent protein with emission at 454 nm after excitation at 399 nm (Subach *et al.* 2011). It is the most pH-resistant fluorescent protein since its pKa (the pH at which fluorescence intensity is half of the maximum) is 2.7. It also benefits from a high brightness, a fast maturation rate and a high photostability. Citrine is a yellow fluorescent protein that emits at 529 nm when excited at 516 nm (Griesbeck *et al.* 2001). Furthermore, it is one of the brightest fluorescent proteins and has a pKa of 5.7. Finally, mCherry is a red fluorescent protein with emission at 610 nm and excitation at 587 nm (Shaner *et al.* 2004). It is highly photostable and has a pKa below 4.5. We generated fusion protein between SRK and TagBFP2, Citrine and mCherry, with fluorescent protein insertion at loop1 and loop2 sites.

We first investigated the subcellular localization of TagBFP2/Citrine/mCherry-loop1/2-SRK14 constructs (**figure 14**). Fluorescence above the background level is seen, indicating that our strategy to use pH-resistant fluorescent proteins is successful. Several intracellular distributions are seen for TagBFP2/Citrine/mCherry-loop1/2-SRK14 but the fluorescence seems to be mainly restricted to a thin zone delimiting the papillae. This is best seen in **figures**

14B, 14H and **14J** and may represent a plasma membrane localization. Crosses with plants expressing plasma membrane markers are in progress to validate this hypothesis. In addition to a putative plasma membrane localization, a diffuse cytoplasmic localization is often seen, revealing the lobes of the vacuole (see **figures 14F, 14G** and **14K**). This diffuse fluorescence sometimes has a reticulate pattern (**figure 14C**). Since SRK14 is likely a type I transmembrane protein, with its N-terminus facing the extracellular side of the plasma membrane or the lumen of secretory/endocytic organelles, it is unlikely that the diffuse labeling arises from cleavage of the fluorescent protein and release into the cytosol. The diffuse and sometimes reticulate distribution is rather consistent with a endoplasmic reticulum labeling. TagBFP2-loop1-SRK14 could sometimes be seen in intracellular compartments (**figure 14D**), reminiscent of the endosomal labeling seen in *Brassica oleracea* (Ivanov and Gaude 2009).

We then characterized the self-incompatible phenotype of first generation transgenic plants expressing TagBFP2/Citrine/mCherry-loop1/2-SRK14 and corresponding to independent insertions of the transgene (**figures 15**, **16**, **17** and **18**). Out of 44 plants analyzed we obtained 17 self-compatible plants, 18 partially self-incompatible plants and 9 self-incompatible plants. We repeated the analysis on the following generation, on selected second generation transgenic plants that correspond to independent single insertions of the transgene (**figure 19**). Unexpectedly, some plants that were previously identified as self-incompatible displayed a self-compatible phenotype or partially self-incompatible phenotype, e.g. TagBFP2-loop1-SRK14 #2, Citrine-loop1-SRK14 #7 and #13, and mCherry-loop1-SRK14 #17. This could arise from an unsufficient sampling number of stigmas for pollination assays in first generation transgenic plants, from silencing of the transgene in second generation transgenic plants, or from bad pollen quality that would impair the ability of pollen grains to germinate on the stigmas. *Arabidopsis lyrata*, the pollen donor in our assays, is difficult to grow in growth chambers and is frequently attacked by pests called thrips which feed on the pollen grains. Nonetheless, we could isolate two plant lines with a significant and repeatable self-incompatible phenotype: Citrine-loop1-SRK14 #1 and mCherry-loop1-SRK14 #18. When investigating the subcellular localization of tagged SRK14 in these lines, it appears that Citrine-loop1-SRK14 #1 (**figure 14G**) and mCherry-loop1-SRK14 #18 (**figure 14K**) display an important diffuse cytoplasmic localization in comparison to partially self-incompatible lines, e.g. Citrine-loop2-SRK14 #7 and mCherry-loop1-SRK14 #17, which display a more plasma membrane-restricted labeling (**figures 14H** and **14J**). Thus, the plasma membrane labeling does not seem to correlate with the self-incompatible phenotype.

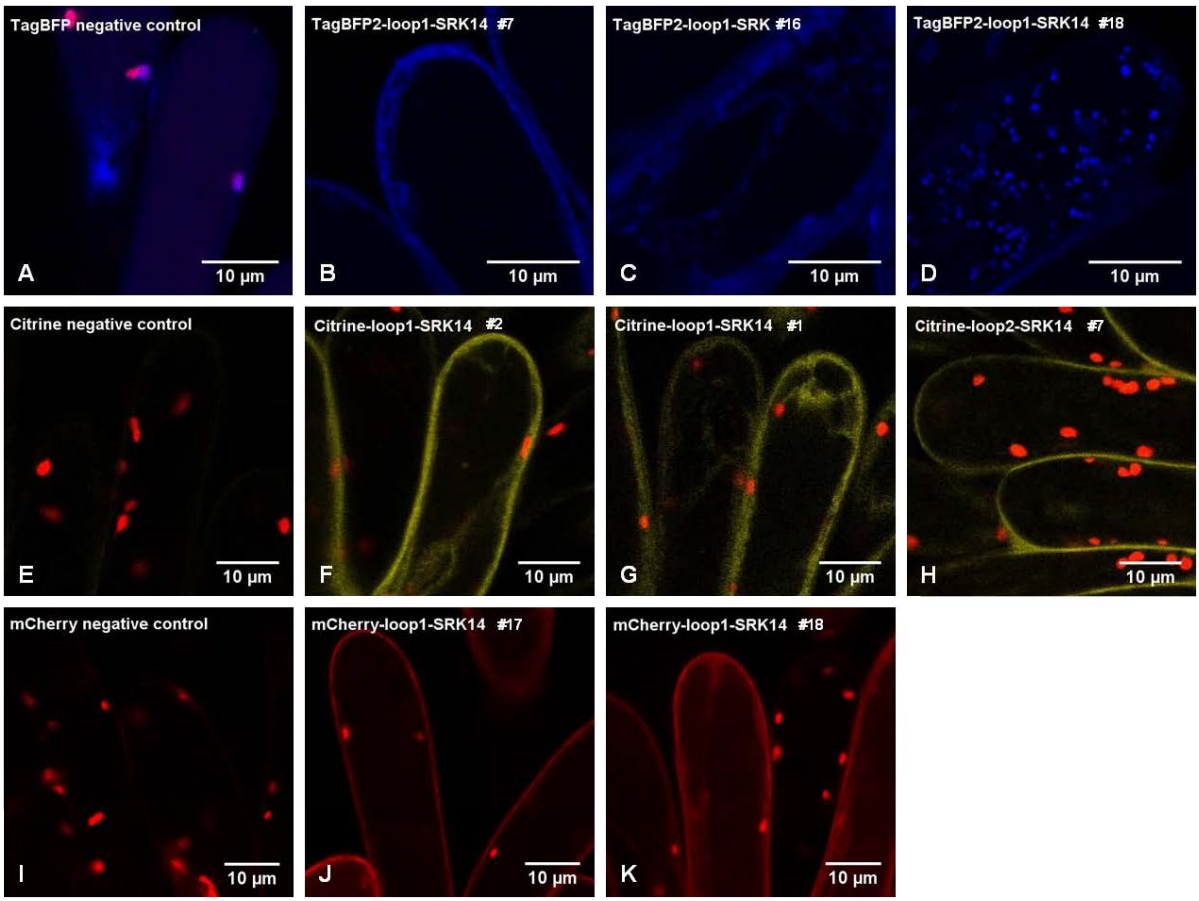

Figure 14: subcellular localization of TagBFP2/Citrine/mCherry-loop1/2-SRK14 in papillae. The papillae were analyzed by confocal microscopy. The name of the construct expressed in papillae and the number of the plant line are shown in the upper left-hand corner of the image. In general the focal plane was adjusted to go through the middle of the papilla, except for images C and D where it passes in the thin cytoplasmic sheath between the vacuole and the plasma membrane.

(A) to (D) Analysis of papillae expressing TagBFP2-loop1-SRK14. A is wild-type Col-0 papillae analyzed with TagBFP2 settings and provides a negative control for TagBFP2 fluorescence.

(E) to (H) Analysis of papillae expressing Citrine-loop1/2-SRK. E is wild-type Col-0 papillae analyzed with Citrine settings and provides a negative control for Citrine fluorescence.

(I) to (K) Analysis of papillae expressing mCherry-loop1-SRK. I is wild-type Col-0 papillae analyzed with mCherry settings and provides a negative control for mCherry fluorescence.

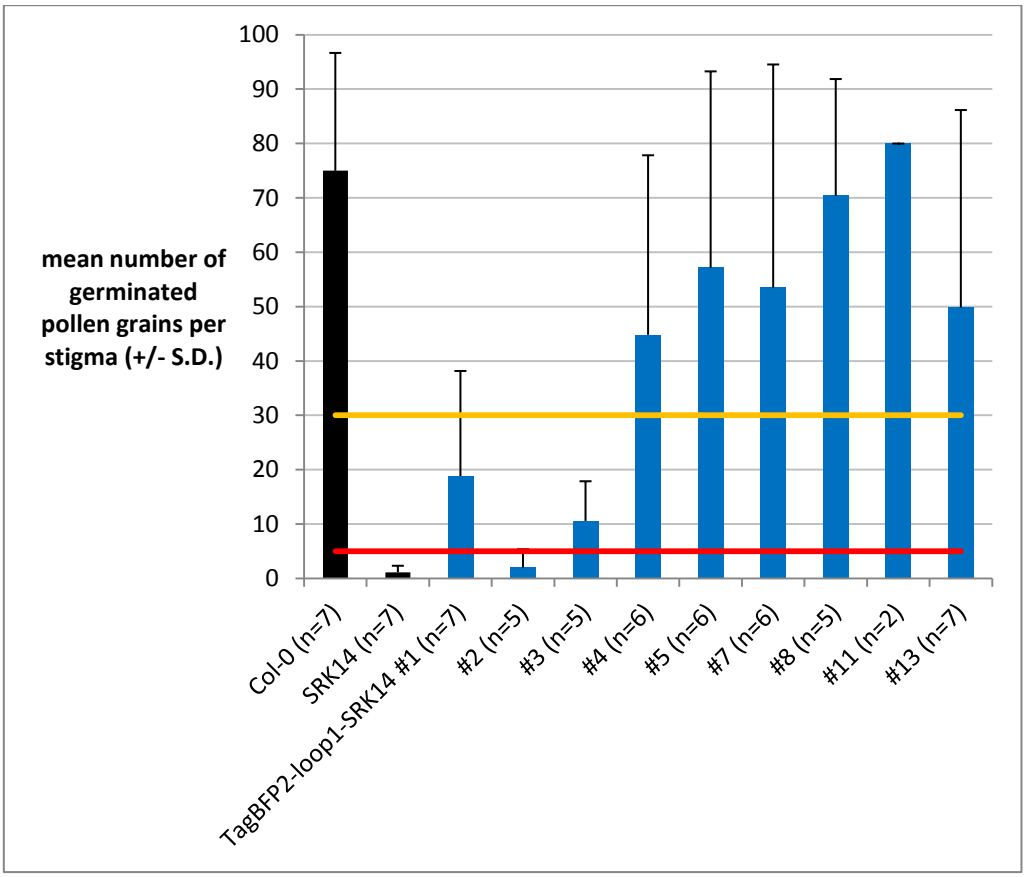

Figure 15: the self-incompatible phenotype of first generation transgenic plants expressing TagBFP2-loop1-SRK14. First generation transgenic plants corresponding to independent transgene insertions were pollinated with incompatible pollen and the number of germinated pollen grains found on the stigma were counted after aniline blue staining. Untagged SRK14 is used as an incompatible control and wild-type Col-0 as a compatible control. The number n of stigmas examined is noted for each genotype. S.D. = standard deviation. The red line marks the upper boundary for a self-incompatible phenotype and the orange line marks the upper boundary for the partial self-incompatible phenotype. Above the orange line plants display a self-compatible phenotype.

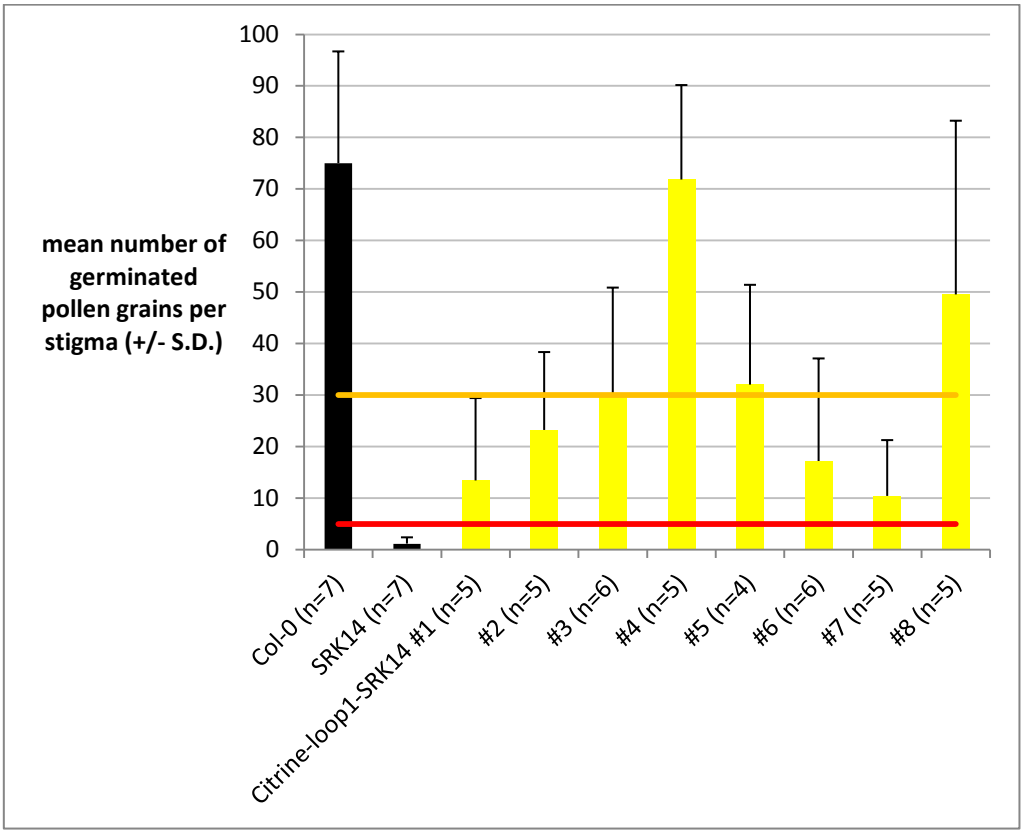

Figure 16: the self-incompatible phenotype of first generation transgenic plants expressing Citrine-loop1-SRK14. First generation transgenic plants corresponding to independent transgene insertions were pollinated with incompatible pollen and the number of germinated pollen grains found on the stigma were counted after aniline blue staining. Untagged SRK14 is used as an incompatible control and wild-type Col-0 as a compatible control. The number n of stigmas examined is noted for each genotype. S.D. = standard deviation. The red line marks the upper boundary for a self-incompatible phenotype and the orange line marks the upper boundary for the partial self-incompatible phenotype. Above the orange line plants display a self-compatible phenotype.

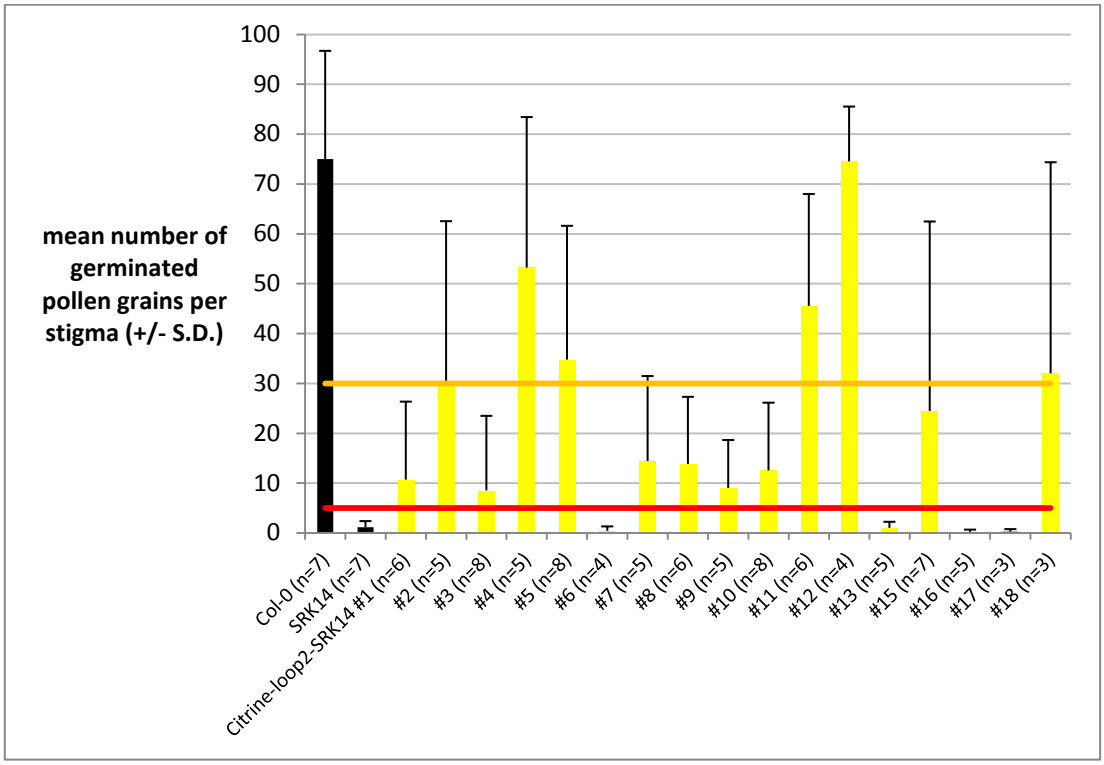

Figure 17: the self-incompatible phenotype of first generation transgenic plants expressing Citrine-loop2-SRK14. First generation transgenic plants corresponding to independent transgene insertions were pollinated with incompatible pollen and the number of germinated pollen grains found on the stigma were counted after aniline blue staining. Untagged SRK14 is used as an incompatible control and wild-type Col-0 as a compatible control. The number n of stigmas examined is noted for each genotype. S.D. = standard deviation. The red line marks the upper boundary for a self-incompatible phenotype and the orange line marks the upper boundary for the partial self-incompatible phenotype. Above the orange line plants display a self-compatible phenotype.

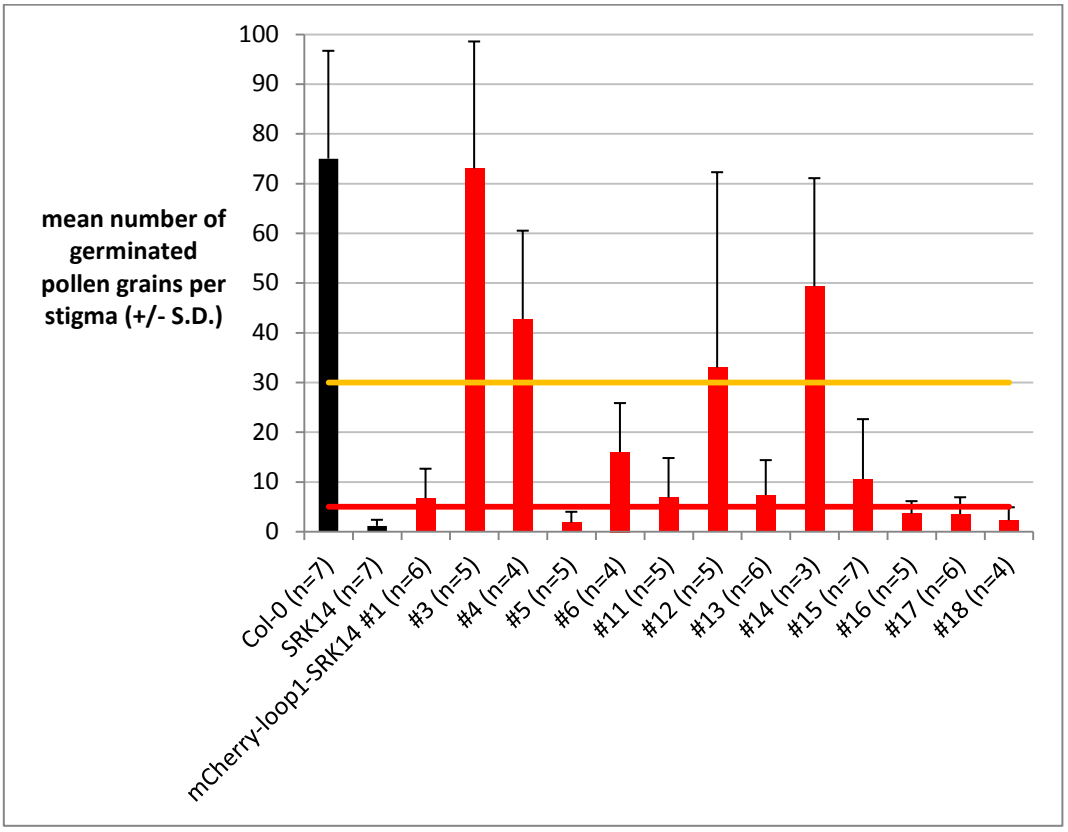

Figure 18: the self-incompatible phenotype of first generation transgenic plants expressing mCherry-loop1-SRK14. First generation transgenic plants corresponding to independent transgene insertions were pollinated with incompatible pollen and the number of germinated pollen grains found on the stigma were counted after aniline blue staining. Untagged SRK14 is used as an incompatible control and wild-type Col-0 as a compatible control. The number n of stigmas examined is noted for each genotype. S.D. = standard deviation. The red line marks the upper boundary for a self-incompatible phenotype and the orange line marks the upper boundary for the partial self-incompatible phenotype. Above the orange line plants display a self-compatible phenotype.

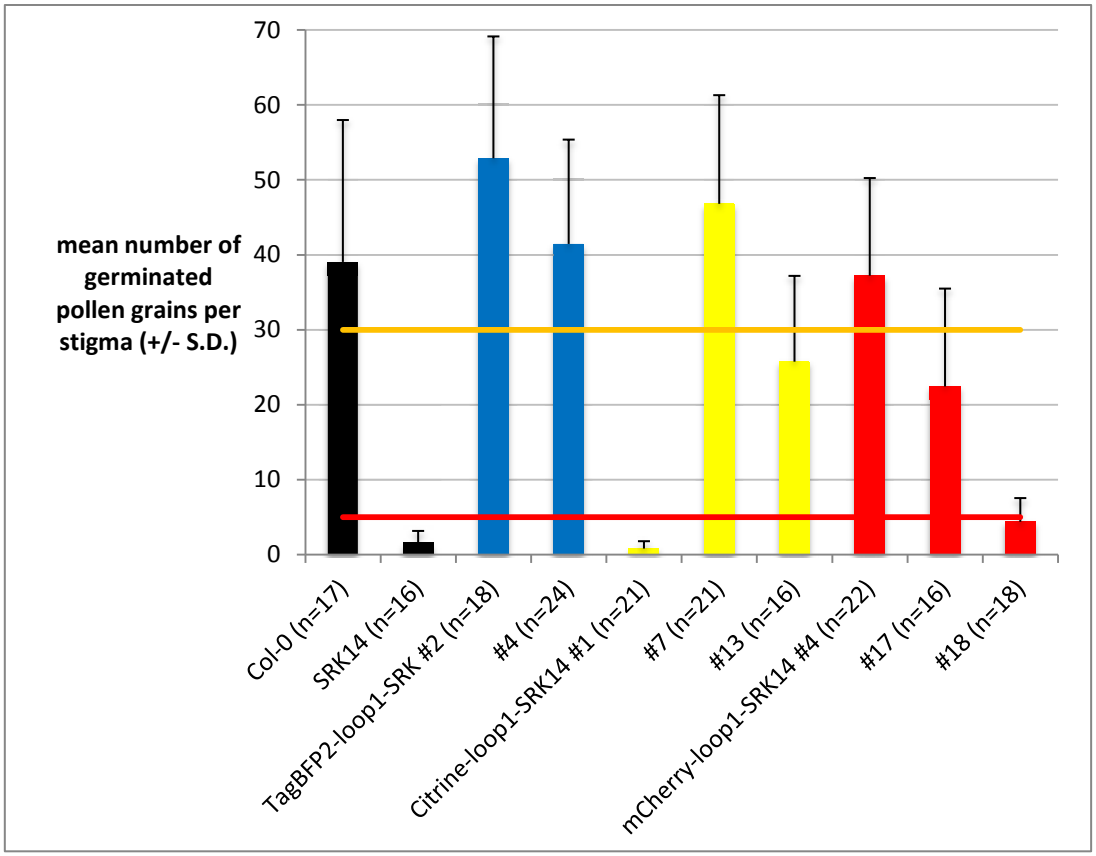

Figure 19: the self-incompatible phenotype of selected second generation transgenic plants expressing TagBFP2-, Citrine- of mCherry-tagged loop1/2-SRK14. Second generation transgenic plants corresponding to independent single transgene insertions were pollinated with incompatible pollen and the number of germinated pollen grains found on the stigma were counted after aniline blue staining. Untagged SRK14 is used as an incompatible control and wild-type Col-0 as a compatible control. The number n of stigmas examined is noted for each genotype. S.D. = standard deviation. The red line marks the upper boundary for a self-incompatible phenotype and the orange line marks the upper boundary for the partial self-incompatible phenotype. Above the orange line plants display a self-compatible phenotype.

7.4. Fluorescent proteins inserted at the N-terminus of SRK14

We generated fluorescent protein fusions in which TagBFP2, Citrine or mCherry were inserted at the N-terminus of SRK14, after the predicted signal peptide (see **figure 11**). We inserted a *PstI* restriction site after the putative signal sequence of SRK14 and inserted the coding sequence of TagBFP2, Citrine or mCherry flanked by *PstI* restriction sites. We added a linker at the C-terminus end of the fluorescent protein. We used either nine alanine residues (later designated 9A) or three repeats of the glycine-alanine dipeptide (later designated GS3). Such a linker provides flexibility in the fusion protein and can help folding and functioning of both proteins participating in the fusion (Snapp 2001). As for the other SRK14 fusion proteins, TagBFP2/Citrine/mCherry-9A/GS3-SRK14 were expressed under the control of *pSLR1*.

We analyzed the subcellular localization of TagBFP2/mCherry-9A/GS3-SRK14 in papillae by confocal microscopy (**figure 20**). We obtained results similar to the localization of loop1/loop2-SRK14 constructs, i.e. consistent with a plasma membrane localization, best seen in **figures 20E**, **20F** and **20G**. Again, a diffuse cytoplasmic fluorescence was seen, highlighting the vacuolar lobes (**figure 20B**), and sometimes displaying a reticulated pattern (**figures 20C** and **20D**), reminiscent of an endoplasmic reticulum labeling. Occasionally, intracellular spots were seen with TagBFP2 constructs (**figure 20H**), as seen with TagBFP2-loop1/2 constructs. This might indicate an endosomal localization.

We then analyzed the self-incompatible phenotype of first generation transformants expressing TagBFP2-9A/GS3-SRK14 and mCherry-9A-SRK14 and corresponding to independent insertions of the transgene (**figures 21**, **22** and **23)**. The generation of transgenic plants expressing constructs containing Citrine or mCherry-GS3 failed because of temporarily uncontrolled growth chamber conditions. New transgenic plants were generated for these constructs and are currently under investigation. However, Col-0 plants still categorize as self-compatible. In comparison to protein fusions in which the fluorescent protein was inserted in loop1 or loop2, a higher frequency of first generation independent lines displayed a self-incompatible phenotype (19/45 versus 9/47). Indeed, the insertion of a fluorescent protein inside predicted loops of the tertiary structure of SRK14 is more likely to perturb the structure or function of SRK14 than an N-terminal fusion. We repeated the analysis of the self-incompatible phenotype on second generation transgenic plants (**figure 24**). Line #5 expressing TagBFP2-9A-SRK14 and line #16 expressing TagBFP2-GS3-SRK14 displayed a stronger self-incompatible phenotype than during the first generation analysis, being categorized now as partially self-incompatible whereas they were self-compatible one generation earlier. Line #5 expressing mCherry-9A-SRK14, on the contrary, was self-incompatible during the first generation and displays a self-compatible

phenotype during the second generation. Despite this, we could obtain two lines that display a strong and repeatable self-incompatible phenotype, namely TagBFP2-9A-SRK14 #6 and #16.

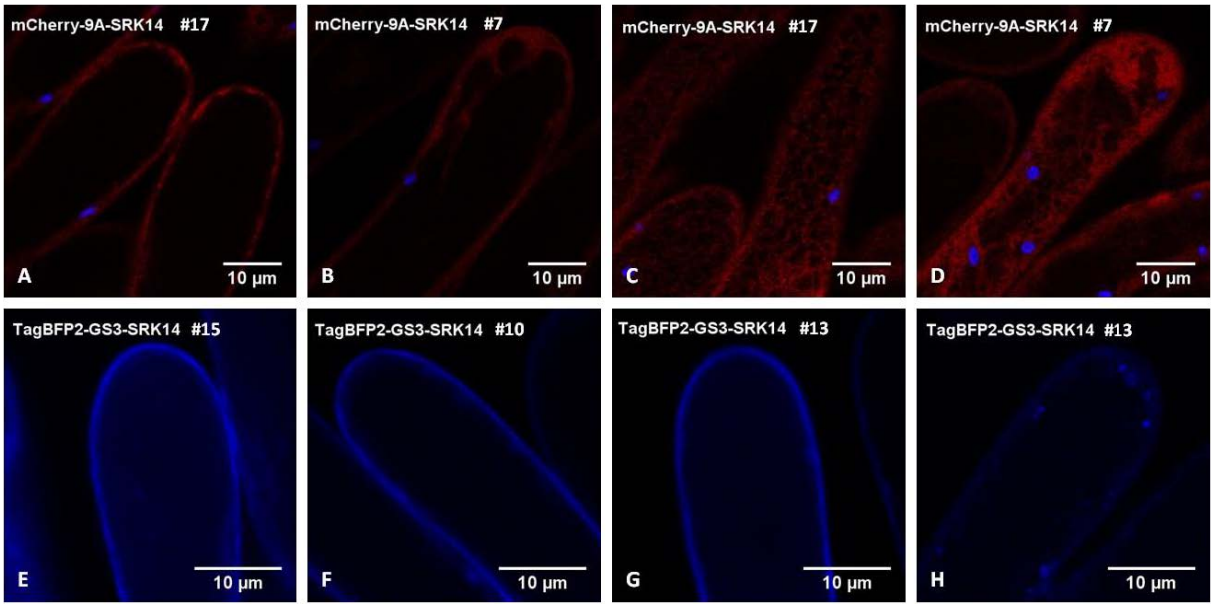

Figure 20: subcellular localization of TagBFP2/mCherry-9A/GS3-SRK14 in papillae. The papillae of first generation transgenic plants corresponding to independent insertions of the transgene were imaged by confocal microscopy. The name of the construct expressed in papillae and number of the plant line are shown in upper left-hand corner. In general, the focal plane was adjusted to go through the middle of the papilla, except for images **C** and **D**, where it passes in the thin cytoplasmic sheath between the vacuole and the plasma membrane.

(A) to **(D)** Analysis of papillae expressing mCherry-9A-SRK14.

(E) to **(F)** Analysis of papillae expressing TagBFP2-GS3-SRK14.

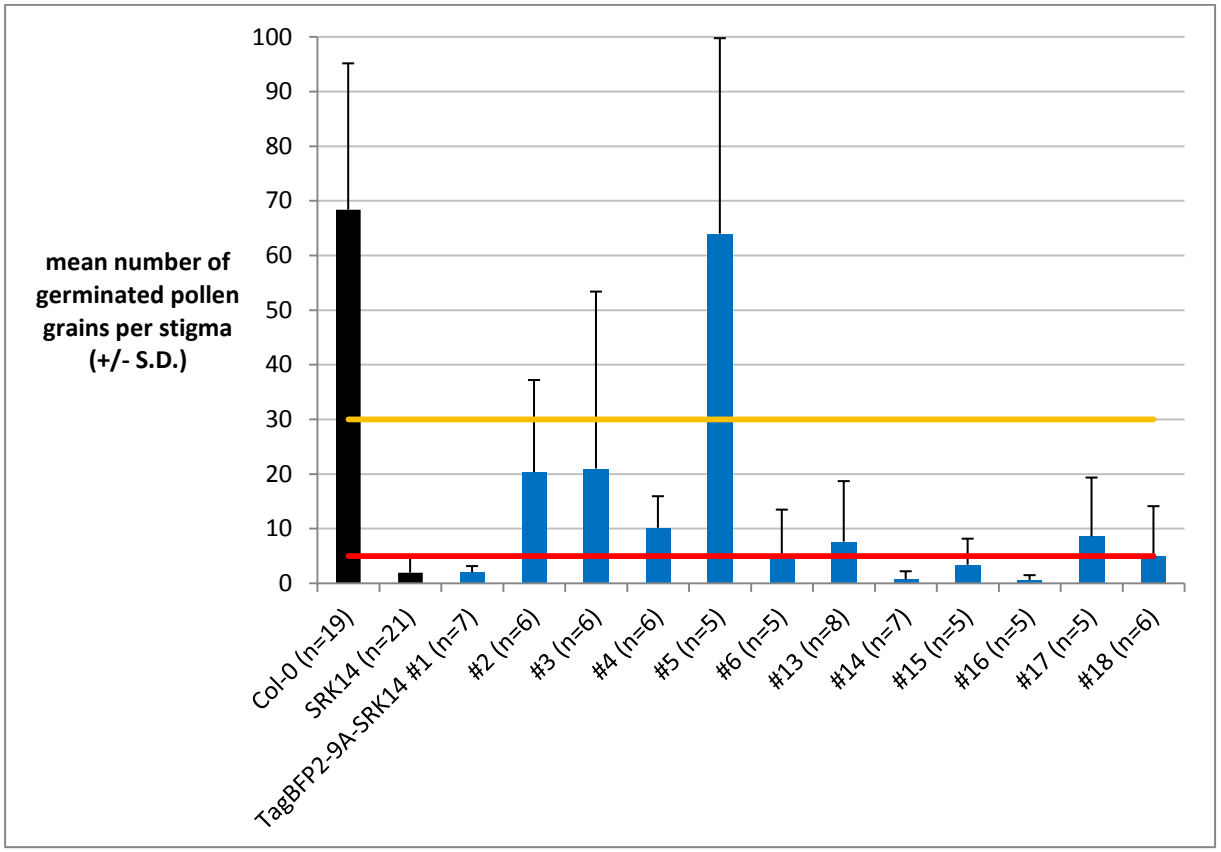

Figure 21: the self-incompatible phenotype of first generation transgenic plants expressing TagBFP2-9A-SRK14. First generation transgenic plants corresponding to independent transgene insertions were pollinated with incompatible pollen and the number of germinated pollen grains found on the stigma were counted after aniline blue staining. Untagged SRK14 is used as a self-incompatible control and wild-type Col-0 as a self-compatible control. The number n of stigmas examined is noted for each genotype. S.D. = standard deviation. The red line marks the upper boundary for a self-incompatible phenotype and the orange line marks the upper boundary for the partial self-incompatible phenotype. Above the orange line plants display a self-compatible phenotype.

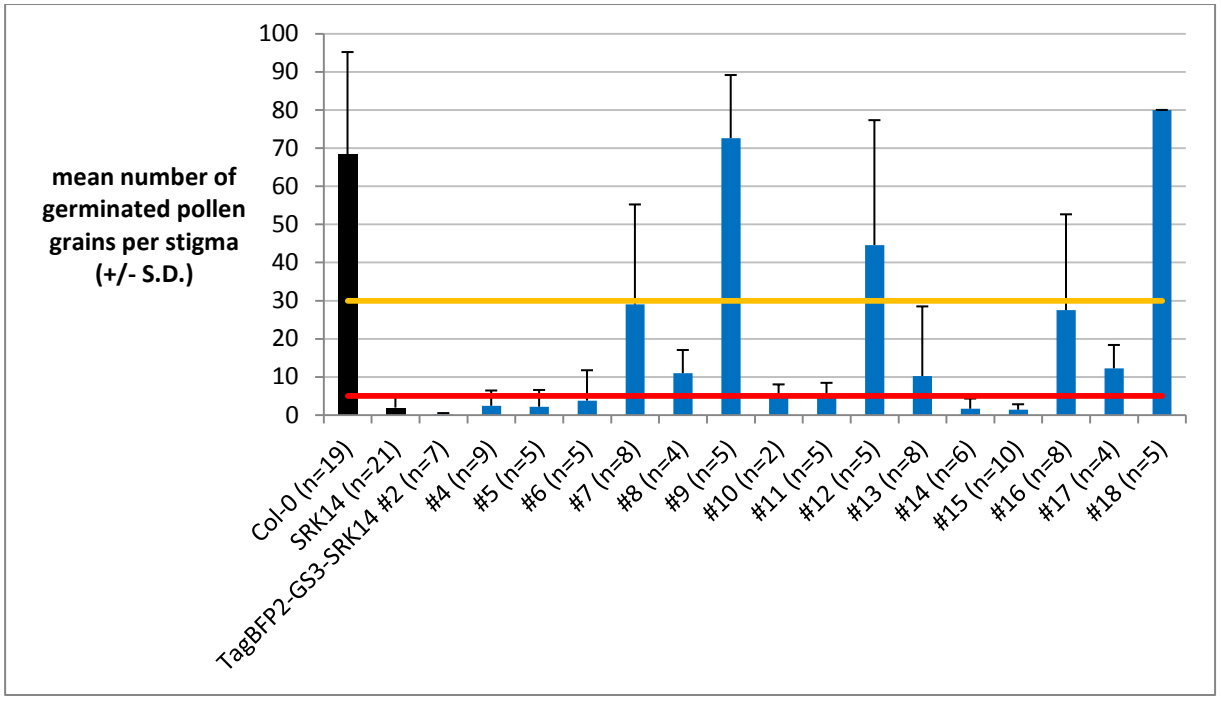

Figure 22: the self-incompatible phenotype of first generation transgenic plants expressing TagBFP2-GS3-SRK14. First generation transgenic plants corresponding to independent transgene insertions were pollinated with incompatible pollen and the number of germinated pollen grains found on the stigma were counted after aniline blue staining. Untagged SRK14 is used as a self-incompatible control and wild-type Col-0 as a self-compatible control. The number n of stigmas examined is noted for each genotype. S.D. = standard deviation. The red line marks the upper boundary for a self-incompatible phenotype and the orange line marks the upper boundary for the partial self-incompatible phenotype. Above the orange line plants display a self-compatible phenotype.

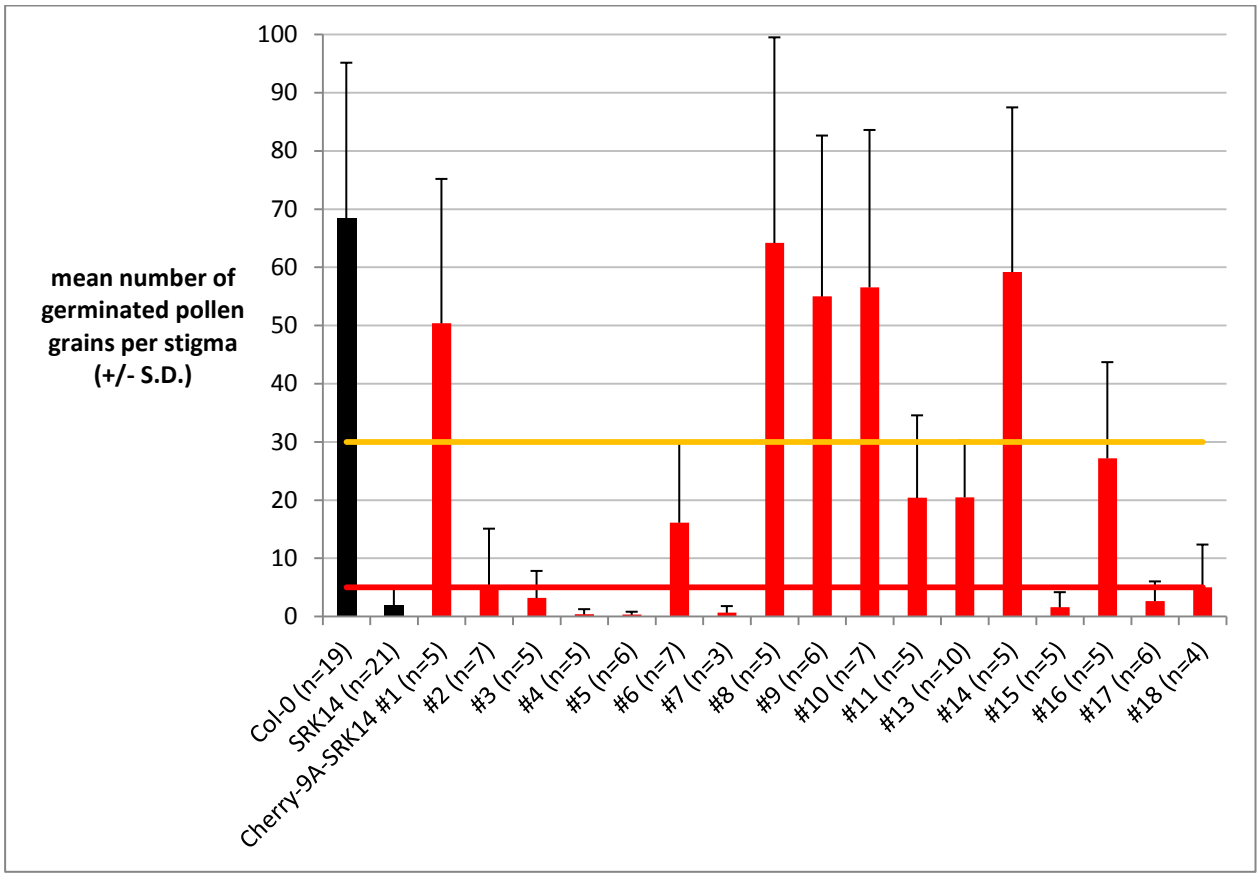

Figure 23: the self-incompatible phenotype of first generation transgenic plants expressing mCherry9A-SRK14. First generation transgenic plants corresponding to independent transgene insertions were pollinated with incompatible pollen and the number of germinated pollen grains found on the stigma were counted after aniline blue staining. Untagged SRK14 is used as a self-incompatible control and wild-type Col-0 as a self-compatible control. The number n of stigmas examined is noted for each genotype. S.D. = standard deviation. The red line marks the upper boundary for a self-incompatible phenotype and the orange line marks the upper boundary for the partial self-incompatible phenotype. Above the orange line plants display a self-compatible phenotype.

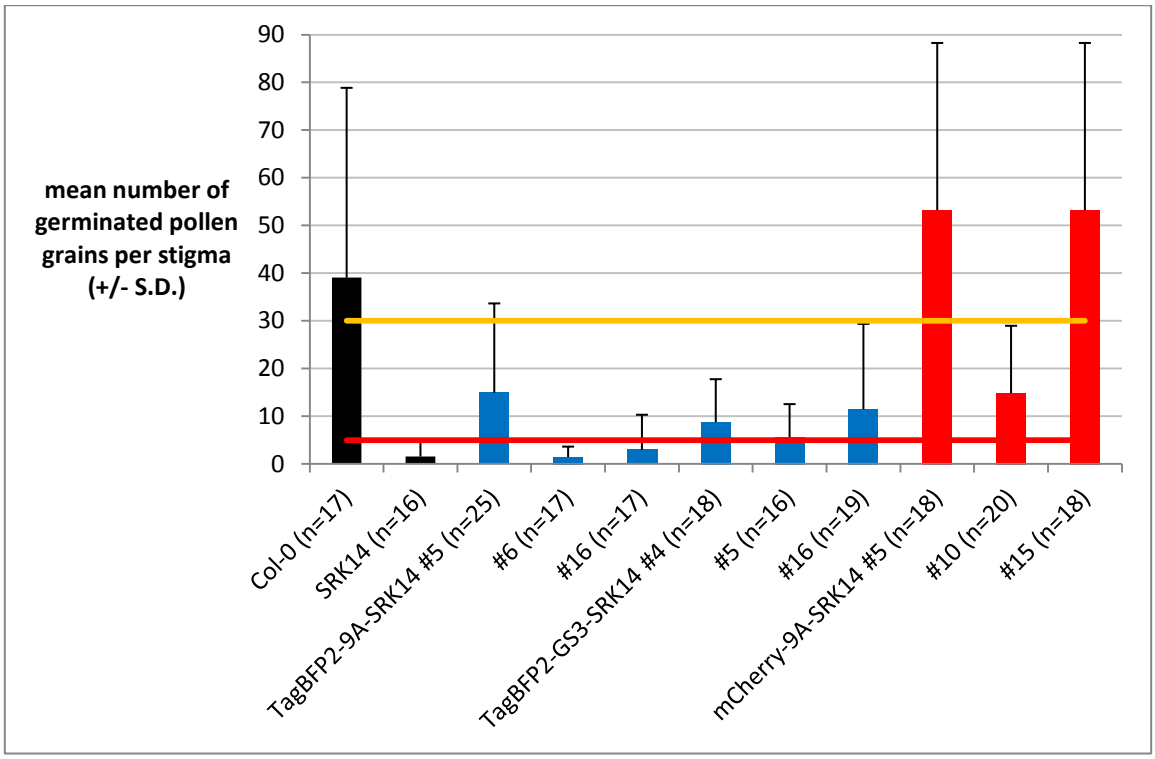

Figure 24: the self-incompatible phenotype of second generation transgenic plants expressing TagBFP2- or mCherry-tagged SRK. Second generation transgenic plants corresponding to independent single transgene insertions were pollinated with incompatible pollen and the number of germinated pollen grains found on the stigma were counted after aniline blue staining. Untagged SRK is used as a self-incompatible control and wild-type Col-0 as a self-compatible control. The number n of stigmas examined is noted for each genotype. S.D. = standard deviation. The red line marks the upper boundary for a self-incompatible phenotype and the orange line marks the upper boundary for the partial self-incompatible phenotype. Above the orange line plants display a self-compatible phenotype.

8. Manuscript in submission

The subcellular localization of *Brassica olerace* SRK3 was investigated using anti-SRK3 antibodies targeted to either the first nine N-terminal amino acids or to part of the C-terminal segment of SRK (Delorme *et al.* 1995, Gaude *et al.* 1993, Ivanov and Gaude 2009). We first undertook the same approach to develop antibodies that bind *Arabidopsis lyrata* SRK14, by using SRK14 peptides, unfortunately without success. We also expressed the extracellular domain of SRK14 in tobacco cells with the aim of developing antibodies against the whole domain, but we could not obtain sufficient amounts of protein to immunize animals. Expression of the extracellular domain of SRK14 in bacteria was not investigated because this domain is highly glycosylated, so antibodies targeted to the unglycosylated protein may not recognize SRK14 *in planta*. We did not generate antibodies against the intracellular domain of SRK14 because the kinase domain is a well-conserved domain among protein kinases, so we were concerned about cross-reactivity of antibodies. The following article describes the strategy that allowed us to characterize the subcellular distribution of SRK14 in *Arabidopsis thaliana*. We also included in the article the most significant results from our investigation of the hypothesized endosomal signaling by SRK.

Loss of function of DYNAMIN-RELATED PROTEIN1A indicates a positive role of endocytosis in S-LOCUS RECEPTOR KINASE signaling

Jonathan Schnabel, Aurélie Chauvet, Thierry Gaude, Isabelle Fobis-Loisy*

Reproduction et Développement des Plantes, UMR5667 CNRS-INRA-ENSL-UCBL, École Normale Supérieure de Lyon, 46 allée d'Italie, 69364 Lyon cedex 07, France

*Corresponding author : isabelle.fobis-loisy@ens-lyon.fr

Abstract

Endocytosis downregulates signaling by removing active receptors from the plasma membrane and leading to their degradation but also brings active receptors in signaling endosomes where sustained and sometimes specific signaling can occur. Given its intriguing predominant localization in endosomal compartments in *Brassica oleracea*, we hypothesized that the female determinant of self-incompatibility S-LOCUS RECEPTOR KINASE (SRK) could be signaling from endosomes. First, we confirmed the subcellular localization of SRK in *Arabidopsis thaliana* papillae by immunolocalization. Then, we investigated the hypothesis of SRK endosomal signaling by perturbing endocytosis in *Arabidopsis thaliana* through a genetic approach. We expressed dominant negative or positive variants of the RAB GTPase ARA7, and used a loss-of-function mutant of DYNAMIN-RELATED PROTEIN (DRP1A). While ARA7 variants partially impaired endocytosis and did not affect self-incompatibility, loss of function of DRP1A led to abolition of self-incompatibility. Our results indicate that endocytosis plays a positive role in self-incompatibility, and suggest that SRK could be signaling from endosomes.

Introduction

Multicellular organisms sense their environment and then elaborate appropriate responses through receptors which translate environmental stresses into cellular signaling. In Angiosperms, plant receptor kinases (PRK) represents the largest family of receptors, with more than 400 members in *Arabidopsis thaliana* around twice as much in rice (Shiu *et al.* 2004). Regulation of PRK signaling is crucial to ensure the success of processes as diverse as reproduction, development and immunity. Intracellular trafficking of active and inactive receptors has long been documented to regulate PRK signaling (Sorkin and von Zastrow 2009). Upon ligand binding at the plasma membrane, many PRK undergo endocytosis and are routed to the lytic compartment for degradation and termination of signaling. In addition, studies in animal models demonstrated that receptor kinases can remain active in endosomes and sustain signaling there. Up to now, endosomal signaling in plants has remained elusive. BRI1, a receptor of plant hormones brassinosteroids, was proposed to signal from endosomes (Geldner *et al.* 2007)

though this hypothesis has been challenged by recent findings (Irani *et al.* 2012, Rubbo *et al.* 2013).

Self-incompatibility is a genetic barrier by which a plant recognizes and rejects its own pollen while allowing pollen from more distantly related plants to germinate. In the *Brassicacea* family, it is controlled by a highly polymorphic locus called the *S*-locus, which contains the male and female determinants of self-incompatibility (Ivanov *et al.* 2010). The female determinant is S-LOCUS RECEPTOR KINASE (SRK), a PRK expressed in the stigma. The male determinant is S-LOCUS CYSTEINE RICH (SCR)/S-LOCUS PROTEIN11 (SP11) and is present at the pollen surface. During pollination, SCR is transported to the plasma membrane of papillae. If SRK and SCR are from the same haplotype of the *S*-locus, their interaction triggers activation of SRK and a downstream signaling cascade leading to self-pollen rejection. If SRK and SCR are from different haplotypes, SRK is not activated and pollen germination can follow, leading to fertilization of the ovules.

To determine the role played by intracellular trafficking of SRK, its subcellular localization was investigated in *Brassica oleracea S3* stigmatic papillae using anti-SRK3 antibodies (Ivanov and Gaude 2009). The results were remarkable, with most of SRK3 being localized to intracellular compartments and to a lesser extent at the plasma membrane. Although ligand stimulation increased SRK3 turnover, this subcellular distribution was constitutive, as it remained unchanged in the presence or absence of ligand. Several PRK and other receptors can be present in endosomal compartments in a constitutive (as seen for the PRK BRASSINOSTEROID INSENSITIVE1 or BRI1, Geldner *et al.* 2007) or ligand-dependent manner (as seen for the PRK FLAGELLIN SENSING2 or FLS2, Robatzek *et al.* 2006 and the receptor-like protein LeEIX2, Bar and Avni 2009). However, the plasma membrane localization is usually predominant, which makes the case of SRK unique. In addition, anti-SRK3 antibodies can activate SRK3 and thus substitute for the ligand. These antibodies bind SRK3 at the plasma membrane and are then endocytosed and colocalize with SRK3 in endosomes, raising the possibility that SRK3 remains active in endosomes. It has also been shown that SRK3 colocalizes in endosomes with THL1 (Ivanov and Gaude 2009), a negative regulator of self-incompatibility (Cabrillac *et al.* 2001). Moreover, SRK3 is internalized and degraded after ligand engagement (Ivanov and Gaude 2009), indicating that endocytosis of SRK3 downregulates signaling by silencing in endosomes through THL1 and by degradation of SRK3. However, given the prevalent localization of SRK3 in endosomal compartments in comparison to the plasma membrane, we hypothesized that SRK3 could be signaling from endosomal compartments before being ultimately silenced.

In this study, we aimed at determining the role of the endosomal localization of SRK in self-incompatibility in *Arabidopsis thaliana* through a genetic approach. Since this species is self-compatible because it expresses non-functional SRK and SCR proteins, we generated transgenic self-incompatible *Arabidopsis*

thaliana that express a functional SRK protein from a related and self-incompatible species called *Arabidopsis lyrata*. We then determined the subcellular localization of SRK by immunolocalization with anti-SRK antibodies and found a localization similar to *Brassica oleracea*. Finally, we aimed at perturbing endocytosis with a loss of function mutant of DYNAMIN-RELATED PROTEIN1A (DRP1A) and dominant-negative/positive mutants of RAB-F2b/ARA7, two proteins involved in endocytic trafficking. Our results indicate that endocytosis plays a positive role in self-incompatibility, suggesting that SRK could signal from endosomal compartments.

Material and methods

Plant material and growth conditions

Wild-type *Arabidopsis thaliana* Col-0 and C24 accessions were obtained from the Notthingham arabidopsis stock centre (university of Notthingham, http://arabidopsis.info/). Transgenic *Arabidopsis thaliana* whose transgene was segregating were sowed on Petri dishes containing Murashige-Skoog medium (Duchefa), 8 g/L Plant Agar (Duchefa), pH 5.7 and appropriate antibiotics depending on the transgene. After sowing seeds, plates were kept for two days at 4 °C to synchronize seed hydration and then place in growth chambers set at 22 °C with 18 h light/6 h dark photoperiod. After 7-10 days, seedlings were transplanted into a soil medium (Argile 10, Favorit) and placed in culture rooms set at 22 °C with 18 h light/6 h dark photoperiod. Transgenic plants homozygous for the transgene and non-transgenic plants were sowed directly in a soil medium.

The *Arabidopsis thaliana* mutant line with a T-DNA insertion in *DRP1A* is SALK_069077 from the SALK mutant collection (http://signal.salk.edu/tabout.html).

Wave line 2Y expressing YFP-ARA7 was described by Geldner *et al.* (2009).

We used *Arabidopsis lyrata ssp petraea* expressing the *S14* haplotype and originating from Czech Republic (seeds generously provided by Dr Pierre Saumitou-Laprade, Université de Lille F59655 Villeneuve d'Ascq cedex, France). *Arabidopsis lyrata* was maintained in culture rooms with the same conditions as *Arabidopsis thaliana* but cultivated in 1L pots containing a mixture of 60 % peat-based compost (Klassman BP substrat 2), 20 % sand and 20 % Pouzzolane (a volcanic rock).

Generation of plasmid vectors

We used Gateway® entry vectors (Life Technologies) and destination vectors described by Karimi *et al.* (2007). The 1569 bp DNA fragment upstream of ATG encoding the *Arabidopsis thaliana* Col-0 pseudo-*SRK* promoter (*pSRK*) was amplified using forward primer 5'-GGGGACAACTTTGTATAGAAAAGTTGTAGGTTCCTTCATTTTAAGGT

G-3' and reverse primer 5'-GGGGACTGCTTTTTTGTACAAACTTGTCTCTCGATCTCTCTCCACCA-3' which contain attB4 and attB1 recombination sites, respectively. The PCR product was subsequently inserted by BP recombination into the pENTR- P4-P1R plasmid. The DNA fragment encoding the *Brassica oleracea SLR1* promoter (*pSLR1*, 1.5 kbp upstream of *SLR1* start codon, Trick *et al.* 1990, Fobis-Loisy *et al.* 2007) was amplified using attB4-containing primer 5'-CCCCACAACTTTGTATAGAAAAGTTGTAGCTCTAGAACTAGTGGATCCC-3' and attB1-containg primer 5'-CCCCACTGCTTTTTTGTACAAACTTGTCTCTCTTCACCACTTTAATTTTC-3'. The PCR product was subsequently inserted by BP recombination into the pENTR-P4-P1R plasmid.

Arabidopsis lyrata SRK14 cDNA was isolated by 5' and 3' Rapid amplification of cDNA ends (RACE) PCR using a primer in the adaptor and a specific primer within the published *S domain* (Charlesworth *et al.* 2003, Castric *et al.* 2008). To obtain a consensus sequence, the complete cDNA was amplified with specific primers on ATG and stop codons (forward primer 5'-GGAAAAATCTGAAATCGATGTGTTAG-3' and reverse primer 5'-GCATCATCGTTAGCCATTGAGAATTG-3'). *SRK14* genomic sequence was amplified with the same primers using genomic DNA from *Arabidopsis lyrata S14* as a template and then inserted by BP recombination into the pDONR-207. We modified the N-terminal protein sequence of *Arabidopsis lyrata* SRK14 to match the sequence of *Brassica oleracea* SRK3 by PCR-mediated mutagenesis with forward primer 5'-TCGATATATGTCAATACTTTGTCTTCTACAGAATC-3' and reverse primer 5'-GATTCTGTAGAAGACAAAGTATTGACATATATCGA-3' and the *SRK14*/pDONR-207 plasmid as a template. The *SLR1* or *pSRK* sequences were then inserted together with either the genomic sequence of *SRK14* or *SRK3:14* by LR recombination in the pK7m24GW,3 or pB7m24GW,3 destination vectors.

RFP-ARA7/pDONR-207 was described by Jaillais *et al.* 2008. We generated the ARA7^{S24N} sequence by PCR-mediated mutagenesis with forward primer 5'-GTTGGTGCTGGAAAAAACAGTCTTGTGTTACGG-3' and reverse primer 5'-CCGTAACACAAGACTGTTTTTTCCAGCACCAAC-3'. We generated the ARA7^{Q69L} sequence with forward primer 5'-GGGATACAGCGGGTCTGGAACGGTACCATAG -3' and reverse primer 5'-CTATGGTACCGTTCCAGACCCGCTGTATCCC-3'. The *SLR1* promoter sequence was then inserted together with the sequence of either *RFP-ARA7*, *RFP-ARA7*^{S24N} or *RFP-ARA7*^{Q69L} by LR recombination in the pH7m24GW,3.

The cDNA encoding *LTI6B* (At3g05890, Nylander *et al.* 2001) was amplified using forward primer 5'-ATGAGTACAGCCACTTTCGTAG-3' and reverse primer 5'-TCAGATGATATAAAGAGCGTAAAG-3' and inserted in

pDONR-207 plasmid. The sequence of *pSLR1*, *LTI6B* and *GFPS65C* were inserted together by LR recombination in the destination vector pB7m34GW,3.

The cDNA encoding *DRP1A* was amplified using forward primer 5'-GGGGACAAGTTTGTACAAAAAAGCAGGCTTAACAATGGAAAATCTGATCTCTCTGG-3' containing the attB1 recombination site and reverse primer 5'-GGGGACCACTTTGTACAAGAAAGCTGGGTGCTTGGACCAAGCAACAGCATG-3' containing the attB2 recombination site. The PCR fragment was inserted by BP recombination in pDONR-Zeo. The sequence of *pSLR1*, *DRP1A* and *GFPS65C* (Fobis-Loisy *et al.* 2007) were inserted together by LR recombination in the destination vector pB7m34GW,3.

PCR-mediated mutagenesis

We followed the protocol described by Fisher and Pei 1997.

Plant transformation

Transgenic plants were generated using *Agrobacterium tumefaciens*-mediated transformation according to Logemann *et al.* (2006), a variation of the flower dip method (Clough and Bent 1998). We used the *Agrobacterium tumefaciens* strain C58PMP90 which is resistant to rifampicin and gentamicin (Hellens *et al.* 2000).

Reverse transcription and real-time quantitative PCR

Thirty stigmas were dissected from buds just before stage 13 (staging according to Smyth *et al.* 1990) and total RNA were extracted with the Arcturus® PicoPure® RNA isolation kit (Life Technologies). 265 ng of total RNA were reverse-transcribed with random hexanucleotides and RevertAid (200 U/µL ; Thermo scientific) and subjected to quantitative real-time PCR with *SRK14* or *ACTIN8* specific primers. Because *Arabidopsis lyrata* and two different accessions of *Arabidopsis thaliana* were compared, we designed primers that amplify a region of the *ACTIN8* cDNA conserved between each species (forward primer 5'-CGACGGACAAGTGATCACGATC-3' and reverse primer 5'-CATAGTTGTACCACCACTGAGCAC-3'). Amplification of *SRK14* was performed with two primers located within the first exon (forward primer 5'-GCCGCCAGACACATCCGGGGC-3' and reverse primer 5'-CAACCCTTCCCACCATCTTGG-3') Absence of contaminating genomic DNA was controlled with primers located within a non coding region close to the *ACTIN8* gene (forward primer 5'-GGCTGTGACAATGCGAAGCCCC-3' and reverse primer 5'-CCCCATTTTGGTATCTAGGG-3'). We performed three biological replicates and two technical replicates. Quantitative analysis of real-time PCR results was performed using the $2^{-\Delta\Delta Ct}$ method (Schmittgen and Livak 2008).

Immunolocalization

The immunolocalization was performed as described (Ivanov and Gaude 2009), with the exception that we used the following blocking solution : 3 % BSA (Sigma) in D-PBS (Gibco). As primary antibodies, we used anti-SRK3-N-ter (mAb85-36-71, Ivanov and Gaude 2009) at 1:500 dilution. As secondary antibodies, we used Alexa 488 donkey anti-mouse (Molecular Probes ref. A21202).

Image acquisition

Pistils were cut at the level of the style and mounted in water for live cell imaging using Zeiss 710 confocal microscope, unless otherwise specified. Immunolocalization were analyzed using a Zeiss 710 confocal microscope. Gain and offset were adjusted for near dark background (outside cells) and maximum signal intensity without saturation.

Drug treatments

Brefeldin A (Sigma) was used at 100 µM in water for 30 min from a 50 mM in ethanol:DMSO 1:1 stock solution. Wortmannin (Sigma) was used at 33 µM in water for 60 min from a 30 mM in DMSO stock solution.

Quantification of internalized LTI6B-GFP

The number of LTI6B-GFP-labeled endosomes was manually determined with the cell counter plug-in of ImageJ and was normalized with the area used to compute the mean gray value. The mean gray value of LTI6B-GFP fluorescence was determined in ImageJ by manually selecting a region of interest that surrounds the cytoplasm of papillae, excluding the plasma membrane. Both quantities were averaged over the number of cells analyzed.

Pollination assays

Arabidopsis thaliana flower buds were emasculated just before anthesis (stage 13, Smyth *et al.* 1990) to avoid pollen contamination and pollinated with pollen from *Arabidopsis lyrata S14*. Pollinated stigmas were harvested 6 h after pollination and placed in FAA (4 % formaldehyde, 5 % acetic acid, 50 % alcohol in water) overnight at 4 °C for fixation. Stigmas were then washed three times with water before being placed in 4 N NaOH for 30 min at room temperature to soften the tissues. Stigmas were then washed three times with water and placed in aniline blue (discolored in 3 % K_3PO_4 in water) overnight at 4 °C to stain pollen grains and tubes. Stigmas were then mounted between plate and coverslip in discolored aniline blue for observation in a Nikon e600 with DAPI filter set. Germinated pollen grains were manually counted and the mean number of germinated pollen grain per stigma was computed for each genotype analyzed. Experiments were replicated at least three times. We distinguish three categories of the degree of

self-incompatibility. Plants are categorized as self-incompatible when they display less than 5 germinated pollen grains per stigma, on the average. Plants are categorized as partially self-incompatible when they display more than 5 but less than 30 germinated pollen grains per stigma. Finally, plants with more than 30 germinated pollen grains per stigma fit in the self-compatible category (Kitashiba *et al.* 2011).

Scanning electron microscopy

Experiments were performed on a Hirox SH-3000 scanning electron microscope. Hydrated samples were mounted on the platform cooled at –10 °C and subsequently cooled at –50 °C for observation.

Results

Molecular cloning of Arabidopsis lyrata SRK14

To obtain the complete cDNA of *SRK14*, we isolated total mRNA from *Arabidopsis lyrata S14* stigmas and performed 5' and 3' RACE PCR with primers annealing within the published sequence encoding the S domain (Charlesworth *et al.* 2003, Castric *et al.* 2008). We generated primers located on the ATG and stop codons to amplify *SRK14* from total genomic DNA and then sequenced the fragment we amplified. Database searches showed that this fragment shares sequence identity with *Arabidopsis lyrata* and *Brassica sp. SRK* alleles, exhibiting the highest sequence identity with *Arabidopsis lyrata SRK13-14* (**figure 1A**). Only 6 nucleotides over the 930 that constitute the highly divergent extracellular domain are different between both sequences. This divergence is compatible with the extent of polymorphism seen in *SRK* sequences that belong to a single *S*-haplotype (Castric *et al.* 2010). Moreover, amino acid sequence alignment with known SRK shows that the fragment we isolated exhibits characteristic features of receptor kinases belonging to the *S*-gene family: a signal sequence, a predicted extracellular S-domain containing 12 conserved cysteine residues, a transmembrane domain, and a kinase domain with conserved residues involved in serine/threonine kinase activity (**supplemental figure 1**). Taken together, our data strongly suggest that the sequence we isolated encodes *SRK14*, which belongs to the B class of *SRK* alleles (Prigoda *et al.* 2005, Castric *et al.* 2008).

Generation of a self-incompatible *Arabidopsis thaliana* by expression of a functional SRK14 from *Arabidopsis lyrata*

SRK belongs to the *S*-gene family which includes members unrelated to the *S*-locus neither to pollen-stigma interaction (Dwyer *et al.* 1994, Pastuglia *et al.* 2002). Thus, a definitive proof that our putative *SRK14* encodes the female self-incompatibility determinant is to complement a natural mutant for self-incompatibility: *Arabidospis thaliana*. Indeed, *Arabidopsis thaliana* is self-fertile due to

the inactivation of *S*-locus recognition genes. However, other components of the *SRK*-mediated signaling cascade are maintained in this species, as self-incompatibility can be restored by the expression of *SRK* and *SCR* isolated from its close self-incompatible relatives *Arabidopsis lyrata* or *Capsella grandiflora* (Nasrallah *et al.* 2002, Boggs *et al.* 2009). Furthermore, it has been observed that different accessions of *Arabidopsis thaliana* exhibited significant differences relative to both the strength of self-incompatibility and the persistence of this response through floral development. For example, self-incompatibility exhibited by C24 transformants is identical to the self-incompatibility observed in naturally self-incompatible *Brassicaceae* species: immature stigmas (corresponding to stage 12 in *Arabidopsis thaliana*, Smyth *et al.* 1990) are self-compatible whereas stigmas from flowers just before opening (stage 13) are fully self-incompatible and this phenotype is maintained throughout stigma development (Nasrallah *et al.* 2002, 2004, Boggs *et al.* 2009). In contrast, stigmas of Col-0 transformants display a transient self-incompatibility meaning that a robust self-incompatibility is observed only during a narrow window of stigma development (stage 13 and early stage 14), with subsequent breakdown of self-incompatibility in mature flower stigmas (stage 14L, Nasrallah *et al.* 2002, Liu *et al.* 2007, Rea *et al.* 2010). Quantitative PCR data indicated that in some *Arabidopsis thaliana* accessions, breakdown of self-incompatibility is due to reduced *SRK* mRNA accumulation, causing suboptimal levels of SRK protein at the latest stages of stigma development (Liu *et al.* 2007, Strickler *et al.* 2013). Furthermore, it was demonstrated that this regulation occurs at the transcriptional level, targeting the promoter of *SRK* (Strickler *et al.* 2013).

To avoid transcriptional regulation affecting *SRK* expression in *Arabidopsis thaliana*, we expressed *SRK14* under the control of the *SLR1* promoter from *Brassica oleracea* (*pSLR1*, Hackett *et al.* 1996, Fobis-loisy *et al.* 2007). *SLR1* gene is a member of the self-incompatibility multigene family of *Brassica sp.* and is expressed in stigma coordinately with *SRK* (Lalonde *et al.* 1989). A DNA fragment of approximately 1500 base pairs upstream of *SLR1* drives in *Arabidospsis thaliana* a high GFP accumulation reaching maximum at flower anthesis (Fobis-Loisy *et al.* 2007). We selected two independent transgenic *Arabidopsis thaliana* Col-0 lines (#10 and #18) and one C24 line (#14) that contain a single transgene insertion. The self-incompatibility phenotype of these lines was characterized (**figure 1B**). Stigmas were emasculated and pollinated at indicated stages of floral development with incompatible pollen from *Arabidopsis lyrata S14*. Col-0 line #10 displayed a strong self-incompatible phenotype from stage 12 to late stage 14 (14L), as did C24 line #14. Indeed, both transgenic lines rejected *Arabidopsis lyrata S14* pollen whereas wild-type Col-0 displayed numerous pollen tubes upon pollination with *Arabidopsis lyrata S14* pollen.

The self-incompatibility phenotype was maintained throughout stigma development and started even earlier than what has been previously reported in a

A

	AlSRK14-Sdom	AlSRK20-Sdom	AlSRK13-Sdom	BoSRK3-SDom	BoSRK6-SDom
AlSRK13-14	99	71	71	66	67
AlSRK14-Sdom		72	73	70	70
AlSRK20-Sdom			72	69	71
AlSRK13-Sdom				73	73
BoSRK3-SDom					89

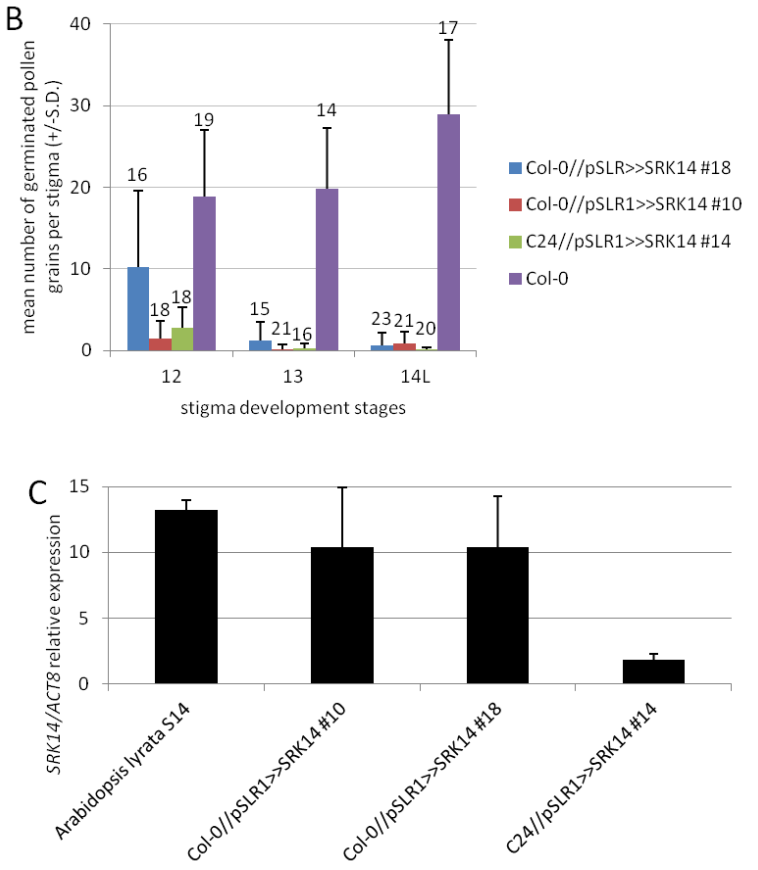

Figure 1: expression of *Arabidopsis lyrata* SRK14 restores self-incompatibility in *Arabidopsis thaliana*.

(A) Nucleotide sequence identity of the S-domain of variants of SRK, AlSRK sequences are from *Arabidopsis lyrata*, BoSRK sequences are from *Brassica oleracea*. AlSRK13-14, Charlesworth *et al.* 2003. AlSRK14, this work. AlSRK13 and AlSRK20, Kusaba *et al.* 2001. BoSRK3, Giranton *et al.* 2000. BoSRK6, Naithani *et al.* 2007.

(B) The self-incompatible phenotype of *Arabidopsis thaliana* expressing *SRK14* from *Arabidopsis lyrata* depends on the developmental stage of flowers. *SRK14* was expressed in *Arabidopsis thaliana* Col-0 or C24 under the control of the *Brassica oleracea SLR1* promoter. Stigmas at development stages 12 or just before anthesis (stage 13), were emasculated and pollinated with pollen from *Arabidopsis lyrata S14*. For stage 14L (14 late), stigmas were emasculated just before anthesis (stage 13) and pollinated 24 hours later. 6 h after pollination, stigmas were harvested, stained with aniline blue and germinated pollen grains with growing pollen tube in the stigma were counted. Numbers on the graph correspond to the number of pollinated stigmas per development stage. S.D. = standard deviation.

(C) Expression level of *SRK14* in stigmas harvested just before stage 13 was quantified by reverse-transcription quantitative PCR. *SRK14* expression measured relative to *ACTIN8 (ACT8)* expression.

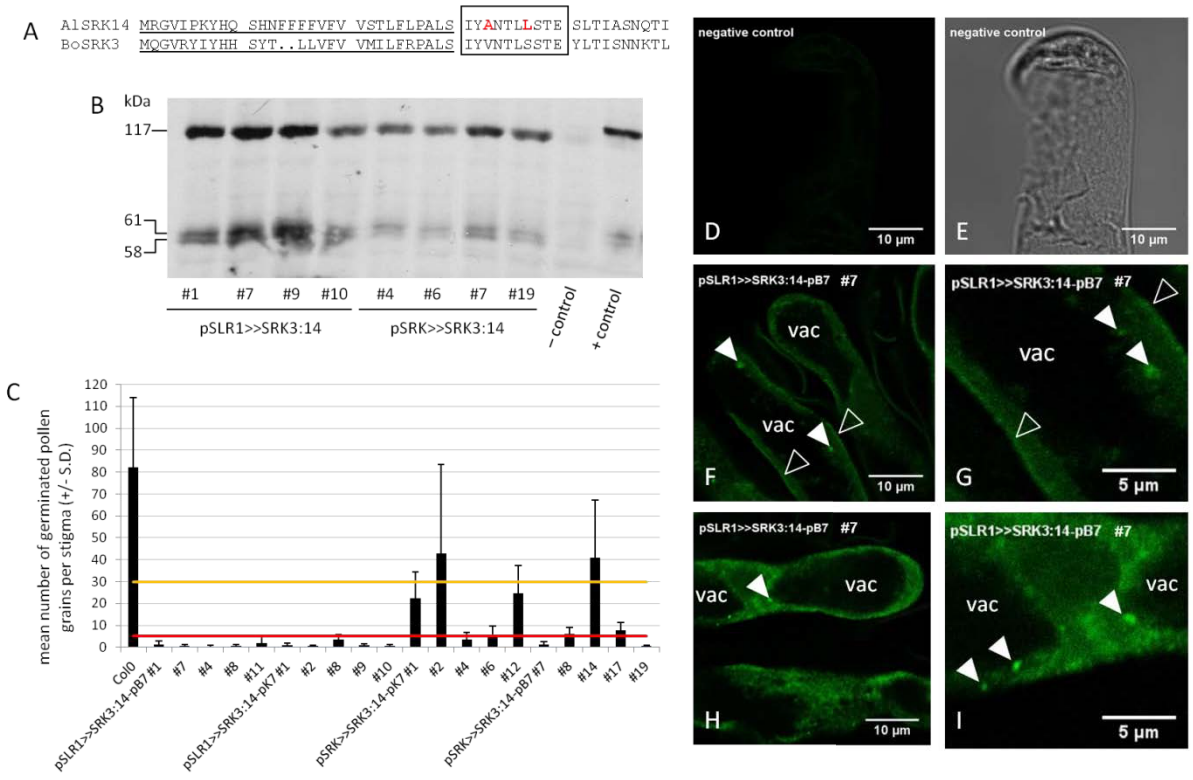

Figure 2: expression of AlSRK3:14 in *Arabidopsis thaliana* papillae.

(A) Alignment of the protein sequence of *Arabidopsis lyrata* SRK14 (AlSRK14) and *Brassica oleracea* SRK3 (BoSRK3) that shows the conservation of the N-terminal peptide (boxed region) where amino acids of AlSRK14 different from BoSRK3 are shown in red. These amino acids were mutated in AlSRK14 sequence to match BoSRK3 and give the protein called SRK3:14.

(B) Immunoblot with anti-SRK3 antibodies on stigma extracts from transgenic *Arabidopsis thaliana* expressing SRK3:14. The construct expressed in stigmas is indicated on the bottom, under the number of the plant line. The negative control (– control) is an *Arabidopsis thaliana* line expressing *pSLR1>>SRK14* and displaying a self-incompatible phenotype. The positive control (+ control) is *Brassica oleracea S3*. The molecular mass of the proteins is indicated on the left (1 kDa = 1000 daltons).

(C) Characterization of the self-incompatible phenotype of plants expressing SRK3:14. Stigmas were pollinated with incompatible pollen from *Arabidopsis lyrata S14*, stained with aniline blue, and the number of germinated pollen grains found on the stigma were counted. *SRK3:14* was expressed either under the control of *Brassica oleracea SLR1* promoter (*pSLR1*) or under the control of Col-0 *pseudo-SRK* promoter (*pSRK*). Promoter and *SRK14* sequences were inserted in a plasmid containing either a kanamycin resistance gene (pK7) or the Basta® resistance gene (pB7), for plant selection. Wild-type Col-0 was used as a self-compatible control. The number n of stigmas examined is noted for each genotype. S.D. = standard deviation. The red line marks the upper boundary for a self-incompatible phenotype and the orange line marks the upper boundary for the partial self-incompatible phenotype. Above the orange line plants display a self-compatible phenotype.

(D) to **(I)** Analysis by confocal microscopy of immunolocalization of SRK3:14 on stigma sections of *Arabidopsis thaliana*. The name of the plant line analyzed is indicated in the upper left part of the image. The *Arabidopsis thaliana* line *pSLR1>>SRK14* #10 was used as a negative control. Putative plasma membrane and endosomes are indicated by open arrowheads and arrowheads, respectively. Vac = vacuole.

C24 background (Nasrallah *et al.* 2002, Liu *et al.* 2007, Rea *et al.* 2010). *Brassica oleracea* SLR1 is abundant in papillae cells and *SLR1* mRNA are detected in early stages of stigma development (Lalonde *et al.* 1989). This might explain why *SRK14* could accumulate above the threshold required for self-incompatibility in stage 12 stigmas in C24 as well as in Col-0. A second transgenic line in Col-0 background was also analyzed. Line #18 displayed a similar self-incompatible phenotype than Col-0 lines #10 and C24 line #14, although it accepted a higher number of incompatible pollen grains at stage 12.

We quantified relative *SRK14* expression in lines #10, #14 and #18 by reverse-transcription followed by real-time quantitative (**figure 1C**). In Col-0 lines #10 and #18, *SRK14* expression was comparable to the expression measured in *Arabidopsis lyrata S14*. In C24 line #14, *SRK14* expression was five to six times lower than in *Arabidopsis lyrata S14* or than in Col-0 lines #10 or #18 but these expression levels were sufficient for the plants to display a self-incompatible phenotype.

Immunolocalization of SRK3:14 in *Arabidopsis thaliana* papillae

The subcellular localization of *Brassica olerace* SRK3 was previously investigated using anti-SRK3 antibodies targeted to either the first nine N-terminal amino acids or to part of the C-terminal segment of SRK (Ivanov and Gaude 2009). We noticed that among the first nine amino acids of SRK14 following the signal peptide, only two were not shared with *Brassica oleracea* SRK3 (**figure 2A**). We mutated these two amino acids by PCR-mediated mutagenesis so that SRK14 first nine amino acids match the homologous sequence of SRK3. This mutated SRK14 protein with the same N-terminus as SRK3 is called SRK3:14. This protein was expressed in Col-0 either under the control of the Col-0 *pseudo-SRK* promoter (*pSRK*), or under the control of *pSLR1*.

To verify that anti-SRK3 antibodies bind to SRK3:14, stigma proteins were extracted from second generation transgenic plants containing independent single transgene insertions, and separated by SDS-PAGE before we performed immunoblots (**figure 2B**). SRK is expressed as a full-length protein and alternative splicing variants comprising the extracellular domain of SRK (eSRK). eSRK has two major glycosylation forms (Ivanov and Gaude 2009). The positive control (**figure 2B**, "+ control" lane) shows that anti-SRK3 antibodies detect the full-length *Brassica oleracea* SRK3 (around 122kDa) and the two major eSRK3 glycosylation forms (around 64 and 61kDa). We used the *Arabidopsis thaliana* line *pSLR1>>SRK14* #10 (see **figure 1**) as a negative control (**figure 2B**, "– control" lane). Since this protein does not contain the SRK3 N-terminal epitope, it should not be recognized by anti-SRK3 antibodies. As expected, no protein was detected in the negative control. We analyzed 5 independent plant lines that express *SRK3:14* under the control of *pSLR1* (*pSLR1>>SRK3:14*) and 5 other independent

lines that express *SRK3:14* under the control of *pSRK* (*pSRK>>SRK3:14*). Anti-SRK3 antibodies bound to SRK3:14 expressed in *Arabidopsis thaliana*, confirming our strategy. Both the full-length protein (around 117kDa) and the two major glycosylation forms of eSRK3:14 (around 61 and 58kDa) were detected.

The self-incompatible phenotype of these plant lines was analyzed (**figure 2C**). Ten out of 10 plants expressing *pSLR1>>SRK3:14* are self-incompatible. Four out of 10 plants expressing *pSRK>>SRK3:14* were self-incompatible, 4/10 were partially self-incompatible and 2/10 were self-compatible.

We then performed immunolocalizations with anti-SRK3 antibodies on stigma sections (**figures 2D** to **2I**). We used the *Arabidopsis thaliana* line *pSLR1>>SRK14* #10 (see **figure 1**) as a negative control—as expected, only a faint background noise was detected (**figures 2D** and **2E**). To investigate the subcellular localization of SRK3:14, we selected the line *pSLR1>>SRK3:14-pB7* #7, which is self-incompatible (**figure 2C**) and expresses a high level of SRK3:14 (**figure 2B**). SRK3:14 was concentrated at the periphery of the papillae along a thin line, consistent with a plasma membrane localization (open arrowheads, **figures 2F** and **2G**). SRK3:14 was also seen in intracellular spots that may correspond to endosomes(arrowheads **figures 2H** and **2I**), as previously seen in *Brassica oleracea* (Ivanov and Gaude 2009).

Overexpression of ARA7^{S24N} or ARA7^{Q69L} partially reduces endocytic trafficking

ARA7 is an *Arabidopsis thaliana* RAB GTPase that controls endosomal trafficking by cycling between a GTP-bound active state and a GDP-bound inactive state (Nielsen *et al.* 2008). A single amino acid substitution can lock ARA7 in one of these nucleotide-bound forms: ARA7^{S24N} is predicted to have impaired GDP exchange and is thus locked in the inactive state, ARA7^{Q69L} putatively has abolished GTPase activity and is thus locked in the active state (Dhonukshe *et al.* 2006). ARA7^{S24N} over-expression was shown to impair endocytosis of FM4-64 and several plasma membrane proteins (Dhonukshe *et al.* 2006, 2008, Irani *et al.* 2012). In addition, ARA7^{S24N} over-expression perturbs trafficking of vacuolar cargos, leading to their secretion (Kotzer *et al.* 2004). ARA7^{Q69L} over-expression induces homotypic fusion of multivesicular bodies, leading to their enlargement (Kotzer *et al.* 2004, Jia *et al.* 2013).

We expressed *pSLR1>>RFP-ARA7^{S24N}* or *pSLR1>>RFP-ARA7^{Q69L}* in a plant line that expresses *pSRK>>SRK14*. This plant line is self-incompatible, since less than 5 pollen grains on average are accepted (data not shown). We used *pSRK* instead of *pSLR1* to drive expression of *SRK14* because of possible co-suppression between *SRK14* and *RFP-ARA7*. We characterized the expression and subcellular localization of RFP-ARA7^{S24N} and RFP-ARA7^{Q69L} in papillae (**figure 3**). The localization of wild-type ARA7 fused to YFP (waveline 2Y, Geldner *et al.* 2009) is also shown. In papillae, YFP-ARA7 displays a dual spotty and diffuse intracellular

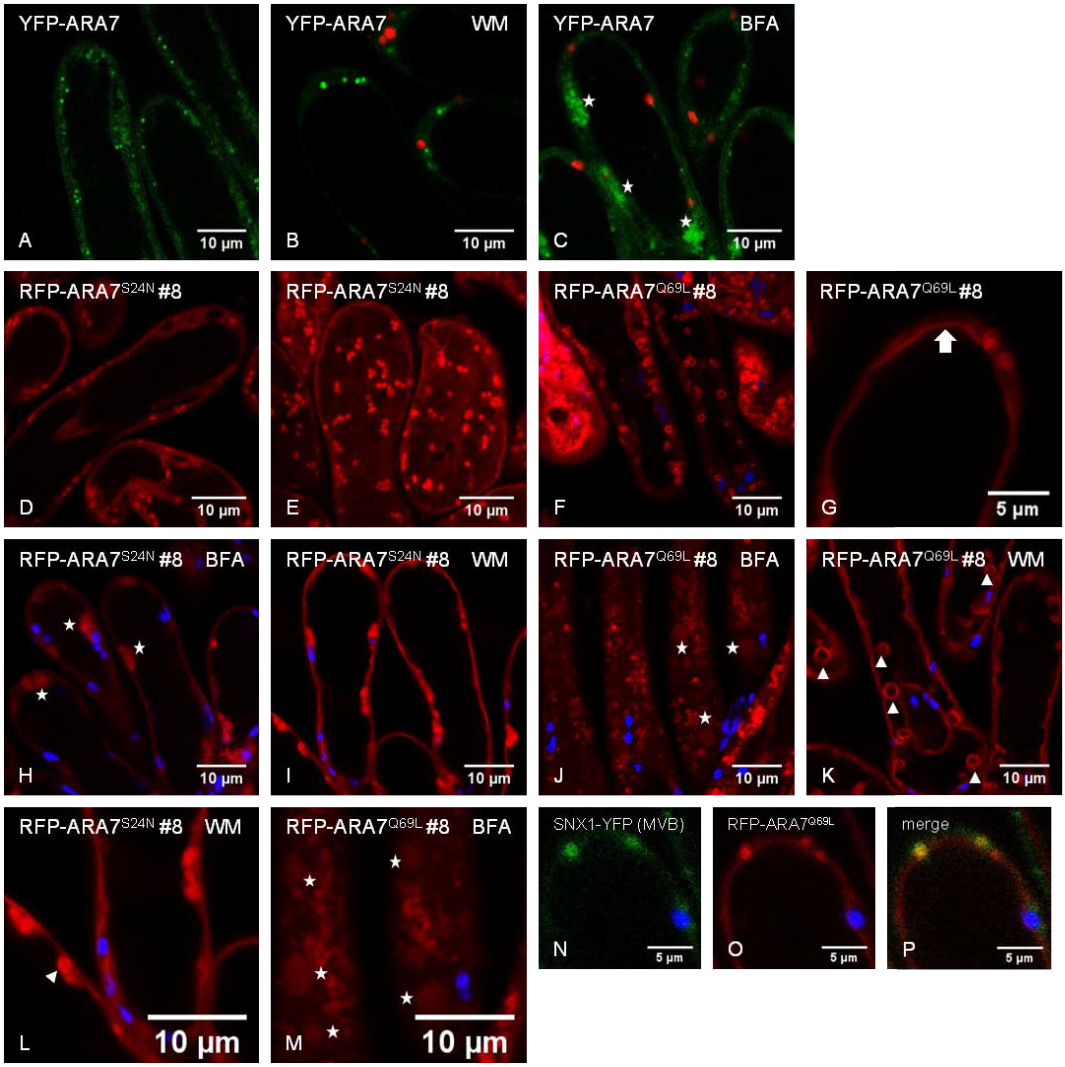

Figure 3: subcellular localization of ARA7 variants in *Arabidopsis thaliana* papillae.

Papillae were analyzed by confocal microscopy. The transgene expressed and the number of the plant lines are indicated on upper left-corner of the images, the eventual drug treatment is indicated in the upper right-hand corner. WM = wortmannin, BFA = brefeldin A. Stars on images **C**, **H**, **J** and **M** indicate BFA bodies, arrowheads on images **K** and **L** indicate swollen intracellular compartments following wortmannin treatment.

(A) to **(C)** YFP-ARA7 (waveline 2Y, Geldner *et al.* 2009) localization and drug sensitivity. YFP fluorescence is shown in green and chloroplasts are shown in red.

(D) to **(G)** Localization of RFP-ARA7^{S24N} and RFP-ARA7^{Q69L}. RFP fluorescent is shown in red and chloroplast fluorescence is shown in blue. The arrow on image **D** indicates the putative tonoplast.

(H) to **(M)** Drug sensitivity of RFP-ARA7^{S24N} and RFP-ARA7^{Q69L}. RFP fluorescent is shown in red and chloroplast fluorescence is shown in blue. **(L)** is a magnification of **(I)** and **(M)** is a magnification of **(J)**.

(N) to **(P)** Co-expression of the multivesicular bodies (MVB) marker SNX1-YFP with RFP-ARA7^{Q69L}. YFP fluorescence is shown in green, RFP fluorescence is shown in red and chloroplasts are shown in blue.

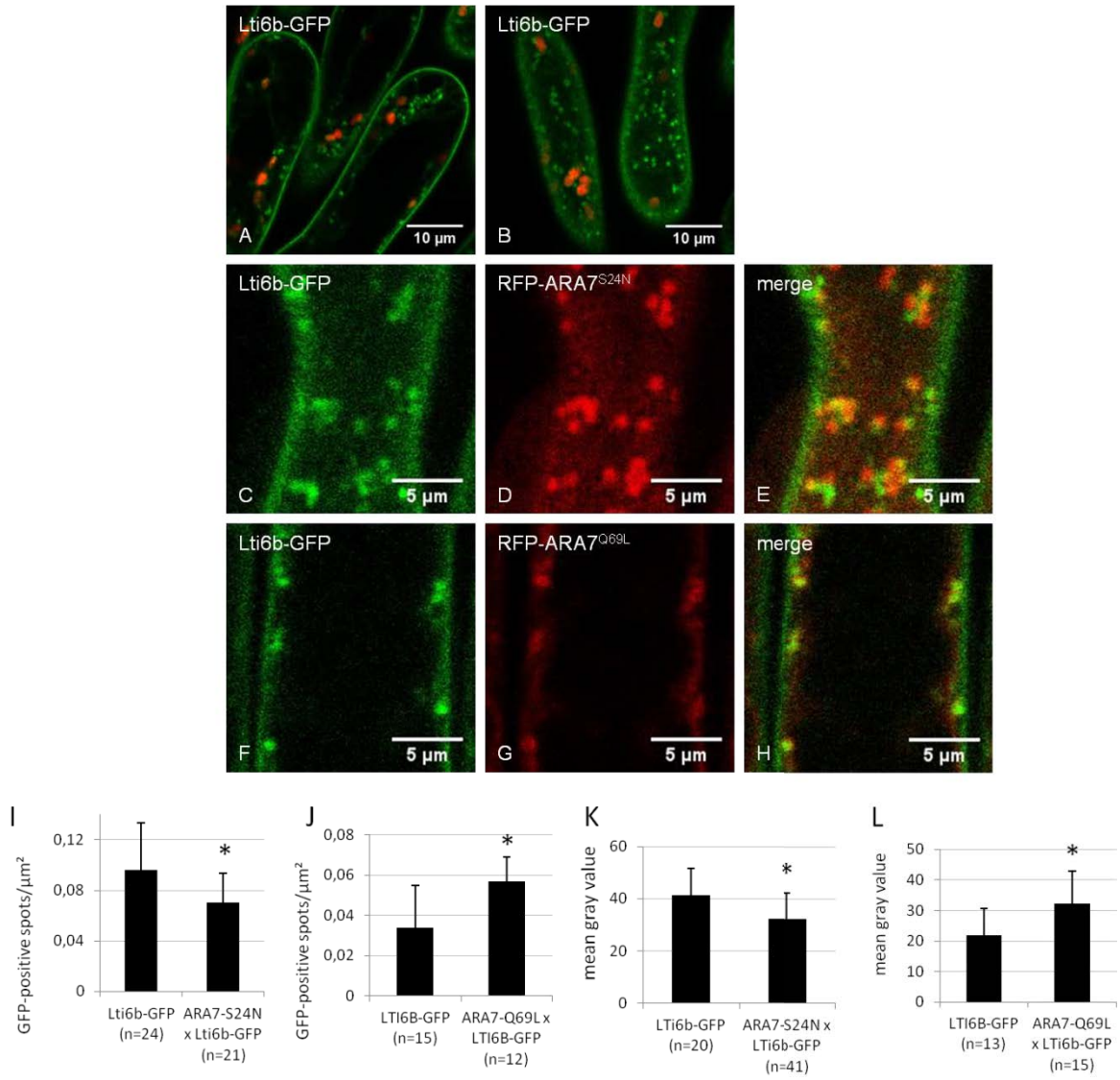

Figure 4: perturbation of endocytosis with RFP-ARA7^{S24N} or RFP-ARA7^{Q69L} over-expression.

(A) to **(H)** Papillae expressing the LTI6B-GFP, RFP-ARA7 variants, or both constructs were analyzed by confocal microscopy. Confocal planes go approximately through the middle of the papillae except on images **B**, **C**, **D** and **E** where the confocal plane goes through the thin cytosolic sheath of the papilla.

(A) and **(B)** Papillae expressing either LTI6B-GFP alone (GFP fluorescence is shown is green and chloroplast fluorescence in red).

(C) to **(E)** Papillae co-expressing LTI6B-GFP and RFP-ARA7^{S24N} (GFP fluorescence is shown in green, RFP fluorescence is shown in red and chloroplast fluorescence is shown in blue).

(F) to **(H)** Papillae co-expressing LTI6B-GFP and RFP-ARA7^{Q69L} (same display settings as RFP-ARA7^{S24N}).

(I) and **(J)** The number of LTI6B-GFP-positive endosomes was quantified manually and averaged for the n cells analyzed using ImageJ. The asterisks indicate statistically significant difference compared to LTI6B-GFP alone (Student's test, p-value < 0.01).

(K) and **(L)** The mean intracellular LTI6B-GFP fluorescence intensity was quantified manually and averaged for the n cells analyzed using ImageJ. The asterisks indicate statistically significant difference compared to LTI6B-GFP alone (Student's test, p-value < 0.01).

distribution, suggesting it partitions between the cytosol and an intracellular compartment (**figure 3A**). This is expected since RAB proteins cycle between inactive and cytosolic and active membrane-bound states and accumulates in multivesicular bodies at steady state (Nielsen *et al.* 2008). We characterized the sensitivity of the YFP-ARA7-positive intracellular compartment to wortmannin and brefeldin A (BFA), two drugs that perturb trafficking (Jaillais *et al.* 2008). Wortmannin is an inhibitor of the PI3-kinase and specifically targets multivesicular bodies, which swell upon wortmannin treatment, leaving other organelles not affected. BFA is an inhibitor of ARF-GEF proteins, and leads to aggregation of endosomal compartments in so called "BFA-bodies", surrounded by Golgi apparatuses. In papillae, YFP-ARA7-labeled compartments were not clearly sensitive to wortmannin, showing a slight enlargement with no vacuolarization visible (**figure 3B**). BFA treatment clearly aggregated most of YFP-ARA7 into BFA-bodies (**figure 3C**, stars).

We selected one single insertion transgenic plant line (#8) homozygous for *RFP-ARA7*^{S24N} and *SRK14* which displays high levels of RFP-ARA7^{S24N} fluorescence. ARA7^{S24N} displayed a cytosolic and punctate distribution (**figures 3D** and **3E**), suggesting that ARA7^{S24N} is recruited to the membrane of an organelle. A similar distribution was reported for ARA7^{S24N} in tobacco epidermal cells and the authors identified the organelles as the Golgi apparatus, based on colocalization with the Golgi marker sialyl-transferase-YFP (Kotzer *et al.* 2004). We then assayed the sensitivity of RFP-ARA7^{S24N}-positive organelles to wortmannin and BFA. The organelles stained by RFP-ARA7^{S24N} were visibly aggregated upon BFA treatment (**figures 3H**, stars), but RFP-ARA7^{S24N} also filled the BFA-bodies, suggesting RFP-ARA7^{S24N} may be located not only at the Golgi, but also at endosomes. Wortmannin treatment perturbed the distribution of RFP-ARA7^{S24N}-positive organelles, which appeared less homogeneously distributed in the cytoplasm (**figure 3I**). Wortmannin also led to enlargement of some RFP-ARA7^{S24N}-positive organelles (**figure 3L**, arrowheads), indicating that part of them are multivesicular bodies. To sum up, the drug sensitivity of RFP-ARA7^{S24N}-stained organelles does not unambiguously point towards a Golgi localization but instead suggests an endosomal localization. A population of these endosomes are multivesicular bodies.

We selected one single insertion transgenic plant line (#8) homozygous for *RFP-ARA7*^{Q69L} and *SRK14* and which displays high levels of RFP-ARA7^{Q69L} fluorescence. RFP-ARA7^{Q69L} was localized at the periphery of circular organelles with a diameter of approximately 1–2μm (**figure 3F**) and was found to delineate the vacuole, likely representing a tonoplast localization (**figure 3G**, arrow). This localization is similar to what was previously reported in tobacco epidermal cells (Kotzer *et al.* 2004) and *Arabidopsis thaliana* protoplasts (Jia *et al* 2013), where RFP-ARA7^{Q69L} induced formation of enlarged multivesicular bodies and also accumulated to the tonoplast. We investigated the sensitivity of RFP-ARA7^{Q69L}-

stained organelles to BFA and wortmannin. BFA seemed to aggregate RFP-ARA7^{Q69L}-positive compartments into weakly fluorescent large structures (**figure 3J** and **3M**, stars) while most of RFP-ARA7^{Q69L}-positive compartments retained their individuality, in line with the fact that multivesicular bodies are weakly sensitive to BFA (Geldner *et al.* 2009, Jaillais *et al.* 2008). Wortmannin treatment dramatically enhanced the diameter of RFP-ARA7^{Q69L}-positive organelles (**figure 3K**, arrowheads), consistent with their identity as being multivesicular bodies. Finally, we co-expressed RFP-ARA7^{Q69L} with SNX1-YFP, a marker of multivesicular bodies (Jaillais 2006, 2008). The two proteins were colocalized to intracellular compartments (**figures 3N** to **3P**). Taken together, these results confirm that ARA7^{Q69L} localization is consistent with published data, i.e. to multivesicular bodies and to the tonoplast.

To verify that ARA7^{S24N} and ARA7^{Q69L} effectively perturbed endocytic trafficking in papillae, we co-expressed these proteins with LTI6B-GFP. LTI6B-GFP labels the plasma membrane and is present in intracellular compartments that are aggregated by BFA (Grebe *et al.* 2003). Moreover, abolition of endocytosis suppressed LTI6B-GFP presence in BFA-bodies and blockage of protein synthesis with cycloheximide did not suppress LTI6B-GFP presence in BFA-bodies (Dhonukshe *et al.* 2007). Altogether, these data indicate that LTI6B-GFP-positive organelles are endosomes. In papillae, LTI6B-GFP was found at the plasma membrane and in putative endosomes (**figures 4A** and **4B**). When RFP-ARA7^{S24N} was co-expressed with LTI6B-GFP, they labeled spatially close but distinct populations of intracellular compartments (**figures 4C** to **4E**). We also noticed that the number of LTI6B-GFP-positive intracellular spots decreased, which was confirmed by quantitative analysis: RFP-ARA7^{S24N}-expressing cells contained 27 % less LTI6B-GFP-positive endosomes than cells not expressing RFP-ARA7^{S24N} (**figure 4I**). However, a decrease in the number of endosomes does not necessarily mean a decrease in the amount of endocytosed material, since the endosomes could contain more material. We therefore quantified the intracellular LTI6B-GFP fluorescence intensity in plants expressing either LTI6B-GFP alone or co-expressing LTI6B-GFP with RFP-ARA7^{S24N} (**figure 4K**). The results indicate that LTI6B-GFP accumulates 22 % less inside cells expressing RFP-ARA7^{S24N}, compared to cells that do not express RFP-ARA7^{S24N}. RFP-ARA7^{Q69L} was colocalized with LTI6B-GFP (**figures 4F** to **4H**). Plants expressing RFP-ARA7^{Q69L} displayed a 69 % increase in the number of LTI6B-GFP-positive endosomes (**figure 4J**) and a 47 % increase in the amount of internalized LTI6B-GFP (**figure 4L**). The data indicate that ARA7 mutants partially perturb endocytosis and have opposite effects: ARA7^{S24N} reduces endocytosis while ARA7^{Q69L} increases endocytosis.

We then analyzed the self-incompatible phenotype of the plants co-expressing either ARA7^{S24N} or ARA7^{Q69L} with SRK14. None of the plants expressing ARA7^{S24N} or ARA7^{Q69L} displayed an altered self-incompatible response (data not shown), thereby suggesting that a partial perturbation of endocytosis does not

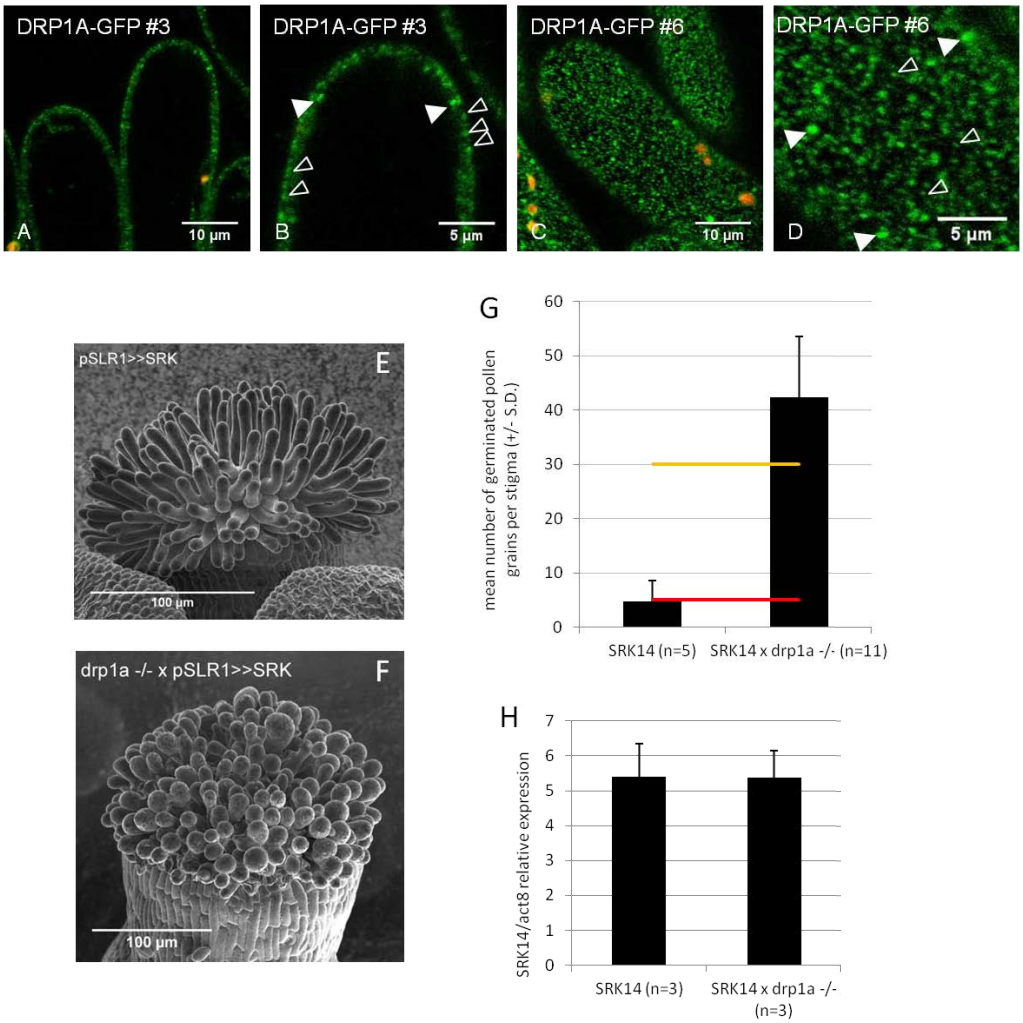

Figure 5: perturbation of endocytosis and self-incompatibility with a *DRP1A* null mutant.

(A) to **(D)** Subcellular localization of DRP1A-GFP in papillae. White arrowheads indicate putative *trans*-Golgi networks, open arrowheads indicate putative endocytic sites.

(E) and **(F)** Scanning electron microscopy of stage 13 stigmas expressing SRK14 in either wild-type (**E**) or loss-of-function mutant (**F**) *DRP1A* background.

(G) Characterization of the self-incompatible phenotype of plants expressing SRK14 in wild-type or loss-of-function mutant *DRP1A* background. Stigmas were pollinated with incompatible pollen from *Arabidopsis lyrata S14* and the number of germinated pollen grains found on the stigma were counted after aniline blue staining. The number n of stigmas examined is noted for each genotype. S.D. = standard deviation. The red line marks the upper boundary for a self-incompatible phenotype and the orange line marks the upper boundary for the partial self-incompatible phenotype. Above the orange line plants display a self-compatible phenotype.

(H) Expression levels of *SRK14* were quantified by reverse-transcription quantitative PCR in stigmas of plants either wild-type or null mutant for *DRP1A*. *SRK14* expression is represented relative to *ACTIN8* (*ACT8*) expression.

affect self-incompatibility, at least not with the amplitude that is realized with RFP-ARA7^{S24N} or RFP-ARA7^{Q69L}.

DRP1A loss of function abolishes self-incompatibility

DRP1A is a GTPase involved in clathrin-mediated endocytosis (Fujimoto and Ueda 2012). It is thought to detach clathrin-coated vesicles from the plasma membrane by conformational changes following GTP hydrolysis. Loss of function of *DRP1A* impairs endocytosis, as seen by a dramatic reduction of FM4-64 endocytosis (Collings *et al.* 2008). Moreover, DRP1A is highly expressed in papillae and loss of function of *DRP1A* leads to defective elongation of papillae and accumulation of excess plasma membrane that forms many indentations, consistent with defective endocytosis (Kang *et al.* 2003).

We selected transgenic plants that express *pSLR1>>DRP1A-GFP* and analyzed the expression and localization of DRP1A-GFP in papillae by confocal microscopy (**figures 5A** to **5D**). DRP1A-GFP was localized to small punctate structures at the periphery of the cell (**figures 5B** and **5D**, open arrowheads) and to larger intracellular spots (**figures 5B** and **5D**, white arrowheads) in all first generation transgenic plants analyzed. This distribution is similar to what was previously published : punctate structures at the cell cortex that colocalize with clathrin light chain and may represent endocytic sites (Fujimoto *et al.* 2010, Konopka and Bednarek 2008) and intracellular compartments that colocalize with a *trans*-Golgi network marker (Sawa *et al.* 2005). We thus hypothesize that the small punctate structures seen at the periphery represent endocytic sites, and that the larger intracellular structures are *trans*-Golgi networks.

We crossed the Col-0 line *pSLR1>>SRK14* #10 with a T-DNA insertion mutant knockout for *DRP1A*. This mutant has a T-DNA insertion in intron 6 of *DRP1A*. We selected *drp1a*$^{-/-}$/*SRK*$^{+}$ plants that contained the *SRK14* transgene (based on amplification of SRK from genomic DNA, data not shown) and homozygous for *drp1a* based on the defective elongation phenotype of papillae, as reported by Kang *et al.* (2003) (**figures 5E** and **5F**). When pollinated with incompatible pollen from *Arabidopsis lyrata*, *drp1a*$^{-/-}$/*SRK*$^{+}$ plants were compatible (**figure 5G**), indicating that DRP1A function is required for self-incompatibility. To verify that the self-compatible phenotype of *drp1a*$^{-/-}$ plants was not the result of downregulation of SRK14 expression, we quantified *SRK14* mRNA levels by reverse transcription followed by quantitative real-time PCR (**figure 5H**). *SRK14* mRNA levels are identical in *drp1a*$^{-/-}$/*SRK*$^{+}$ and *DRP1A* wild-type plants, indicating that *drp1a*$^{-/-}$/*SRK*$^{+}$ plants express sufficient quantities of SRK14 to mount a self-incompatible response.

Discussion

Endocytic trafficking plays both positive and negative roles in the regulation of receptor kinase signaling (Sorkin and von Zastrow 2009). Silencing of activated receptors is realized by endocytosis and degradation of receptors in the lytic compartment. During intracellular trafficking through endosomal compartments, the ligand-receptor interaction can be maintained, enabling sustained and sometimes specific signaling from endosomal compartments. The subcellular localization of SRK3 in *Brassica oleracea* revealed that most of SRK3 is localized to endosomes, where it is routed after activation, raising the possibility that SRK could be signaling from endosomal compartments (Ivanov and Gaude 2009). In this work, we reintroduced self-incompatibility in *Arabidopsis thaliana* by expression of the functional *SRK14* from *Arabidopsis lyrata* and then studied the relationship between SRK14 endocytic trafficking and self-incompatibility.

When self-incompatibility is reintroduced in *Arabidopsis thaliana*, the expression of self-incompatibility depends on the ecotype (Nasrallah *et al.* 2004). Indeed, only C24 was found to display a strong and robust self-incompatibility that peaked at stage 13 of flower development and last until late stage 14, as in *Arabidopsis lyrata*. Col-0 displayed a strong self-incompatible phenotype at stage 13 but a subsequent breakdown of the phenotype (Nasrallah *et al.* 2002, 2004). This breakdown was linked to polymorphism in at least three modifier loci: *PUB8* (Liu *et al.* 2007), *NRDP1A* (Strickler *et al.* 2013) and an unkown gene (Boggs *et al.* 2009). It was shown that *PUB8* and *NRDP1A* affect *SRK* expression levels (Liu *et al.* 2007, Strickler *et al.* 2013). In the present article, we demonstrate that the expression of self-incompatibility in Col-0 can be as robust as in *Arabidopsis lyrata*, contrary to what was previously reported. This may be due to the use of the strong *SLR1* promoter to control the expression of SRK instead of *Arabidopsis lyrata SRK14* endogenous promoter. The *SLR1* promoter could allow SRK14 expression to be above the threshold required for self-incompatibility throughout stigma development.

Performing immunolocalization on papillae expressing SRK3:14, we found SRK3:14 in intracellular compartments that could represent endosomes but we also found a significant amount of SRK3:14 at the plasma membrane. In *Brassica oleracea*, SRK3 was almost uniquely found in endosomes, with few patches at the plasma membrane (Ivanov and Gaude 2009). This contrasts with immunolocalization of SRK3:14 in *Arabidopsis thaliana*, where significant amounts of SRK apparently localize to the plasma membrane. It was proposed that the constitutive and predominant localization of *Brassica oleracea* SRK3 in endosomes served the purpose of regulating the amount of SRK that is available for ligand binding at the plasma membrane (Ivanov and Gaude 2009), which is a paradigm for mammalian RTK function (Sorkin and von Zastrow 2009). Indeed, a single papilla can distinguish between a compatible pollen grain and an incompatible pollen grain at the same time and mount a self-incompatible response against the

latter while allowing the former to germinate (Sarker *et al.* 1988). Since SRK can *trans*-phosphorylate (Giranton *et al.* 2000), this dual competence of papillae implies that some mechanisms must prevent SRK signaling from spreading along the plasma membrane when it is activated. Such a mechanism could be a high endocytosis/recycling ratio that concentrates SRK in endosomes and leaves only a few amounts at the plasma membrane (Ivanov and Gaude 2009). However, it is currently unknown if this dual competence of papillae is conserved in *Arabidopsis thaliana*. Since *Arabidopsis thaliana* is naturally self-compatible, compatible and incompatible pollen grains do not compete at the stigma surface. As a result, evolutionary pressure to maintain this dual competence may be released, allowing SRK to accumulate at the plasma membrane in *Arabidopsis thaliana*.

We aimed at perturbing endocytosis by over-expression of the dominant negative mutant ARA7^{S24N}, a strategy that was previously reported to reduce endocytosis in *Arabidopsis thaliana* roots (Dhonukshe *et al.* 2006, 2008, Irani *et al.* 2012). We also investigated the effect of the dominant positive mutant ARA7^{Q69L}. We first characterized the subcellular localization of wild-type ARA7 and the two ARA7 mutants. Wild-type ARA7 was reported to be localized at the multivesicular bodies (Haas *et al.* 2007, Kotzer *et al.* 2004, Lee *et al.* 2004). In papillae, wild-type ARA7-labeled compartments were poorly sensitive to wortmannin and highly sensitive to BFA. However, these results were unexpected because ARA7-labeled multivesicular bodies are strongly sensitive to wortmannin A and weakly to BFA in root cells (Geldner *et al.* 2009, Jaillais *et al.* 2008). Instead, our results are more consistent with YFP-ARA7 being localized to a population of endosomes that is earlier on the endocytic pathway than multivesicular bodies—perhaps *trans*-Golgi networks which are not sensitive to wortmannin and moderately sensitive to BFA. When comparing different cell types, it is not uncommon to see differences of trafficking that translate in differences in the compartments that are labeled by a particular protein at steady state (Robinson *et al.* 2008, Jaillais *et al.* 2008). *Trans*-Golgi networks are believed to progressively mature to form multivesicular bodies (Scheuring *et al.* 2011). It is possible that the unique properties of papillae regarding trafficking lead to accumulation of YFP-ARA7 in a population of endosomes that is between *trans*-Golgi networks and multivesicular bodies, which would explain the atypical drug sensitivity of ARA7-labeled compartments seen in papillae.

We confirmed that targeting ARA7 function indeed perturbed endocytosis, as monitored by quantitative imaging of LTI6B-GFP. Our data indicate that RFP-ARA7^{S24N} and RFP-ARA7^{Q69L} partially perturb endocytosis in papillae and have opposite effects: RFP-ARA7^{S24N} decreases endocytosis while RFP-ARA7^{Q69L} increases it, in line with the fact that these proteins are dominant-negative and dominant positive mutants of ARA7, respectively. However, over-expression of ARA7 mutants in papillae does not perturb self-incompatibility. We also aimed at perturbing endocytosis with a loss-of-function mutant of *DRP1A*. Plants

expressing SRK14 and homozygotes for *DRP1A* loss-of-function were self-compatible, contrary to plants expressing SRK14 in a *DRP1A* wild-type background. This confirms the link between endocytosis and self-incompatibility. The partial perturbation of endocytosis realized with ARA7 mutants may leave SRK signaling unaffected. Our next goal is to determine the subcellular localization of SRK3:14 in a *DRP1A* loss-of-function background, in which we expect to see a reduction in the amount of internalized SRK3:14.

Taken together, our data indicate that endosomal signaling of SRK might happen and raises important questions. In what type of endosomes is SRK signaling? Is SRK endosomal signaling a sustained process initiated at the plasma membrane, or are there specific signaling proteins recruited to endosomes? Transgenic self-incompatible *Arabidopsis thaliana* lines are powerful tools to study pollen-stigma interactions through genetic approaches and allowed to uncover the specificities of SRK signaling in *Arabidopsis* (Kitashiba *et al.* 2011, Yamamoto and Nasrallah 2013). We demonstrate here that they are also amenable to investigation of the subcellular events that govern self-incompatibility, and believe that they will help to answer the questions raised by the unique properties of SRK signaling.

Acknowledgements

We thank Frédérique Rozier for helpful discussions about immunolocalization. We thank Christophe Chamot and Claire Lionnet from the Unité Mixte de Services (UMS3444/US8) and Plateau technique d'imagerie et de microscopie (PLATIM) for technical assistance in confocal microscopy.

References

Bar, M., and Avni, A. (2009). EHD2 inhibits ligand-induced endocytosis and signaling of the leucine-rich repeat receptor-like protein LeEix2. The Plant Journal *59*, 600–611.

Boggs, N.A., Nasrallah, J.B., and Nasrallah, M.E. (2009). Independent S-Locus Mutations Caused Self-Fertility in Arabidopsis thaliana. PLoS Genet *5*, e1000426.

Cabrillac, D., Cock, J.M., Dumas, C., and Gaude, T. (2001). The S-locus receptor kinase is inhibited by thioredoxins and activated by pollen coat proteins. Nature *410*, 220–223.

Castric, V., Bechsgaard, J., Schierup, M.H., and Vekemans, X. (2008). Repeated adaptive introgression at a gene under multiallelic balancing selection. PLoS Genet. *4*, e1000168.

Castric, V., Bechsgaard, J.S., Grenier, S., Noureddine, R., Schierup, M.H., and Vekemans, X. (2010). Molecular evolution within and between self-incompatibility specificities. Mol. Biol. Evol. *27*, 11–20.

Charlesworth, D., Mable, B.K., Schierup, M.H., Bartolomé, C., and Awadalla, P. (2003). Diversity and linkage of genes in the self-incompatibility gene family in Arabidopsis lyrata. Genetics *164*, 1519–1535.

Clough, S.J., and Bent, A.F. (1998). Floral dip: a simplified method forAgrobacterium-mediated transformation ofArabidopsis thaliana. The Plant Journal *16*, 735–743.

Collings, D.A., Gebbie, L.K., Howles, P.A., Hurley, U.A., Birch, R.J., Cork, A.H., Hocart, C.H., Arioli, T., and Williamson, R.E. (2008). Arabidopsis dynamin-like protein DRP1A: a null mutant with widespread defects in endocytosis, cellulose synthesis, cytokinesis, and cell expansion. J. Exp. Bot. *59*, 361–376.

Delorme, V., Giranton, J.-L., Hatzfeld, Y., Friry, A., Heizmann, P., Ariza, M.J., Dumas, C., Gaude, T., and Cock, J.M. (1995). Characterization of the S locus genes, SLG and SRK, of the Brassica S3 haplotype: identification of a membrane-localized protein encoded by the S locus receptor kinase gene. The Plant Journal *7*, 429–440.

Dhonukshe, P., Baluska, F., Schlicht, M., Hlavacka, A., Samaj, J., Friml, J., and Gadella, T.W.J., Jr (2006). Endocytosis of cell surface material mediates cell plate formation during plant cytokinesis. Dev. Cell *10*, 137–150.

Dhonukshe, P., Aniento, F., Hwang, I., Robinson, D.G., Mravec, J., Stierhof, Y.-D., and Friml, J. (2007). Clathrin-Mediated Constitutive Endocytosis of PIN Auxin Efflux Carriers in Arabidopsis. Current Biology *17*, 520–527.

Dhonukshe, P., Tanaka, H., Goh, T., Ebine, K., Mähönen, A.P., Prasad, K., Blilou, I., Geldner, N., Xu, J., Uemura, T., et al. (2008). Generation of cell polarity in plants links endocytosis, auxin distribution and cell fate decisions. Nature *456*, 962–966.

Dwyer, K.G., Kandasamy, M.K., Mahosky, D.I., Acciai, J., Kudish, B.I., Miller, J.E., Nasrallah, M.E., and Nasrallah, J.B. (1994). A superfamily of S locus-related sequences in Arabidopsis: diverse structures and expression patterns. Plant Cell *6*, 1829–1843.

Fisher, C.L., and Pei, G.K. (1997). Modification of a PCR-based site-directed mutagenesis method. BioTechniques *23*, 570–571, 574.

Fobis-Loisy, I., Chambrier, P., and Gaude, T. (2007). Genetic transformation of Arabidopsis lyrata: specific expression of the green fluorescent protein (GFP) in pistil tissues. Plant Cell Rep *26*, 745–753.

Fujimoto, M., and Ueda, T. (2012). Conserved and Plant-Unique Mechanisms Regulating Plant Post-Golgi Traffic. Frontiers in Plant Science *3*.

Fujimoto, M., Arimura, S., Ueda, T., Takanashi, H., Hayashi, Y., Nakano, A., and Tsutsumi, N. (2010). Arabidopsis dynamin-related proteins DRP2B and DRP1A participate together in clathrin-coated vesicle formation during endocytosis. PNAS *107*, 6094–6099.

Geldner, N., Hyman, D.L., Wang, X., Schumacher, K., and Chory, J. (2007). Endosomal signaling of plant steroid receptor kinase BRI1. Genes Dev. *21*, 1598–1602.

Geldner, N., Dénervaud-Tendon, V., Hyman, D.L., Mayer, U., Stierhof, Y.-D., and Chory, J. (2009). Rapid, combinatorial analysis of membrane compartments in intact plants with a multicolor marker set. The Plant Journal *59*, 169–178.

Giranton, J.-L., Dumas, C., Cock, J.M., and Gaude, T. (2000). The integral membrane S-locus receptor kinase of Brassica has serine/threonine kinase

activity in a membranous environment and spontaneously forms oligomers in planta. Proceedings of the National Academy of Sciences *97*, 3759–3764.

Grebe, M., Xu, J., Möbius, W., Ueda, T., Nakano, A., Geuze, H.J., Rook, M.B., and Scheres, B. (2003). Arabidopsis Sterol Endocytosis Involves Actin-Mediated Trafficking via ARA6-Positive Early Endosomes. Current Biology *13*, 1378–1387.

Haas, T.J., Sliwinski, M.K., Martínez, D.E., Preuss, M., Ebine, K., Ueda, T., Nielsen, E., Odorizzi, G., and Otegui, M.S. (2007). The Arabidopsis AAA ATPase SKD1 Is Involved in Multivesicular Endosome Function and Interacts with Its Positive Regulator LYST-INTERACTING PROTEIN5. Plant Cell *19*, 1295–1312.

Hackett, R.M., Cadwallader, G., and Franklin, F.C. (1996). Functional analysis of a Brassica oleracea SLR1 gene promoter. Plant Physiol. *112*, 1601–1607.

Hellens, R., Mullineaux, P., and Klee, H. (2000). Technical Focus:a guide to Agrobacterium binary Ti vectors. Trends Plant Sci. *5*, 446–451.

Irani, N.G., Rubbo, S.D., Mylle, E., Begin, J.V. den, Schneider-Pizoń, J., Hniliková, J., Šíša, M., Buyst, D., Vilarrasa-Blasi, J., Szatmári, A.-M., et al. (2012). Fluorescent castasterone reveals BRI1 signaling from the plasma membrane. Nature Chemical Biology *8*, 583–589.

Ivanov, R., and Gaude, T. (2009). Endocytosis and Endosomal Regulation of the S-Receptor Kinase during the Self-Incompatibility Response in Brassica oleracea. Plant Cell *21*, 2107–2117.

Ivanov, R., Fobis-Loisy, I., and Gaude, T. (2010). When no means no: guide to Brassicaceae self-incompatibility. Trends in Plant Science *15*, 387–394.

Jaillais, Y., Fobis-Loisy, I., Miège, C., Rollin, C., and Gaude, T. (2006). AtSNX1 defines an endosome for auxin-carrier trafficking in Arabidopsis. Nature *443*, 106–109.

Jaillais, Y., Fobis-Loisy, I., Miège, C., and Gaude, T. (2008). Evidence for a sorting endosome in Arabidopsis root cells. The Plant Journal *53*, 237–247.

Jia, T., Gao, C., Cui, Y., Wang, J., Ding, Y., Cai, Y., Ueda, T., Nakano, A., and Jiang, L. (2013). ARA7(Q69L) expression in transgenic Arabidopsis cells induces the formation of enlarged multivesicular bodies. J. Exp. Bot.

Kang, B.-H., Busse, J.S., and Bednarek, S.Y. (2003). Members of the Arabidopsis Dynamin-Like Gene Family, ADL1, Are Essential for Plant Cytokinesis and Polarized Cell Growth. Plant Cell *15*, 899–913.

Karimi, M., Depicker, A., and Hilson, P. (2007). Recombinational Cloning with Plant Gateway Vectors. PLANT PHYSIOLOGY *145*, 1144–1154.

Kitashiba, H., Liu, P., Nishio, T., Nasrallah, J.B., and Nasrallah, M.E. (2011). Functional test of Brassica self-incompatibility modifiers in Arabidopsis thaliana. Proc. Natl. Acad. Sci. U.S.A. *108*, 18173–18178.

Konopka, C.A., and Bednarek, S.Y. (2008). Comparison of the Dynamics and Functional Redundancy of the Arabidopsis Dynamin-Related Isoforms DRP1A and DRP1C during Plant Development. Plant Physiol. *147*, 1590–1602.

Kotzer, A.M., Brandizzi, F., Neumann, U., Paris, N., Moore, I., and Hawes, C. (2004). AtRabF2b (Ara7) acts on the vacuolar trafficking pathway in tobacco leaf epidermal cells. J Cell Sci *117*, 6377–6389.

Kusaba, M., Dwyer, K., Hendershot, J., Vrebalov, J., Nasrallah, J.B., and Nasrallah, M.E. (2001). Self-Incompatibility in the Genus Arabidopsis: Characterization of the S Locus in the Outcrossing A. lyrata and Its Autogamous Relative A. thaliana. Plant Cell *13*, 627–643.

Lalonde, B.A. (1989). A Highly Conserved Brassica Gene with Homology to the S-Locus-Specific Glycoprotein Structural Gene. THE PLANT CELL ONLINE *1*, 249–258.

Lee, G.-J., Sohn, E.J., Lee, M.H., and Hwang, I. (2004). The Arabidopsis Rab5 Homologs Rha1 and Ara7 Localize to the Prevacuolar Compartment. Plant Cell Physiol *45*, 1211–1220.

Liu, P., Sherman-Broyles, S., Nasrallah, M.E., and Nasrallah, J.B. (2007). A cryptic modifier causing transient self-incompatibility in Arabidopsis thaliana. Curr. Biol. *17*, 734–740.

Logemann, E., Birkenbihl, R.P., Ulker, B., and Somssich, I.E. (2006). An improved method for preparing Agrobacterium cells that simplifies the Arabidopsis transformation protocol. Plant Methods *2*, 16.

Naithani, S., Chookajorn, T., Ripoll, D.R., and Nasrallah, J.B. (2007). Structural modules for receptor dimerization in the S-locus receptor kinase extracellular domain. PNAS *104*, 12211–12216.

Nasrallah, M.E., Liu, P., and Nasrallah, J.B. (2002). Generation of Self-Incompatible Arabidopsis thaliana by Transfer of Two S Locus Genes from A. lyrata. Science *297*, 247–249.

Nasrallah, M.E., Liu, P., Sherman-Broyles, S., Boggs, N.A., and Nasrallah, J.B. (2004). Natural variation in expression of self-incompatibility in Arabidopsis thaliana: Implications for the evolution of selfing. PNAS *101*, 16070–16074.

Nielsen, E., Cheung, A.Y., and Ueda, T. (2008). The Regulatory RAB and ARF GTPases for Vesicular Trafficking. Plant Physiol. *147*, 1516–1526.

Nylander, M., Heino, P., Helenius, E., Palva, E.T., Ronne, H., and Welin, B.V. (2001). The low-temperature- and salt-induced RCI2A gene of Arabidopsis complements the sodium sensitivity caused by a deletion of the homologous yeast gene SNA1. Plant Mol. Biol. *45*, 341–352.

Pastuglia, M., Swarup, R., Rocher, A., Saindrenan, P., Roby, D., Dumas, C., and Cock, J.M. (2002). Comparison of the expression patterns of two small gene families of S gene family receptor kinase genes during the defence response in Brassica oleracea and Arabidopsis thaliana. Gene *282*, 215–225.

Prigoda, N.L., Nassuth, A., and Mable, B.K. (2005). Phenotypic and genotypic expression of self-incompatibility haplotypes in Arabidopsis lyrata suggests unique origin of alleles in different dominance classes. Mol. Biol. Evol. *22*, 1609–1620.

Rea, A.C., Liu, P., and Nasrallah, J.B. (2010). A transgenic self-incompatible Arabidopsis thaliana model for evolutionary and mechanistic studies of crucifer self-incompatibility. J. Exp. Bot. *61*, 1897–1906.

Robatzek, S., Chinchilla, D., and Boller, T. (2006). Ligand-induced endocytosis of the pattern recognition receptor FLS2 in Arabidopsis. Genes Dev. *20*, 537–542.

Rubbo, S., Irani, N.G., Kim, S.Y., Xu, Z.-Y., Gadeyne, A., Dejonghe, W., Vanhoutte, I., Persiau, G., Eeckhout, D., Simon, S., et al. (2013). The Clathrin Adaptor Complex AP-2 Mediates Endocytosis of BRASSINOSTEROID INSENSITIVE1 in Arabidopsis. Plant Cell.

Sarker, R.H., Elleman, C.J., and Dickinson, H.G. (1988). Control of pollen hydration in Brassica requires continued protein synthesis, and glycosylation in necessary for intraspecific incompatibility. PNAS *85*, 4340–4344.

Sawa, S., Koizumi, K., Naramoto, S., Demura, T., Ueda, T., Nakano, A., and Fukuda, H. (2005). DRP1A Is Responsible for Vascular Continuity Synergistically Working with VAN3 in Arabidopsis. Plant Physiol. *138*, 819–826.

Scheuring, D., Viotti, C., Krüger, F., Künzl, F., Sturm, S., Bubeck, J., Hillmer, S., Frigerio, L., Robinson, D.G., Pimpl, P., et al. (2011). Multivesicular Bodies Mature from the Trans-Golgi Network/Early Endosome in Arabidopsis. Plant Cell *23*, 3463–3481.

Schmittgen, T.D., and Livak, K.J. (2008). Analyzing real-time PCR data by the comparative C(T) method. Nat Protoc *3*, 1101–1108.

Shiu, S.-H., Karlowski, W.M., Pan, R., Tzeng, Y.-H., Mayer, K.F.X., and Li, W.-H. (2004). Comparative Analysis of the Receptor-Like Kinase Family in Arabidopsis and Rice. Plant Cell *16*, 1220–1234.

Smyth, D.R., Bowman, J.L., and Meyerowitz, E.M. (1990). Early flower development in Arabidopsis. Plant Cell *2*, 755–767.

Sorkin, A., and Zastrow, M. von (2009). Endocytosis and signalling: intertwining molecular networks. Nature Reviews Molecular Cell Biology *10*, 609–622.

Strickler, S.R., Tantikanjana, T., and Nasrallah, J.B. (2013). Regulation of the S-Locus Receptor Kinase and Self-Incompatibility in Arabidopsis thaliana. G3: Genes|Genomes|Genetics *3*, 315–322.

Trick, M. (1990). Genomic sequence of a Brassica S locus-related gene. Plant Mol. Biol. *15*, 203–205.

Yamamoto, M., and Nasrallah, J.B. (2013). In planta assessment of the role of thioredoxin h proteins in the regulation of S-locus receptor kinase signaling in transgenic Arabidopsis thaliana. Plant Physiol.

Supplemental figure 1: alignment of the predicted AlSRK14.

Arabidopsis lyrata SRK: AlSRK14, this work; AlSRK13 and AlSRK20, Kusaba *et al.* 2001. *Brassica sp. SRK*: BoSRK3, Delorme *et al.* 1995; BoSRK6, Naithani *et al.* 2007. The putative peptide sequences are underlined. The black stars indicate the 12 cysteines that are conserved in the S-domains of genes in the S-gene family. The red boxes indicate amino acid involved in phospho-transfer. The lysine residue in red corresponds to the catalytic lysine. The black boxes indicate residues in the kinase domain that are conserved in serine/threonine protein kinases.

```
          1                                                   50
AlSRK14   MRGVIPKYHQ SHNFFFFVFV VSTLFLPALS IYANTLLSTE SLTIASNQTI
AlSRK13   MRVVVPNCHH FY....IFFV VLILIRSVFS SYVHTLSSTE SLTISSKQTI
AlSRK20   .....PNKHH YYSFSFVFLF FFLILFPDFS ISTNTLSATE SLTISSNKTI
 BoSRK3   MQGVRYIYHH SYT..LLVFV VMILFRPALS IYVNTLSSTE YLTISNNKTL
 BoSRK6   MKGARNIYHH SYMSFLLVFV VMILIHPALS IYINTLSSTE SLTISSNKTL

          51                                                 100
AlSRK14   VSLGDDFELG FFKPAASLRD GDRWYLGIWY KTISIRTYVW VANRDHPLYS
AlSRK13   VSPGEVFELG FFNPAATSRD GDRWYLGIWF KTNLERTYVW VANRDNPLYN
AlSRK20   VSLGDVFELG FFT.....IL GDSWYLGIWY KKIPEKTYVW VANRDNPIST
 BoSRK3   VSPGDVFELG FFKTTS.... SSRWYLGIWY KTLSDRTYVW IANRDNPISN
 BoSRK6   VSPGSIFEVG FFRTN..... .SRWYLGMWY KKVSDRTYVW VANRDNPLSN

          101                                                150
AlSRK14   SAGTLKISGI NLVLLNQSNI AVWSTNLT.G AVRSPPVAEL LPNGNFVLRY
AlSRK13   STGTLKISDT NLVLLDQFDT LVWSTNLT.G VLRSPVVAEL LSNGNLVLKD
AlSRK20   STGILKISNA NLVLLNHFDT PVWSTNLT.A EVKSPVVAEL LDNGNFVLRD
 BoSRK3   STGTLKISGN NLVLLGDSNK PVWSTNLTRR SERSPVVAEL LANGNFVMRD
 BoSRK6   AIGTLKISGN NLVLLDHSNK PVWWTNLTRG NERSPVVAEL LANGNFVMRD

          151                                                200
AlSRK14   SKTNGQDILL WQSFDYPTDT LLPHMKLGLD LKTGNNRLLT SWKNSFDPSS
AlSRK13   SKTNDKDGIL WQSFDYPTDT LLPQMKMGWD VKKGLNRFLR SWKSQYDPSS
AlSRK20   SKTNGSDEFL WQSFDFPTDT LLPQMKLGLD HKKRLNKFLR SWKSSFDMSS
 BoSRK3   SNNNDASQFL WQSFDYPTDT LLPDMKLGYD LKTGLDRFLT SWRSLDDPSS
 BoSRK6   SSNNDASEYL WQSFDYPTDT LLPEMKLGYN LKTGLNRFLT SWRSSDDPSS

          201                                                250
AlSRK14   GYISYKLETL GLPEFFMWRN EVPIFRSGPW DGTRLSGIPE MQRWKDINIS
AlSRK13   GDFSYKLETR GFPEFFLLWR NSRVFRSGPW DGLRFSGIPE MQQWEYM..V
AlSRK20   GDYLFKIETL GLPEFFIWMS DFRVFRSGPW NGIRFSGMLE MQKWDDI..I
 BoSRK3   GNFSYRLETR KFPEFYLRSG IFRVHRSGPW NGIRFSGIPD DQKLSYM..V
 BoSRK6   GNFSYKLETQ SLPEFYLSRE NFPMHRSGPW NGIRFSGIPE DQKLSYM..V

          251                                                300
AlSRK14   YNFTENKEEV AFTFRVTTPN VYSRLIMNSE GFLQLSRWNP TLSEWNVFWR
AlSRK13   SNFTENREEV AYTFQITNHN IYSRFTMSST GALKRFRWIS SSEEWNQLWN
AlSRK20   YNLTENKEEV AFTFRPTDHN LYSRLTINYA GLLQQFTWDP IYKEWNMLWS
 BoSRK3   YNFTDNSEEV AYTFRMTNNS IYSRLTVSFL GHFERQTWNP SLGMWNAFWS
 BoSRK6   YNFIENNEEV AYTFRMTNNS FYSRLTLISE GYFQRLTWYP SIRIWNRFWS

          301                                                350
AlSRK14   S.STSDCNGY QSCTPYSYCD TNTTPNCNCI KGFAPQNPQE GALDNTNTEC
AlSRK13   K.PNDHCDMY KRCGPYSYCD MNTSPICNCI GGFKPRNLHE WTLRNGSIGC
AlSRK20   TSTDNACETY NPCGPYAYCD MSTSPMCNCV EGFKPRNPQE WALGDVRGRC
 BoSRK3   FILDSQCDIY KMCGPYAYCD VNTSPICNCI QGFNPSDVEQ WDRRSWAGGC
 BoSRK6   SPVDPQCDTY IMCGPYAYCD VNTSPVCNCI QGFNPRNIQQ WDQRVWAGGC
```

```
          351                                                       400
AlSRK14   VRKTQLSCDG DGFFWLRNMK PPDTSGAIVD KRIGLKECEE RCIKECNCTA
AlSRK13   VRKTRLNCGG DGFLCLRKMK LPDSSAAIVD RTIDLGECKK RCLNDCNCTA
AlSRK20   QRTTPLNCGR DGFTQLRKIK LPDTTAAILD KRIGFKDCKE RCAKTCNCTA
 BoSRK3   IRRTRLSCSG DGFTRMKNMK LPETTMAIVD RSIGVKECEK KCLSDCNCTA
 BoSRK6   IRRTQLSCSG DGFTRMKKMK LPETTMATVD RSIGVKECKK RCISDCNCTA

          401                                                       450
AlSRK14   FSNMNIQDGG KGCVIWTKEL ADIRRYADG. ..GQDLYVRL AAVDLVTEKA
AlSRK13   YASTDIQNGG LGCVIWIEEL LDIRNYASG. ..GQDLYVRL ADVDIGDERN
AlSRK20   FANTDIRNGG SGCVIWIGRF VDIRNYAAD. ..GQDLYVRV AAANIGDRKH
 BoSRK3   FSNADIRNGG MGCVIWTGRL DDMRNYAAD. ..GQDLYFRL AAVDLVKKRN
 BoSRK6   FANADIRNGG SGCVIWTERL EDIRNYATDA IDGQDLYVRL AAADIAKKRN

          451                                                       500
AlSRK14   NNNSGKTRTI IGLSVGAIAL IFLSFTIFFL WRRHKKAREI AQYTECGQRV
AlSRK13   .....IRGKI IGLAVGASVI LFLSSIMFCV WRRKQKLLRA TEAPIVYPTI
AlSRK20   .....ISGQI IGLIVGVSLL LLVSFIMYWF WKKKQKQARA TAAPNVYRER
 BoSRK3   .....ANWKI ISLTVGVTVL LLL..IMFCL WKRKQKRAKA NATSIVNRQR
 BoSRK6   .....ASGKI ISLTVGVSVL LLL..IMFCL WKRKQKRAKA SAISIANTQR

          501                                                       550
AlSRK14   GR........ .....QNLLE TDEDDLKLPL MEYDVVAMAT DDFAITNKLG
AlSRK13   NQGLLMNRLE ISSGRHLSED NQTEDLELPL VEFEAVVMAT ENFSNSNKLG
AlSRK20   TQ.HLTNGVV ISSGRHLFGE NKTEELELPL TEFEAVVMAT DNFSDSNILG
 BoSRK3   NQNLPMNGMV LSSKTEFSEE NKIEELELPL IDLETVVKAT ENFSNCNKLG
 BoSRK6   NQNLPMNEMV LSSKREFSGE YKFEELELPL IEMETVVKAT ENFSSCNKLG

          551                                                       600
AlSRK14   EGGFGTVYKG RLIDGEEIAV KKLSDVSTQG TNEFRTEMIL IAKLQHINLV
AlSRK13   EGGFGVVYKG RLLDGQEIAV KRLSTTSIQG ICEFRNEVKL ISKLQHINLV
AlSRK20   QGGFGVVYMG RLPDGQEIAV KRLSMVSLQG VNEFKNEVKL IARLQHINLV
 BoSRK3   QGGFGIVYKG RLLDGKEIAV KRLSKTSVQG TDEFMNEVTL IARLQHINLV
 BoSRK6   QGGFGIVYKG RLLDGKEIAV KRLSKTSVQG TDEFMNEVTL IARLQHINLV

          601                                                       650
AlSRK14   RLLGCFADAD DKILVYEYLE NLSLDYYIFD ETKSSDLNWQ TRFNIINGIA
AlSRK13   RLFGCCVDEN EKMLIYEYLE NLSLDSHLFN KSLSCKLNWQ MRFDITNGIA
AlSRK20   RLFSCCIYAD EKILIYEYLE NGSLDSHLFK KVQSSKLNWQ KRFNIINGIA
 BoSRK3   QIIGCCIEAD EKMLIYEYLE NLSLDSFLFG KTRRSKLNWK ERFDITNGVA
 BoSRK6   QVLGCCIEGD EKMLIYEYLE NLSLDSYLFG KTRRSKLNWN ERFDITNGVA

          651                                                       700
AlSRK14   RGLLYLHKDS RCKVIHRDLK TSNILLDKDM IPKISDFGLA RIFARDEEEA
AlSRK13   RGLLYLHQDS RFRIIHRDLK ASNVLLDKDM TPKISDFGMA RIFGRDETEA
AlSRK20   RGLLYLHQDS RFKIIHRDLK ASNVLLDKDM TPKISDFGMA RIFEREETEA
 BoSRK3   RGLLYLHQDS RFRIIHRDLK VSNILLDKNM IPKISDFGMA RMFAREETEA
 BoSRK6   RGLLYLHQDS RFRIIHRDLK VSNILLDKNM IPKISDFGMA RIFERDETEA

          701                                                       750
AlSRK14   TTRRIVGTYG YMAPEYAMDG VYSEKSDVFS FGVVILEIVT GKKNRGFTSS
AlSRK13   NTRKVVGTYG YMSPEYAMDG IFSVKSDVFS FGVLVLEIVS GKKNRGFYNS
AlSRK20   STKKVVGTYG YMSPEYAMDG IFSVKSDVFS FGVLVLEIVS GKRNRGFYNS
```

```
 BoSRK3  STMKVVGTYG YMSPEYAMHG IFSEKSDVFS FGVIVLEIVT GKRNSGFNNL
 BoSRK6  NTMKVVGTYG YMSPEYAMYG IFSEKSDVFS FGVIVLEIVS GKKNRGFYNL

         751                                                 800
AlSRK14  DLDTNLLSYV WRNMEEGTGY KLLDPNMMDS SSQ...AFKL DEILRCITIG
AlSRK13  NQDNNLLGYA WRNWKEGKGL EILDPFIVDS SSS.PSAFRP HEVLRCIQIG
AlSRK20  NQDNNLLSYT WDHWKEGKWL EIADPIIVGT SSS.SSTFRP HEVLRCLQIG
 BoSRK3  NYEDHLLNYA WSHWKEGKAL EIVDPVTVDS L...PSTFQK QEVLKCIQIG
 BoSRK6  DYENDLLSYV WSRWKEGRAL EIVDPVIVDS LSSQPSIFQP QEVLKCIQIG

         801                                                 850
AlSRK14  LTCVQEYAED RPMMSWVVSM LGSN.TDIPK PKPPGYCLAI S....SDP..
AlSRK13  LLCVQERAED RPVMSSVVVM LRSETETIPQ PKPPGYCVGR SPFETDSSTH
AlSRK20  LLCVQERAED RPKMSSVVFM LGNEKGEIPQ PKPPGYCIGR SFLETDSSSS
 BoSRK3  LLCVQELAEN RPTMSSVVWM LGSEATEIPQ PKPPGYCIRR SPYELDPSSS
 BoSRK6  LLCVQELAEH RPAMSSVVWM FGSEATEIPQ PKPPGYCVRR SPYELDPSSS

         851                   873
AlSRK14  ......WTST TIEYTTTEVE PR.
AlSRK13  EQRD..ESCT VNQITISAID PR.
AlSRK20  TQRN..ESST INQFTVSVIN AR.
 BoSRK3  RQYD.NDEWT VNQYTCSFID AR.
 BoSRK6  WQCDENESWT VNQY...... ...
```

9. Effects of perturbing endocytic trafficking on self-incompatibility

9.1. Perturbation of clathrin activity with the clathrin-hub

As discussed in the introduction, clathrin-mediated endocytosis is a major internalization route. Over-expression of the C-terminal part of clathrin heavy chain, called the clathrin-hub, impairs clathrin-mediated endocytosis in a dominant-negative manner (Liu *et al.* 1998). In *Arabidopsis thaliana*, clathrin-hub was shown to impair endocytosis of FM4-64, PIN proteins and H^+ plasma membrane ATPase (Dhonukshe *et al.* 2007, Kitakura *et al.* 2011), and ligand-bound BRI1 (Irani *et al.* 2012). Although the clathrin-hub may inhibit clathrin-mediated bud of vesicles at the *trans*-Golgi networks, it was reported that secretion of plasma membrane proteins is not inhibited by the clathrin-hub (Dhonukshe *et al.* 2007).

We generated a construct in which the *pSLR1* drives the expression of a GFP-clathrin-hub protein fusion, with GFP at the N-terminal side of the hub (GFP-hub). This construct was expressed in self-incompatible plants that express *Arabidopsis lyrata SRK14* under the control of *pSRK*. The expression of GFP-hub in papillae was monitored by confocal microscopy in second generation transgenic plants (**figure 25**). Most of the GFP-hub displayed an intracellular spotty distribution and to a smaller extent a cytosolic localization (**figures 25A**, **25B** and **25C**, large arrowheads), indicating that the clathrin-hub is likely recruited to intracellular membranes. These membranes may be *trans*-Golgi networks, since clathrin-coated vesicles bud from this compartment (Sauer *et al.* 2013). This localization seems to contrast with the published localization of the clathrin-hub. Indeed, the clathrin-hub is mainly cytosolic in animal cultured cells (Liu *et al.* 1998) and in plant protoplasts (Dhonukshe *et al.* 2007), although membrane-associated hubs are visible after cytosol removal (Liu *et al.* 1998), and a spotty pattern is also detected in *Arabidopsis thaliana* roots cells expressing RFP-hub (Kitakura *et al.* 2011). Moreover, the clathrin-hub is sometimes incorporated in structures formed by wild-type membrane-associated clathrin heavy chains, although the function of these structures is perturbed (Liu *et al.* 1998). These data indicate that our finding that GFP-hub may associate with intracellular membranes in papillae is not surprising. We also noticed a population of smaller spots that were more numerous than the bigger ones (which likely are *trans*-Golgi networks), often seen when the confocal plan was tangential to the periphery of the papillae (**figure 25C**, small arrowheads). This dual localization is similar to what is obtained for clathrin light chain (Konopka *et al.* 2008): part of clathrin is localized to the plasma membrane at endocytic sites (the small spots) and part is localized

to the *trans*-Golgi networks (the big spots). The small spots seen in papillae might thus represent clathrin structures at the plasma membrane.

We plan to verify whether endocytosis is indeed perturbed in papillae by expression of the clathrin-hub or not. To do so, we will investigate if GFP-hub expression reduces endocytosis of LTI6B-GFP, as performed for ARA7 mutants (see part 8).

We then investigated whether expression of GFP-hub perturbs the self-incompatibility phenotype (**figure 26**). Out of 5 independent lines that co-express GFP-hub and SRK14, three lines were self-incompatible and two were partially self-incompatible (lines #10 and #11). However, the high standard deviation of the mean of lines #10 and #11 indicates these results are likely not significant. Collectively, our data indicate that the clathrin-hub over-expression in papillae does not impair self-incompatibility.

9.2. Perturbation of endocytosis with dominant negative mutants of DYNAMIN RELATED PROTEIN 1A

DYNAMIN-RELATED PROTEIN 1A (DRP1A) is a GTPase involved in clathrin-mediated endocytosis. It is thought to detach clathrin-coated vesicles from the plasma membrane by conformational changes following GTP hydrolysis. DRP1A is highly expressed in papillae and loss of function of DRP1A leads to defective elongation of papillae and accumulation of excess plasma membrane that forms many indentations, consistent with defective endocytosis (Kang *et al.* 2003). In animals, mutation of lysine 44 involved in GTPase activity was used to study the function of Dynamin1. The mutant Dynamin1^{K44A} has 90% reduced GTPase activity and its over-expression leads to abolished endocytosis of transferrin and EGF receptor in a dominant negative manner (Bliek *et al.* 1993, Herskovits *et al.* 1993, Damke *et al.* 1994). In plant cells, over-expression of the homologous mutant of DRP1A, DRP1A^{K47M}, perturbed transport of Golgi-derived vesicles to the cell plate (Hong *et al.* 2003). Other dominant-negative mutants of animal Dynamin1 were studied. Dynamin1^{T68A} has null GTPase activity and its over-expression blocks endocytosis of transferrin (Marks *et al.* 2001). We mutated DRP1A to obtain DRP1A^{K47M} and DRP1A^{T68A}, the latter being a mutation homologous to the one studied by Marks *et al.* (2001). Wild-type DRP1A or DRP1A mutants fused to GFP or mCherry were expressed under the control of *pSLR1* in papillae that express *SRK14* under the control of *pSRK*.

We analyzed the expression and localization of fluorescently-tagged DRP1A wild-type and variants in papillae of first generation transgenic plants corresponding to independent transgene insertions (**figure 27**). Wild-type DRP1A-GFP (**figures 27A** to **27D**) was localized to small punctate structures at the periphery of the cell (**figures 27B** and **27D**, open arrowheads) and to larger intracellular spots (**figures 27B** and **27D**, arrowheads). This distribution is similar

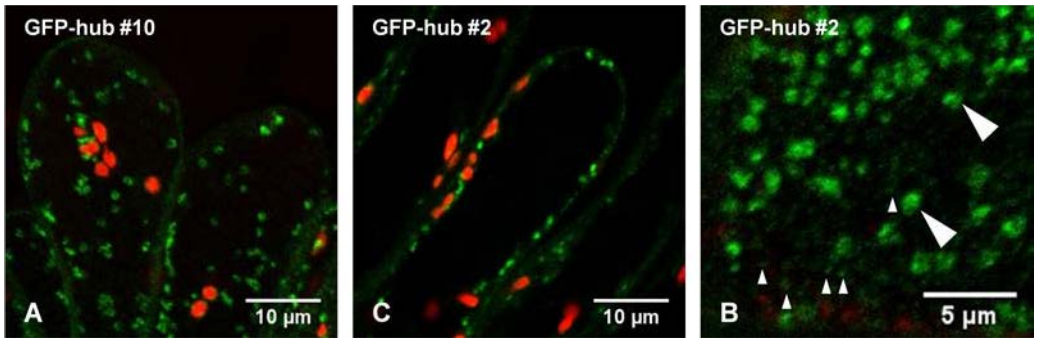

Figure 25: expression and subcellular localization of GFP-hub in papillae. *GFP-hub* was expressed under the control of the *SLR1* promoter in plants expressing *SRK14* under the control of Col-0 *pseudo-SRK* promoter. GFP-hub fluorescence and subcellular localization was analyzed by confocal microscopy. The number of the plant line is indicated on the upper left-hand corner. Large arrowheads indicate putative *trans*-Golgi networks, small arrowheads indicate putative endocytic sites at the plasma membrane.

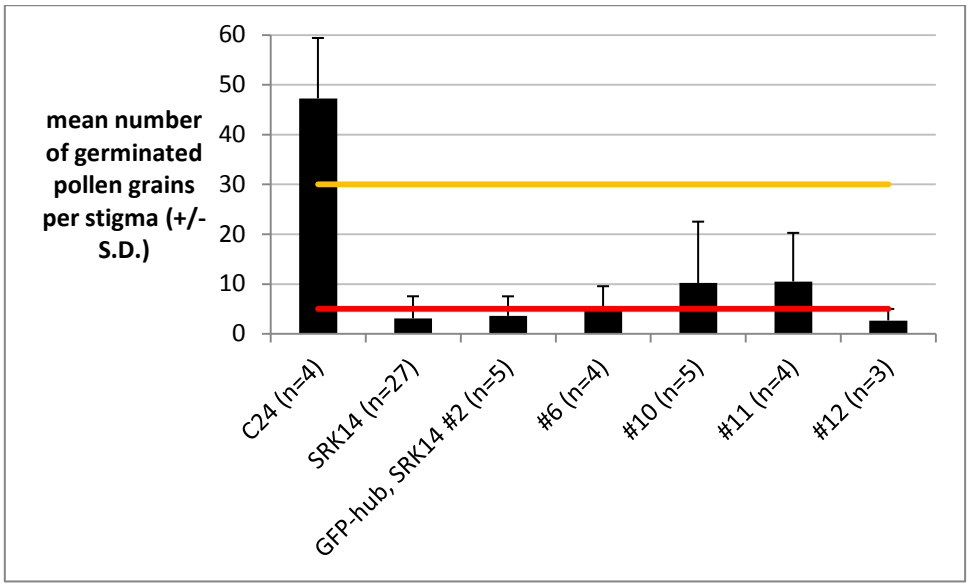

Figure 26: the self-incompatible phenotype of second generation transgenic plants co-expressing GFP-hub and SRK14. Second generation transgenic plants corresponding to independent single transgene insertions were pollinated with incompatible pollen and the number of germinated pollen grains found on the stigma were counted after aniline blue staining. *GFP-hub* was expressed under the control of *Brassica oleracea SLR1* promoter (*pSLR1*) and *SRK14* was expressed under the control of Col-0 *pseudo-SRK* promoter (*pSRK*). Wild-type C24 was used as a self-compatible control and a transgenic line expressing *SRK14* only was used as a self-incompatible control. The number n of stigmas examined is noted for each genotype. S.D. = standard deviation. The red line marks the upper boundary for a self-incompatible phenotype and the orange line marks the upper boundary for the partial self-incompatible phenotype. Above the orange line plants display a self-compatible phenotype.

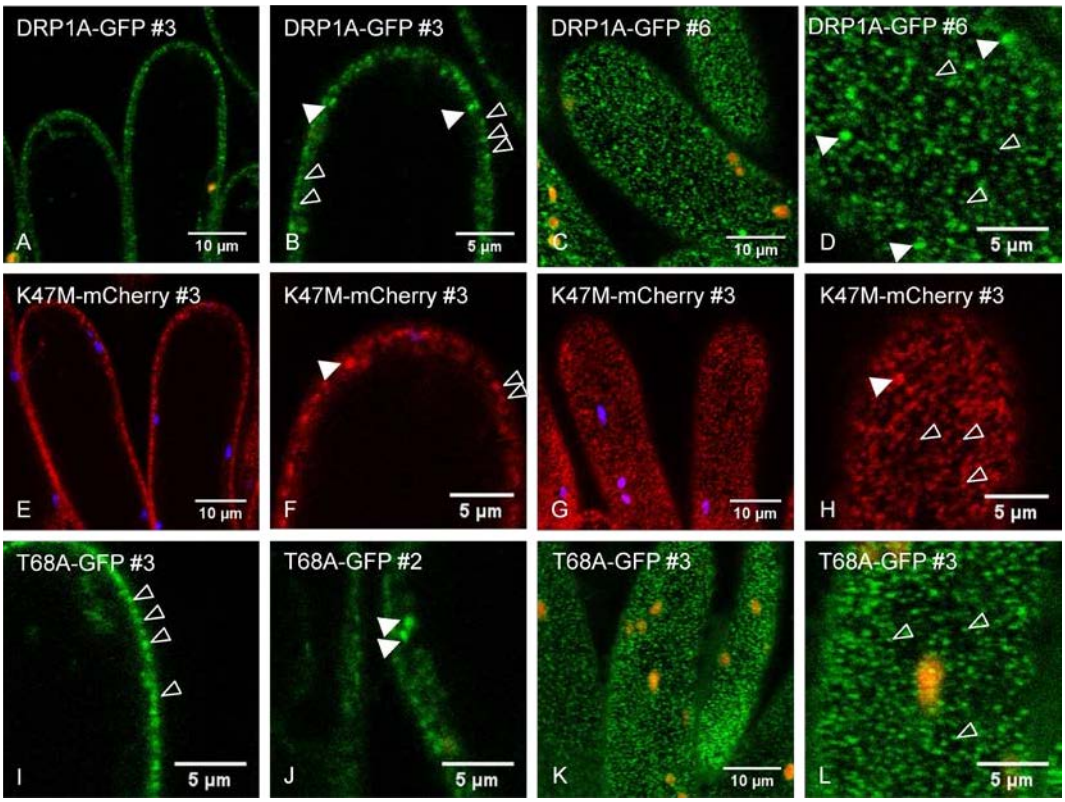

Figure 27: subcellular localization of DRP1A, DRP1A^{K47M} and DRP1A^{T68A} fused to either GFP or mCherry. The name of the construct expressed by papillae is indicated in the upper left-hand corner, together with the number of the plant line. Papillae were analyzed by confocal microscopy. White arrowheads point at putative *trans*-Golgi networks, open arrowheads point at putative endocytic sites. The confocal plane went through the middle of the cell, except on images **C**, **D**, **G**, **H**, **K** and **L** where the confocal plane is tangential to the periphery of the cell.

(A) to **(D)** Papillae co-expressing *Arabidopsis lyrata* SRK14 and wild-type DRP1A-GFP. GFP fluorescence is shown in green, chloroplast fluroescence is shown in red.

(E) to **(H)** Papillae co-expressing *Arabidopsis lyrata* SRK14 and DRP1A^{K47M}-mCherry. mCherry fluorescence is shown in red, chloroplast fluorescence is shown in blue.

(I) to **(L)** Papillae co-expressing *Arabidopsis lyrata* SRK14 and DRP1A^{T68A}-GFP. GFP fluorescence is shown in green, chloroplast fluroescence is shown in red.

to what was previously published: punctate structures at the cell cortex that colocalize with clathrin light chain and may represent endocytic sites (Fujimoto *et al.* 2010, Konopka and Bednarek 2008) and intracellular compartments that colocalize with a *trans*-Golgi network marker (Sawa *et al.* 2005). We thus hypothesize that the small punctate structures seen at the periphery represent endocytic sites, and that the larger intracellular structure are *trans*-Golgi networks. DRP1A^{K47M}-mCherry (**figures 27E** to **27H**) and DRP1A^{T68A}-GFP (**figures 27I** to **27L**) displayed a distribution similar to DRP1A-GFP, as expected. Indeed, these two DRP1A mutants are mutated at residues required for GTP hydrolysis, but their membrane binding and protein-protein interaction domains are not affected. Consequently, they are expected to be recruited to their site of activity and impair the function of their interacting partners, hence the dominant-negative property. Whether DRP1A proteins were tagged with GFP or mCherry did not affect the distribution of DRP1A variants in papillae.

We selected several first generation transgenic plant lines corresponding to independent transgene insertions. We selected plant lines that displayed high expression of DRP1A transgenes, based on levels of GFP or mCherry fluorescence, and determined the self-incompatibility phenotype of these plants (**figure 28**). Over-expression of wild-type DRP1A-GFP did not affect self-incompatibility, as the plants were self-incompatible (only line #3 is represented, this line was used as a self-incompatible control). Over-expression of DRP1A^{K47M}-GFP/mCherry or DRP1A^{T68A}-GFP/mCherry did not affect self-incompatibility, as the plants displayed pollen rejection similar to plants expressing wild-type DRP1A. Only line DRP1A^{K47M}-mCherry #2 and line DRP1A^{T68A}-GFP #1 had slightly more germinated incompatible pollen grains in comparison to the other lines. However, the fact that this phenotype is seen in only two lines over nine analyzed and the size of the standard deviation compared to the mean make us believe that this result likely not significant. Altogether, our results indicate that over-expression of DRP1A dominant-negative mutants does not perturb self-incompatibility.

We are currently verifying that DRP1A mutants effectively perturb endocytic trafficking by crossing them with plants expressing LTI6B-GFP and monitor the changes in the amount of internalized LTI6B-GFP.

9.3. Perturbation of SRK endocytic trafficking by mutation of a conserved tyrosine-based motif of SRK

The sequence of the intracellular region of SRK14 contains several motifs putatively involved in endocytosis, among them three YXXΦ motifs, where Y is a tyrosine, X is any amino acid, and Φ is a hydrophobic residue. This motif is involved in clathrin-mediated endocytosis by binding to the μ subunit of the AP-2 complex, which bridges cargo and clathrin molecules (Kurten 2003). The YDVV motif starting at tyrosine 525 is located in the juxtamembrane segment of SRK14, the YYIF motif (tyrosine 618) is located inside the kinase domain, as the YEYL motif (tyrosine 608). The YEYL motif is very well conserved among many PRK and was proposed to be a common endocytic motif for PRK endocytosis (Geldner and Robatzek 2008). The tyrosine of this motif is actually the gatekeeper residue. Among the kinase domains encoded by the human genome, 20 % have a threonine and 60 % have a methionine as a gatekeeper. The presence of a tyrosine at this position is specific for the IRAK family of kinases (Wang *et al.* 2006), which is homologous to the family composed by the kinase domains of PRK (Shiu and Bleecker 2001b). When the atomic structure of IRAK4 was solved, it was determined that the gatekeeper tyrosine interacts with a conserved residue in the N-terminal lobe of the kinase domain and stabilizes the active conformation of the kinase (Wang *et al.* 2006). PRK, being phylogenetically related to the IRAK family, have a tyrosine as a gatekeeper. Mutation of the gatekeeper of *Arabidopsis thaliana* BRI1 (tyrosine 956, Oh *et al.* 2009), of *Medicago truncatula* LYK3 (tyrosine 390, Klaus-Heisen *et al.* 2011) and of *Arabidopsis thaliana* SYMRK (tyrosine 970, Samaddar *et al.* 2013) results in a severely impaired kinase activity, consistent with the role of the gatekeeper in stabilizing the active conformation of PRK kinase domains.

We investigated the role of the YEYL motif by mutating the first tyrosine (tyrosine 608) into alanine. We selected 7 second generation transgenic plant lines expressing SRK14^{Y608A} and corresponding to independent single insertions of the transgene. All the lines displayed a self-compatible phenotype, in contrast to plants expressing a wild-type SRK14 (**figure 29A**). We verified by reverse transcription quantitative PCR that the compatible phenotype of SRK14^{Y608}-expressing plants was not the result of low expression levels of *SRK14* (**figure 29B**). Only plant line #15 is represented, as all plant lines displayed similar expression levels.

As tyrosine 608 is the probable gatekeeper residue of SRK14, we investigated the effect of this mutation on the kinase activity of SRK14. We fused the cytoplasmic domain of SRK14 (SRK14cd), from amino acids 487 to 851 (comprising the juxtamembrane segment, the kinase domain and the C-terminal tail) with an N-terminal HA epitope and inserted the construct in a plasmid for *in vitro* transcription and translation. We expressed wild-type SRK14cd, SRK14^{Y608A}cd,

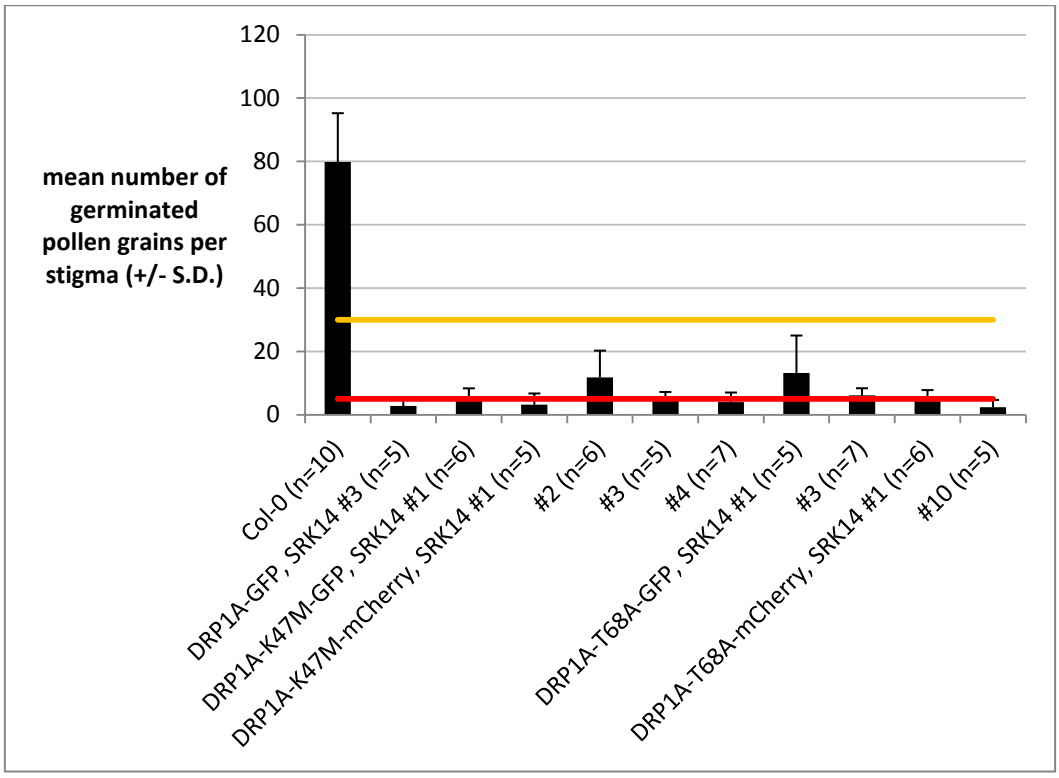

Figure 28: the self-incompatible phenotype of plants co-expressing either DRP1A^{K47M}-GFP/mCherry or DRP1A^{T86A}-GFP/mCherry with SRK14. First generation transgenic plants corresponding to independent transgene insertions were pollinated with incompatible pollen and the number of germinated pollen grains found on the stigma were counted after aniline blue staining. DRP1A^{K47M}-GFP/mCherry or DRP1A^{T68A}-GFP/mCherry were expressed under the control of *Brassica oleracea SLR1* promoter (*pSLR1*) and *SRK14* was expressed under the control of Col-0 *pseudo-SRK* promoter (*pSRK*). Wild-type Col-0 was used as a self-compatible control and a transgenic line co-expressing wild-type DRP1A-GFP and SRK14 only was used as a self-incompatible control. The number n of stigmas examined is noted for each genotype. S.D. = standard deviation. The red line marks the upper boundary for a self-incompatible phenotype and the orange line marks the upper boundary for the partial self-incompatible phenotype. Above the orange line plants display a self-compatible phenotype.

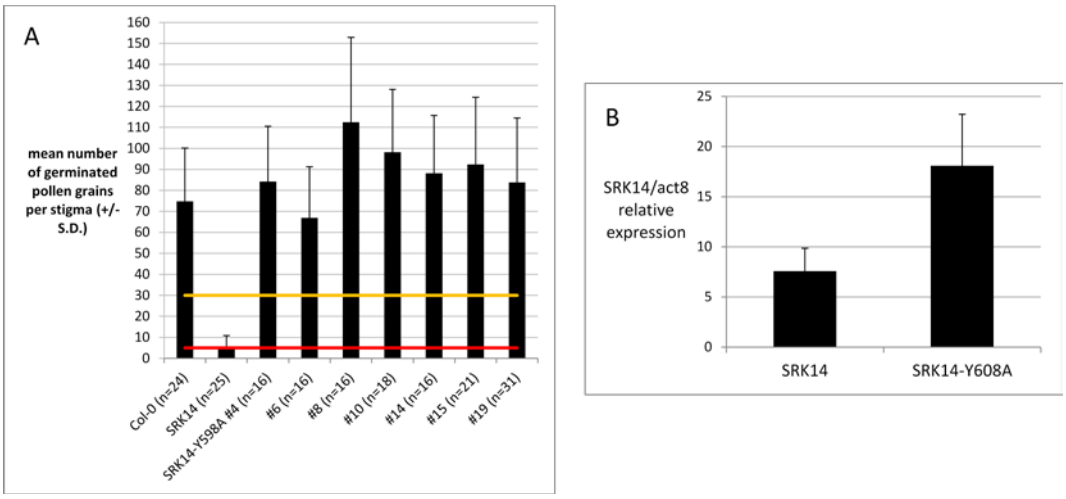

Figure 29: effect of mutation of the gatekeeper tyrosine of SRK14 on self-incompatibility.
(A) Characterization of the self-incompatible phenotype plants expressing SRK14^{Y608A}. Second generation transgenic plants corresponding to independent single transgene insertions were pollinated with incompatible pollen and the number of germinated pollen grains found on the stigma were counted after aniline blue staining. The red line marks the upper boundary for a self-incompatible phenotype and the orange line marks the upper boundary for the partial self-incompatible phenotype. Above the orange line plants display a self-compatible phenotype.
(B) Reverse transcription quantitative PCR was performed to quantify *SRK14^{Y608}* mRNA levels on plant line #15. All plant lines displayed similar expression levels.

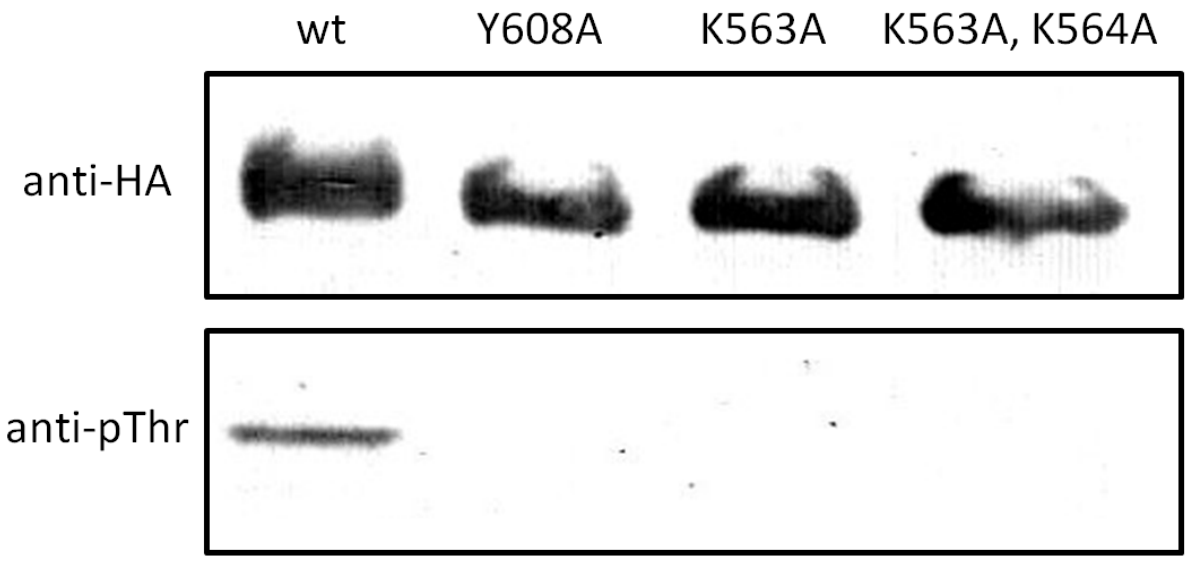

Figure 30: monitoring of trans-phosphorylation of SRK kinase domain in the Y608A mutant. The cytoplasmic domain (containing the kinase domain) of wild-type SRK14, SRK14^{Y608A}, SRK14^{K563A} and SRK14$^{K563A,\ K564A}$, were fused to the hemagglutinin epitope (HA) expressed *in vitro* and proteins were subjected to immunoblotting with anti-HA antibodies (upper panel). The same proteins expressed *in vitro* were subjected to immunoblotting with anti-phospho-threonine antibodies (anti-pThr) (lower panel).

SRK14^{K563A}cd and SRK14$^{K563A, K564A}$cd. Lysine 563 of SRK14 is the putative catalytic lysine. As lysine 563 is immediately followed by another lysine, we also generated an SRK14cd in which both lysines were mutated (SRK14$^{K563A, K564A}$cd) in case lysine 564 could be involved in the phosphotransfer reaction.

We expressed all the SRK14cd variants in a cell-free wheat germ extract and analyzed the expression products by Western-blot with anti-HA antibodies (**figure 30**, upper panel). All constructs gave a strong and sharp band at the expected size (45 kDa), indicating they were well expressed. We also performed a Western blot with anti-phosphothreonine (anti-pThr) antibodies (**figure 30**, lower panel). As expected, wild-type SRK14 (wt lane) showed a band of approximately 45 kDa while the kinase-dead variants did not (K563A and K563A, K564A lanes). This result indicates that wild-type SRK14cd can *trans*-phosphorylate in the *in vitro* reaction mixture to produce an SRK14cd protein phosphorylated on threonines, while the kinase-dead variants cannot. Unfortunately, we did not detect phosphorylated SRK14^{Y608A}cd, indicating that this mutant as an abolished kinase activity. We thus conclude that the self-compatible phenotype of the plants expressing SRK14^{Y608A} most likely arises from the abolition of the kinase activity of SRK14, and not from a mis-localization of the receptor at the subcellular level because of impaired endocytosis.

DISCUSSION

10. Subcellular localization of SRK14

10.1. Summary of the approaches implemented

Managing to detect SRK at the subcellular level in *Arabidopsis thaliana* stigmatic papillae proved to be a much more challenging task than expected. Many PRK can bear the insertion of a fluorescent protein at their C-terminus and retain functionality (BRI1, Friedrichsen *et al.* 2000; BAK1, Li *et al.* 2002; FLS2, Robatzek *et al.* 2006; CLV1, Nimchuk *et al.* 2011; ACR4, Gifford *et al.* 2003; NFP, Lefebvre *et al.* 2012; Xa21, Chen *et al.* 2010a). SRK14, however, lost functionality when either GFP (27 kDa) or smaller tags like hemagglutinin or FLAG epitopes (10 Da) were inserted at its C-terminus. We overcame this difficulty by inserting fluorescent protein within the N-terminus of SRK14, in regions predicted to be loops in the 3D structure of the extracellular domain, and succeeded in generating functional fusions. Experimental evidence shows that the extracellular space has a pH in the 5–6 range (Fasano *et al.* 2001) and the lumen of endosomes has a pH of 6.2 to 6.3 (Shen *et al.* 2010). SRK is predicted to be a type I transmembrane protein (Stein *et al.* 1990), so the N-terminal domain is located either in the extracellular space if SRK is at the plasma membrane, or in the lumen of endosomes if SRK is endocytosed. In other words, the fluorescent proteins inserted in the extracellular domain of SRK are in an acidic environment. To address this issue, we took advantage of pH-resistant fluorescent proteins, namely TagBFP2 (Subach *et al.* 2011), Citrine (Griesbeck *et al.* 2001) and mCherry (Shaner *et al.* 2004). These N-terminal fusions between fluorescent proteins and SRK14 allowed subcellular localization in live papillae. As a final approach, we mutated two amino acids at the N-terminus of SRK14 to take advantage of antibodies targeted at the first nine amino acids of *Brassica oleracea* SRK3. These anti- SRK3 antibodies allowed us to visualize the subcellular localization of SRK14 on stigma sections using secondary antibodies coupled to fluorochromes.

10.2. SRK14 may localize to the plasma membrane and to endosomes in *Arabidopsis thaliana*

SRK14 tagged at the N-terminus with fluorescent proteins displayed a diffuse cytoplasmic localization, a reticulate pattern that could correspond to an endoplasmic reticulum labeling and a putative plasma membrane localization. Performing immunolocalization on papillae expressing SRK3:14, we found SRK3:14 in intracellular compartments that could represent endosomes but we also found a significant amount of SRK3:14 at the plasma membrane. These localizations will be confirmed by colocalization with characterized markers of intracellular compartments. We have *Arabidopsis thaliana* plant lines expressing fluorescently-tagged markers of all major compartments, including the Wave lines (Geldner *et al.* 2009) and several additional lines that we developed. We already

crossed these marker-lines with plants expressing tagged SRK14 and the progeny of these crosses will be analyzed soon. In addition, we plan to use drugs that perturb trafficking to verify that the intracellular compartments labeled by SRK3:14 are endosomes. We will treat papillae with tyrphostin A23, or BFA in conjunction with cycloheximide, or wortmannin prior to immunolocalization. If these intracellular compartments are endosomes, and if SRK14 endocytosis depends on one or several YXXΦ motifs, tyrphostin A23 should decrease the number and/or the intensity of the intracellular spots. In addition, BFA plus cycloheximide treatment should lead to aggregation of these structures into BFA-bodies. However, the compartments may be endosomes weakly sensitive to BFA, such as multivesicular bodies. In this case, wortmannin treatment should alter the structure of these compartments.

The significance of the localization of SRK14 tagged at loop1/2 or at the N-terminus with fluorescent proteins is unclear. Indeed, the endoplasmic reticulum is not likely to be relevant for SRK14 signaling and may represent defects during SRK14 biosynthesis. The presence of the fluorescent protein at loop1/2 or at the N-terminus of SRK may perturb folding of SRK into the native structure and activate endoplasmic reticulum quality control mechanisms, which could lead to mis-folded tagged-SRK retention in the endoplasmic reticulum by binding to chaperones (Gidalevitz *et al.* 2013).

The relevance of the putative plasma membrane localization of fluorescently-tagged SRK14 is also enigmatic, since its correlation with self-incompatibility is not clear. The plant lines in which the plasma membrane localization of SRK14 is most evident are not the lines that display the strongest self-incompatible phenotype. Conversely, the plant lines that display the strongest self-incompatible phenotype show a diffuse cytoplasmic localization of the fluorescent protein. Such a diffuse fluorescence may not reflect the localization of functional fusions, but rather the localization of cytosolic fluorescent protein fusions after failure of protein addressing to the endoplasmic reticulum. In the case of the N-terminal fusions, the presence of an ectopic fluorescent protein close to the signal peptide could perturb signal peptide recognition by the signal recognition particle (SRP), blocking addressing of tagged-SRK14 to the endoplasmic reticulum (Snapp *et al.* 2001). It is unlikely that the fluorescent protein is cleaved from SRK14, since we did not see labeling of the nucleus, which occurs when a fluorescent protein is expressed alone. In addition, diffuse cytoplasmic localization displayed by tagged-SRK could arise from high levels of SRK14 expression. Indeed, this may lead to problems of secretion and release of tagged-SRK14 in the cytosol but allow enough protein to reach the compartment(s) that is (are) relevant for SRK14 signaling, explaining both the diffuse localization and the strong self-incompatible phenotype.

By performing immunolocalization with anti-SRK3 antibodies we found SRK3:14 in intracellular compartments that could represent endosomes but we

also found a significant amount of SRK3:14 at the periphery of papillae, probably representing a plasma membrane localization. However, live cell imaging of SRK14 tagged with fluorescent proteins rarely showed intracellular compartments, contrasting with the immunolocalization data. We favor the results obtained with immunolocalization of SRK3:14 for two reasons: first, they are more consistent with results obtained in *Brassica oleracea* than live cell imaging of SRK tagged at loop1/2 or at the N-terminus with fluorescent proteins; second, SRK3:14 contains no additional tag and is different from SRK14 by only two amino acid substitutions at locations not involved in ligand binding, receptor activation or kinase activity. This should minimally perturb the function/localization of SRK14 and is attested by the higher frequency of self-incompatible phenotype of the plants expressing SRK3:14 in comparison to plants expressing tagged SRK.

10.3. Why is SRK localization different between *Brassica oleracea* and *Arabidopsis thaliana*?

In *Brassica oleracea*, SRK3 was almost uniquely found in endosomes, with few patches at the plasma membrane (Ivanov and Gaude 2009). This contrasts with immunolocalization of SRK3:14 in *Arabidopsis thaliana*, where significant amounts of SRK apparently localize to the plasma membrane. It has been stated that the constitutive and predominant localization of *Brassica oleracea* SRK3 in endosomes served the purpose of regulating the amount of SRK that is available for ligand binding at the plasma membrane (Ivanov and Gaude 2009), which is a paradigm for mammalian RTK function (Sorkin and von Zastrow 2009). Indeed, a single papilla can distinguish between a compatible pollen grain and an incompatible pollen grain at the same time and mount a self-incompatible response against the latter while allowing the former to germinate (Sarker *et al.* 1988). Since SRK can *trans*-phosphorylate (Giranton *et al.* 2000), this dual competence of papillae implies that some mechanisms must prevent SRK signaling from spreading along the plasma membrane. Such a mechanism could be a high endocytosis/recycling ratio that concentrates SRK in endosomes and leaves only little amounts at the plasma membrane (Ivanov and Gaude 2009). However, it is currently unknown if this dual competence of papillae is conserved in *Arabidopsis thaliana*. Since *Arabidopsis thaliana* is naturally self-compatible, compatible pollen grains do not compete with incompatible pollen grains at the stigma surface, so evolutionary pressure to maintain this dual competence may be released, allowing SRK to accumulate at the plasma membrane in *Arabidopsis thaliana*.

11. Perturbation of endocytic trafficking

11.1. Endocytosis is required for self-incompatibility

At the beginning of this work we noted that SRK-GFP was mainly localized at the plasma membrane and was not functional. Interestingly enough, SRK3:14—a functional protein—is localized to endosomal compartments, in addition to being localized at the plasma membrane. This is consistent with the hypothesis that SRK requires to be in endosomal compartments to activate its signaling pathway.

We used several approaches to perturb endocytic trafficking and monitor the effect on self-incompatibility. We targeted clathrin function by over-expression of the clathrin-hub, which is composed of the C-terminal region of clathrin heavy chain and impairs clathrin-mediated endocytosis in a dominant-negative manner (Dhonukshe *et al.* 2007, Liu *et al.* 1998, 1995). However, the clathrin-hub did not impair self-incompatibility. We plan to verify that clathrin-hub indeed perturbed endocytosis in papillae by quantitative imaging of internalized LTI6B-GFP.

We also investigated the role of the RAB GTPase ARA7 by over-expression of either dominant-negative or dominant-positive variants, which were reported to perturb endocytosis and trafficking to the vacuole (Dhonukshe *et al.* 2006, Kotzer *et al.* 2004). We could confirm that targeting ARA7 function indeed perturbed endocytosis, as monitored by localization of LTI6B-GFP to intracellular compartments. On the one hand, over-expression of the dominant-negative ARA^{S24N} led to a partial reduction of the number of LTI6B-GFP-labeled intracellular compartments and the amount of intracellular LTI6B-GFP. On the other hand, over-expression of the dominant-positive ARA^{Q69L} led to a partial increase of the same parameters. The contrasting effects of ARA^{S24N} and ARA^{Q69L} on endocytosis are consistent with the dominant-negative and dominant-positive properties, respectively, of these proteins. Over-expression of ARA7 variants did not affect self-incompatibility, suggesting that a partial perturbation of endocytosis leaves SRK function unaffected. Conversely, SRK may follow a trafficking pathway that is independent of ARA7 function. If SRK signals from endosomes, it could be expected that over-expression of ARA^{Q69L} leads to an amplification of self-incompatibility, since ARA^{Q69L} over-expression increases endocytosis. We plan to verify if over-expression of ARA^{Q69L} can turn a partial self-incompatible phenotype into a full self-incompatible phenotype. To do so, we will take advantage of lines that express *SRK* under the control of *pSRK*, as some of these lines display a partial self-incompatible phenotype.

We then targeted dynamin function with GTPase-defective variants and a loss-of-function mutant of DRP1A, a protein involved in clathrin-coated vesicle budding from the plasma membrane (Collings *et al.* 2008, Fujimoto *et al.* 2010). While GTPase-defective variants did not affect self-incompatibility, loss of

function of DRP1A abolished it. It is surprising that expression of dominant-negative variants of DRP1A does not have the same effect as a loss-of-function mutant. A similar result was reported for Rab7 in cultured mammalian cells. Indeed, siRNA-mediated knockdown of Rab7 blocks EGFR recycling in absence of ligand, blocking EGFR in aberrant endosomes (Rush and Ceresa 2013) while $Rab7^{N125I}$ (a dominant negative mutant) does not alter the distribution of EGFR (Ceresa and Bahr 2006). The origin of these differences is not clear. It is possible that endogenous wild-type proteins are in sufficient amounts to prevent dominant negative effects of mutant proteins, or that inhibition of endocytosis is only partial. We plan to perform quantitative imaging of LTI6B-GFP internalization to verify these hypotheses. We also introgressed *SRK14* in *ARA7* or clathrin heavy chain mutant lines, in order to verify if we can obtain a stronger phenotype than with dominant negative mutants.

Overall, our findings support a model in which endocytosis is required for self-incompatibility, perhaps by leading to SRK signaling from endosomes. It was demonstrated that upon activation, SRK is endocytosed and colocalizes with THL1, a negative regulator of self-incompatibility, before being degraded in the vacuole (Ivanov and Gaude 2009). Endocytosis thus seems to play a dual role in self-incompatibility by regulating both positively and negatively SRK signaling. SRK may sustain signaling from an early population endosomes, before being silenced by contacting THL1 and being routed to the vacuole for degradation. Further investigation will determine if SRK signaling is an endosomal-specific process or if it starts at the plasma membrane and sustains in endosomes.

11.2. SRK could undergo clathrin-independent endocytosis

Targeting DRP1A function links endocytosis to SRK signaling, but targeting clathrin function with over-expression of clathrin-hub does not perturb self-incompatibility, although the two proteins are believed to function together to mediate endocytosis (Chen *et al.* 2011). Clathrin-independent endocytosis probably occurs in plant cells (Bandmann and Homann 2012, Li *et al.* 2012, Moscatelli *et al.* 2007, Onelli *et al.* 2008) and may depend on dynamin-related proteins. Indeed, several clathrin-independent endocytosis routes characterized in animal cells require the function of dynamin. Flotillin-mediated endocytosis is clathrin-independent, dynamin-dependent (at least for some cargos) and is involved in internalization of cell surface proteoglycans, interleukin2-receptor β and IgE (Doherty and McMahon 2009). In addition, flotillin localizes to a population of lipid rafts, which are enriched in sterols, sphingolipids and saturated fatty acids (Parton and Simon 2007). Flotillin-dependent endocytosis was studied in plant cells and is sensitive to cholesterol depletion (Li *et al.* 2012). To investigate if SRK endocytosis and signaling are dependent on clathrin-independent pathways,

we could investigate the effect of cholesterol depletion (by using methyl-β-cyclodextrin) on self-incompatibility. We crossed *Arabidopsis thaliana* lines expressing SRK14 with *fad2* and *fad3* mutants, which are impaired in saturated fatty acid biosynthesis (Hugly and Somerville 1992), and planned to test the self-incompatible phenotype of these mutants. Third, we could investigate the association of SRK with detergent insoluble membranes, which are the biochemical counterparts of *in vivo* lipid rafts. This is performed by extraction of stigma proteins with a mild detergent (e.g. Triton X100) and centrifugation of the protein extract. Co-sedimentation of SRK with a lipid raft marker such as remorin (Simon-Plas *et al.* 2011) would suggest association of SRK with lipid rafts *in vivo*. Results obtained with this biochemical approach should be confirmed by *in planta* imaging of SRK association with cholesterol- and saturated fatty acid-dependent microdomains. Although such microdomains can been seen by confocal microscopy (Raffaele *et al.* 2009), they are 30–70nm wide so their investigation requires techniques such as super-resolution microscopy (Owen *et al.* 2012) and immunolocalization by freeze-fracture electron microscopy (Raffaele *et al.* 2009).

11.3. Investigating the function of linear motifs of SRK

We sought to perturb the endocytic trafficking of SRK 14 in a specific manner by mutating the YEYL motif located in the kinase domain of SRK. This motif was suggested to be a conserved motif among PRK involved in interaction with the adaptor protein complex AP2 which bridges clathrin and endocytosed cargo (Geldner and Robatzek 2008). However, this motif turned out to contain the gatekeeper tyrosine, an amino acid involved in stabilizing the 3D structure of the kinase domain (Wang *et al.* 2006). Mutation of this motif impairs the kinase activity and function of *Arabidopsis thaliana* BRI1 (Oh *et al.* 2009) and SYMRK (Samaddar *et al.* 2013), as well as the kinase activity of *Medicago truncatula* LYK3 while leaving its biological function intact (Klaus-Heisen *et al.* 2011). We analyzed five independent lines of plants expressing $SRK14^{Y608A}$ and all were self-compatible although they expressed high levels of SRK14. However, the kinase activity of $SRK14^{Y608A}$ was abolished, suggesting that the self-incompatible phenotype of these plants arises from a lack of kinase activity of SRK14, and not from a mis-localization of $SRK14^{Y608A}$ because of defective endocytosis. This confirms published results showing that the kinase activity of SRK910 is required for self-incompatibility in *Brassica napus* (Stahl *et al.* 1998).

In comparison with the use of drugs and mutants to perturb endocytosis, targeting specific motifs in the endocytic cargo has the advantage of specifically altering trafficking of the cargo while preserving the global physiology of the plant. Analysis of the primary sequence of SRK14 with an online prediction software called Eukaryotic linear motif resource (Dinkel *et al.* 2012) revealed several other linear motifs putatively involved in endocytosis and regulation of signaling. It would be interesting to characterize the effect of substitution or

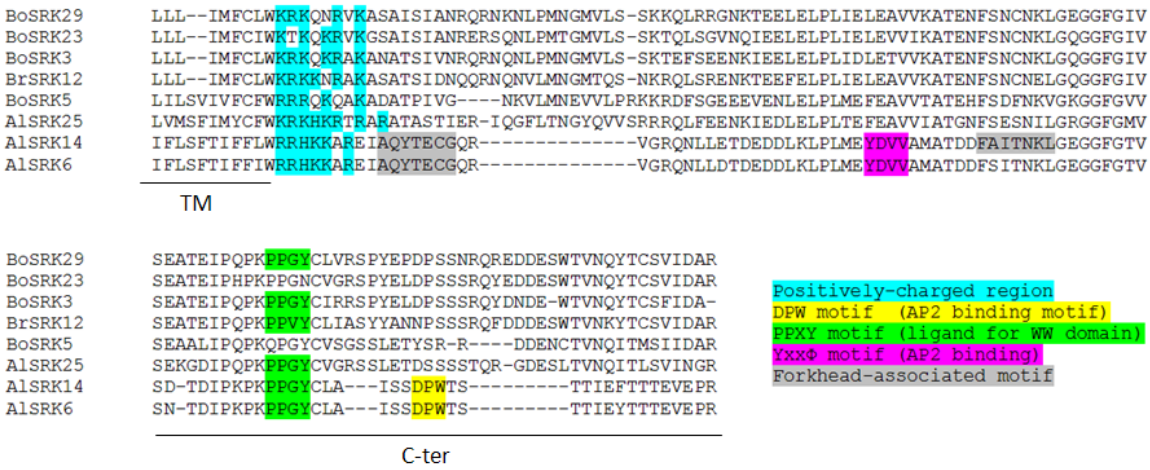

Figure 31: conservation of linear motifs in different SRK variants. The sequence of *Brassica oleracea* SRK29 (BoSRK29, Genbank accession number Z30211.1), SRK23 (BoSRK23, Genbank accession number BAA34233.1), SRK3 (BoSRK3, EMBL Data Library accession number X79432), SRK5 (BoSRK5, Genbank accession number CAB41878.1), *Brassica rapa* SRK12 (BrSRK12, Genbank accession number BAA07577.2), *Arabidopsis lyrata* SRK14 (AlSRK14, cf. supplemental figure 1 of part 8) and SRK6 (AlSRK6, Genbank accession number ACU29642.1) were aligned using ClustalW (Combet *et al.* 2000). The upper alignment shows the end of the transmembrane segment (TM) followed by the juxtamembrane segment. The lower alignment shows the C-terminal segment (C-ter).

deletion of these motifs on self-incompatibility, on the subcellular localization of SRK3:14 in papillae, and on the interaction of SRK3:14 with candidate proteins. Several of these motifs may play a role in clathrin-dependent endocytosis. Although I proposed in the previous paragraph that SRK could be internalized through clathrin-independent endocytosis, a clathrin-dependent endocytic pathway cannot be ruled out yet. Furthermore, SRK trafficking may involve both clathrin-dependent and clathrin-independent pathways. The engagement of a specific endocytic pathway could depend on SRK activation, as seen for EGFR and FLS2. Indeed, FLS2 is constitutively endocytosed and recycles through a BFA-sensitive pathway, while activated receptors traffic via ARA7- and ARA6-positive endosomes (Beck *et al.* 2012). EGFR is endocytosed through a clathrin-dependent pathway and then recycled when activated with a low ligand concentration while it follows an additional clathrin-independent route that promotes receptor degradation when subjected to high ligand concentration (Sigismund *et al.* 2008).

To begin with, a YDVV motif is found in the juxtamembrane segment of SRK14 (**figure 31**, purple). This motif is a tyrosine-based motif putatively involved in clathrin-mediated endocytosis through interaction with the μ subunit of the AP2 complex. It would be possible to investigate the function of this motif in self-pollen rejection and SRK3:14 subcellular localization by mutating the first tyrosine into alanine. Moreover, we could also test the involvement of this motif in interaction with AP2-μ by co-immunoprecipitation.

The C-terminal tail of SRK14 contains a DPW motif (**figure 31**, yellow). This motif is present in adaptor proteins like epsin and is involved in clathrin recruitment by endocytic cargos through interaction with the α and β subunits of AP-2 (Owen 2004). We could mutate the DPW motif of SRK14 and test the outcome on self-pollen rejection and SRK14 subcellular localization. Plants that express a tagged AP2-α protein were recently described and used to purify the whole AP2 complex by tandem affinity purification (Rubbo *et al.* 2013). Similarly, we could perform co-immunoprecipitation of SRK3:14 and AP2-α. As a complementary approach, we can characterize the effect of loss-of-function of AP2 subunits on self-incompatibility. Several AP2 mutants were recently described and display impaired endocytosis of FM4-64 and BRI1 (Rubbo *et al.* 2013).

The C-terminal tail of SRK14 also contains a PPGY motif that is well conserved among SRK sequences from different *Brassicaceae* species (**figure 31**, green). PPXY motifs are ligands for group I WW domains, which are involved in protein-protein interactions (Kay 2000). We plan to investigate if mutation of the PPGY motif perturbs self-incompatibility. If so, this motif could be used as a bait in co-immunoprecipitation experiments to identify binding partners.

Finally, the juxtamembrane segment of SRK14 contains two forkhead-associated (FHA) motifs (**figure 31**, gray). FHA motifs interact with phospho-threonines and phospho-serines and are found in a variety of proteins, among

them KAPP (Stone 1994). KAPP is a cytosol-oriented, membrane-anchored type 2C phosphatase that interacts with the kinase domain of several PRK, including KIK1 of maize (Braun *et al.* 1997), HAESA (Stone *et al.* 1994), CLV1 (Williams *et al.* 1997), SERK1 (Shah *et al.* 2002), SERK1 (Ding *et al.* 2007), FLS2 (Gomez-Gomez *et al.* 2001) and *Brassica oleracea* SRK29 (Vanoosthuyse *et al.* 2003). It has been demonstrated that KAPP is phosphorylated by CLV1 and SRK29 and dephosphorylates them *in vitro*. Moreover, KAPP negatively regulates CLV1, BRI1 and FLS2 signalling (Ding *et al.* 2007, Williams *et al.* 1997, Gomez-Gomez *et al.* 2001, Vanoosthuyse *et al.* 2003), suggesting that KAPP has a general role in receptor kinase downregulation through its phosphatase activity. KAPP has affinity for the sequence [YAF]-A-[YF]-pT-[VQELI]-X-[SA] (where amino acids between brackets allow any of the indicated amino acids to be present at this position, pT represents a phosphorylated tyrosine and X represents any amino acid, Durocher *et al.* 2000). Far Western experiments demonstrated that KAPP binds BAK1 to the LLATQSS sequence (Ding *et al.* 2007), which differs from the canonical KAPP binding sequence by 3 amino acids (favored amino acids at +1 and +3). This sequence is found with mismatches in the juxtamembrane segment of SRK14: AQYTECG (2 mismatches, favored amino acids at -3, -1 and +1) and FAITNKL (3 mismatches, favored amino acids at -3 and -2). To characterize the function of KAPP in self-incompatibility, we can investigate the effect of either KAPP loss of function or KAPP over-expression. Since KAPP is likely involved in downregulation of SRK signaling, a KAPP loss of function mutant would increase the strength of the self-incompatible phenotype, in other words, turn a partial self-incompatible phenotype into a self-incompatible phenotype. More specifically, we can cross *Arabidopsis thaliana* that expresses SRK14 and displays a partial self-incompatible phenotype with the *rag1-2* mutant, which is a T-DNA insertion null mutant for KAPP (SAIL_1255_D05, Manabe *et al.* 2008). Conversely, KAPP over-expression would decrease the strength of the self-incompatible phenotype, e.g. turn a self-incompatible phenotype into a partial self-incompatible phenotype or self-compatible phenotype. To verify this hypothesis, we can overexpress KAPP in stigmatic papillae using the *Brassica oleracea SLR1* promoter. KAPP was reported to be localized at the plasma membrane in *Arabidopsis thaliana* protoplasts, and to induce accumulation of the PRK SERK1 in intracellular compartments (Shah *et al.* 2002). It would be interesting to investigate the localization of KAPP in stigmatic papillae, and the effect of KAPP over-expression on SRK14 localization in papillae.

12. Miscellaneous perspectives

12.1. SRK dimerization and activation at the plasma membrane

SRK displays an oligomeric state at the plasma membrane in absence of ligand (Giranton *et al.* 2000). Over-expression of SRK in a heterologous system leads to auto-activation in absence of ligand (Giranton *et al.* 2000), and this auto-activation can be silenced by the addition of THL1 (Cabrillac *et al.* 2001). THL1 is an inhibitor of self-incompatibility which colocalizes with SRK in endosomes but which is absent from the plasma membrane (Ivanov and Gaude 2009). This raises a series of important questions. How are SRK dimers stabilized in absence of ligand? What are the mechanisms that prevent *trans*-phosphorylation by the kinase domain of SRK in the oligomer at the plasma membrane? How are these mechanisms relieved to activate SRK upon ligand binding?

Several RTK form oligomers that exist even in the absence of ligand, a property linked with dimerization motifs. Indeed, RTK encode in their transmembrane helix a propensity to form dimers (Finger *et al.* 2009), thanks to motifs such as the Steinberg-Gullick motif, also referred to as the GG4-like motif (Cymer and Schneider 2010). This motif is composed of two small residues (alanine, serine, threonine or glycine) separated by three residues and provides a groove for close contact between transmembrane helices in the receptor dimer. RTK from the EGFR family generally possess two GG4-like motifs in their transmembrane segments. It was proposed that interaction between the C-terminal GG4-like motifs stabilizes the inactive dimer. Ligand binding to the receptor induces structural rearrangements in the extracellular domain that allow to occur the more energetically favored interaction between the N-terminal GG4-like motif, thereby stabilizing the active dimer (Cymer and Schneider 2010). Moreover, substitution of the glycines of this motif by larger hydrophobic residues like valine or isoleucine reduces ligand-induced endocytosis and degradation of EGFR, and leads to sustained signaling (Heukers *et al.* 2013). The GG4-like motif can thus play a role in signal transduction and endocytic trafficking by receptor kinases.

The extracellular part of SRK (eSRK) was demonstrated to contain a dimerization determinant, namely the PAN domain (Naithani *et al.* 2007). However, eSRK was found mainly monomeric *in planta* while SRK was dimeric (Giranton *et al.* 2000). In addition, eSRK does not bind SCR while artificial eSRK dimerization with a helix-loop-helix zipper induces SCR binding with affinity similar to SRK (Shimosato *et al.* 2007), highlighting the lack of a dimerization determinant in eSRK compared to SRK. The transmembrane segment of SRK14 contains a GLSGV motif that is well conserved among SRK from different

Brassicaceae species. The functional significance of this motif is currently unknown and could be responsible for efficient SRK dimerization *in vivo*.

EGFR activation is uncharacteristic, as the activation loop of EGFR is in an active conformation even when unphosphorylated. EGFR is thus primed and ready for activation before ligand binding. Because of this, mechanisms to control auto-activation of EGFR in the absence of ligand were acquired by cells during evolution. One such mechanism is proposed in the "electrostatic engine model" (McLaughlin *et al.* 2005). According to this model, EGFR is maintained inactive at the plasma membrane thanks to binding of both the juxtamembrane segment and the kinase domain to positively charged lipids (such as phosphoinositides) through positively charged amino acid residues (arginine, lysine, histidine). A fast calcium influx at the early stage of EGFR activation triggers calmodulin binding to the juxtamembrane segment of EGFR, which shields the negative charges and repels both the juxtamembrane segment and the kinase domain from the plasma membrane, allowing full activation of EGFR. EGFR over-expression leads to its auto-activation, a phenomenon that can reach the same levels as ligand-induced EGFR activation, maybe by titration of phospholipids by the over-expressed receptor (Endres *et al.* 2013).

Interestingly enough, activation of SRK shares many features with EGFR activation. First of all, SRK is in an oligomeric state at the plasma membrane in absence of ligand and over-expression of SRK in a heterologous system leads to auto-activation in absence of ligand (Giranton *et al.* 2000). Secondly, SRK was proposed to be in a ready-to-be-activated state at the plasma membrane, since SRK is present at the plasma membrane as patches devoid of the negative regulator THL1, which is specifically localized in endosomes (Ivanov and Gaude 2009). Thirdly, the juxtamembrane segment of SRK14 contains 6 adjacent positively charged residues (RRHKKAR), which are well-conserved among different SRK sequences (**figure 31**, blue). Finally, a calcium influx is seen in papillae upon self-pollen addition (Iwano *et al.* 2004) and calmodulin interacts with the kinase domain of SRK29 (Vanoosthuyse *et al.* 2003). Calmodulin was shown to interact with an amphipathic helix of SRK29 kinase domain, which does not appear as rich in positively charged residues in SRK14. However, binding to the juxtamembrane may occur anyway. Taken as a whole, these data indicate that some mechanisms are likely to prevent SRK auto-activation at the plasma membrane, and that these mechanisms could share similarities with those discussed for EGFR.

To verify these hypotheses, a first approach could be to substitute the positively charged amino acids of the juxtamembrane of SRK14 by alanine residues. We expect to monitor a stronger self-incompatible phenotype compared to wild-type SRK14, i.e. a shift from a partial self-incompatible phenotype to a self-incompatible phenotype. A second approach could be to manipulate the levels of phosphoinositides at the plasma membrane of papillae by expression of enzymes involved in the metabolism of such lipids. An increase of phosphoinositides

should lead to a weaker self-incompatible phenotype, while a decrease of phosphoinositides should make the self-incompatible phenotype stronger. The manipulation of calmodulin function may be difficult. Indeed, the calmodulin family in *Arabidopsis thaliana* contains many members and a single mutant might not give a measurable phenotype. Over-expression of the identified calmodulin-binding peptide of SRK (Vanoosthuyse *et al.* 2003) in papillae could saturate calmodulin and prevent the putative calmodulin-induced SRK activation.

12.2. Phosphorylated amino acids of SRK

Studies in *Brassica sp.* demonstrated that SRK is phosphorylated on serine and threonines upon activation (Giranton *et al.* 2000, Cabrillac *et al.* 2001). This occurs through *trans*-phosphorylation between SRK molecules (Giranton *et al.* 2000) and between MLPK and SRK molecules (Kakita *et al.* 2007b). Phosphorylated residues then probably serve as binding sites for proteins of the signaling pathway, such as ARC1 (Gu *et al.* 1998). Although the C-terminal segment of SRK contains phosphorylated residues (Giranton *et al.* 2000), the exact identity of these amino acids remains unknown. The C-terminal segment of SRK14 contains several serine and threonine residues that are conserved between different SRK alleles. A simple experiment would be to generate a truncated SRK14 without the C-terminal segment, and to test the self-incompatibility phenotype of plants expressing this truncated receptor. The function of putatively phosphorylated residues in self-incompatibility and partner binding could be further investigated by replacing them with either alanine (a loss-of-phosphorylation mutation) or aspartate (a gain-of-phosphorylation mutation).

13. Conclusion

In this study, we investigated the role of endocytic trafficking in regulation of self-incompatibility. We first generated transgenic self-incompatible *Arabidopsis thaliana* that express a functional S-LOCUS RECEPTOR KINASE (SRK) protein from a related and self-incompatible species called *Arabidopsis lyrata*. We then determined the subcellular localization of SRK by immunolocalization with anti-SRK antibodies and found a localization similar to *Brassica oleracea*. Indeed, significant amounts of SRK are seen in putative endosomes, suggesting that endosomes play an important role in SRK signaling. We then implemented genetic approaches to perturb endocytic trafficking. Among the various strategies we undertook, loss of function of DYNAMIN-RELATED PROTEIN1A resulted in abolished self-incompatibility, indicating that endocytic trafficking positively regulates self-incompatibility. This contrasts with the negative role that has been previously attributed to endocytosis in regulation of self-incompatibility and suggests that control of SRK signaling is complex and relies on antagonistic pathways. We also validated *Arabidopsis thaliana* as a model to study the subcellular events that govern self-incompatibility. Stigmatic papillae of *Arabidopsis thaliana* are amenable to expression of fluorescent protein fusions and quantitative confocal imaging. This species will certainly be a useful model to explore the complex relationships between intracellular trafficking and self-incompatibility, and help to verify the hypotheses that were formulated through the realization of this study.

MATERIAL AND METHODS

Materials and methods related to experimental results presented in the article in submission (part 8) are included in the article itself. Methods that are used in the article are not described again in this section.

14. Plant material and growth conditions

Wild-type *Arabidopsis thaliana* Col-0 and C24 accessions were obtained from the Notthingham arabidopsis stock centre (university of Notthingham, UK, http://arabidopsis.info/). Transgenic *Arabidopsis thaliana* whose transgene was segregating were sowed on Petri dishes containing Murashige-Skoog medium (Duchefa), 8 g/L Plant Agar (Duchefa), pH 5.7 and appropriate antibiotics depending on the transgene. After sowing seeds, plates were kept for two days at 4 °C to synchronize seed hydration and then place in growth chambers set at 22 °C with 18 h light/6 h dark photoperiod. After 7-10 days, seedling were transplanted on earth medium (Argile 10, Favorit) and placed in culture rooms set at 22 °C with 18 h light/6 h dark photoperiod. Transgenic plants homozygous for the transgene and non-transgenic plants were sowed directly on earth medium.

Arabidopsis lyrata ssp petraea expressing the *S14* haplotype originates from the Czech Republic (seeds generously provided by Dr Pierre Saumitou-Laprade, Université de Lille F59655 Villeneuve d'Ascq cedex, France). *Arabidopsis lyrata* was maintained in culture rooms with the same conditions as *Arabidopsis thaliana* but cultivated in 1L pots containing a mixture of 60 % peat-based compost (Klassman BP substrat 2), 20 % sand and 20 % Pouzzolane (a volcanic rock).

15. Arabidopsis thaliana transformation

Transgenic plants were generated using *Agrobacterium tumefaciens*-mediated transformation according to Logemann *et al.* 2006. This is a variation of the flower dip method (Clough and Bent 1998) that is less labor-intensive and that uses *Agrobacterium tumefaciens* culture on Petri dishes containing a rich medium instead of liquid culture. We used the *Agrobacterium tumefaciens* strain C58PMP90 which is resistant to rifampicin and gentamicin (Hellens *et al.* 2000). Briefly, *Agrobacterium tumefaciens* that contain the transgene of interest plus the resistance marker are cultured on Petri dishes and put into suspension. *Arabidopsis thaliana* flowers are dipped into the bacterial suspension, enabling the bacteria to penetrate the developing female organs. The bacteria then infect the ovules and inject the transgene of interest and the resistance marker which are stably inserted into the genome of *Arabidopsis thaliana*.

The batch of seeds obtained after transgenesis is sowed on a selective medium and gives birth to first generation transgenic plants, which carry one (sometimes more) transgene insertion that is independent between each plant. First generation transgenic plants are all heterozygous for the transgene. A "transgenic plant line" is defined as a group of plants with a genealogical relationship and contain an independent transgene insertion. The seeds obtained from first generation transgenic plants are sowed on a selective

medium and plants that contain a single transgene insertion are identified based on segregation of the resistance phenotype: 25 % sensitive plants and 75 % resistant plants). The second generation transgenic plants contain a mixture of heterozygous and homozygous plants in a 2:1 ratio. Finally, the seeds obtained from second generation transgenic plants are sowed on a selective medium and plants that were homozygous for the transgene during the second generation are identified because all of their progeny is resistant to selection.

16. PCR-mediated mutagenesis

The protocol for PCR-mediated mutagenesis has been previously described (Fisher and Pei 1997).

17. Generation of plasmid vectors

We used Gateway® entry plasmid vectors (Life Technologies) and destination vectors described by Karimi *et al.* 2007.

GFPS65C/pDONR-207 has been described (Fobis-loisy *et al.* 2007).

For the SRK14-GFP construct, the sequence of *pSLR1, SRK14* and *GFPS65C* were inserted together by LR recombination in the destination vector pK7m34GW,3.

For the SRK-HA/FLAG construct, the sequence of *pSLR1*, *SRK14* and *HA* or *FLAG* were inserted together by LR recombination in the destination vector pK7m34GW,3.

A *PstI* restriction site was inserted at loop1 and loop2 by PCR-mediated mutagenesis. For loop1, we used primers 5'-CTTCAAACCGGCTGCAGGTCTTCGAGACG-3' and 5'-CGTCTCGAAGACCTGCAGCCGGTTTGAAG-3'. For loop2, we used primers 5'-CTCCAAAACCAATCTGCAGGATATATTATTGTGGC-3' and 5'-GCCACAATAATATATCCTGGAGATTGGTTTTGGAG-3'. We amplified the cDNA of TagBFP2, Citrine and mCherry with primers containing a *PstI* site to generate a DNA fragment encoding the fluorescent protein flanked with *PstI* sites. This fragment was digested with *PstI* and ligated with an entry plasmid containing *PstI*-loop1/2-*SRK14* previously digested with *PstI* and dephosphorylated. The sequence of *pSLR1* and *TagBFP2/Citrine/mCherry-loop1/2-SRK14* were inserted together by LR recombination in the destination vector pK7m24GW.

A *PstI* restriction site was inserted at the mature N-terminus (after the predicted signal sequence) of *SRK14* by PCR-mediated mutagenesis with primers 5'-CTCTCGATATATCTGCAGACTTTGTTGTCTAC-3' and 5'-GTAGACAACAAAGTCTGCAGATATATCGAGAG-3'. We amplified the cDNA of TagBFP2, Citrine and mCherry with primers containing an amino acid linker (9A or GS3) coding sequence and a *PstI* site to generate a DNA fragment encoding the fluorescent protein flanked with *PstI* sites. This fragment was digested with *PstI* and ligated with an

entry plasmid containing *PstI-Nter-SRK14* previously digested with *PstI* and dephosphorylated. The sequence of *pSLR1* and *TagBFP2/Citrine/mCherry-9A/GS3-SRK14* were inserted together by LR recombination in the destination vector pK7m24GW.

For the GFP-clathrin-hub construct, a 1860 bp DNA fragment corresponding from *CLATHRIN HEAVY CHAIN 1* (At3g11130) encoding the C-terminal region of the protein was amplified with attB1-containing primer 5'-GGGGACAGCTTCTTGTACAAAGTGGTAAAGAAGTTTAACTTAAATGTTCA-3' and attB3-containing primer 5'-GGGGACAACTTTGTATAATAAAGTTGTTAGTAGCCGCCCATCGGTGG-3'. The PCR product was then inserted by BP recombination into the entry plasmid pDONR-P2R-P3. The sequence of *pSLR1*, *GFPS65C* and *Hub1*were inserted together by LR recombination in the destination vector pH7m34GW,3.

DRP1A variants were generated by PCR-mediated mutagenesis with plasmids containing the cDNA sequence of *DRP1A* as a template. We generated the $DRP1A^{K47M}$ sequence with the forward primer 5'-GGTCAGAGCTCAGGGATGTCTTCAGTCCTGG-3' and reverse primer 5'-CCAGGACTGAAGACATCCCTGAGCTCTGACC-3'. We generated the $DRP1A^{T68A}$ sequence with the forward primer 5'-GGATCTGGCATTGTTGCTCGAAGGCCCCTTGTC-3' and the reverse primer 5'-GACAAGGGGCCTTCGAGCAACAATGCCAGATC-3'.

18. Pollination assays

We pollinated stage 13 (according to Smyth *et al.* 1990) *Arabidopsis thaliana* stigmas with pollen from *Arabidopsis lyrata S14*. Pollinated stigmas were harvested 6 h after pollination and placed in FAA (4 % formaldehyde, 5 % acetic acid, 50 % alcohol in water) overnight at 4 °C for fixation. Stigmas were then washed three times with water before being placed in 4 N NaOH for 30 min at room temperature to soften the tissues. Stigmas were then washed three times with water and placed in aniline blue (discolored in 3 % K_3PO_4 in water) overnight at 4 °C to stain pollen grains and tubes. Stigmas were then mounted between plate and coverslip in discolored aniline blue for observation in a Nikon e600 with DAPI filter set. Germinated pollen grains were manually counted and the mean number of germinated pollen grain per stigma was computed for each genotype analyzed. We distinguish three categories of the self-incompatibility degree. Plants are categorized as self-incompatible when they display less than 5 germinated pollen grains per stigma, on the average. Plants are categorized as partially self-incompatible when they display more than 5 but less than 30 germinated pollen grains per stigma. Finally, plants with more than 30 germinated pollen grains per stigma fit in the self-compatible category (Kitashiba *et al.* 2011).

19. Reverse transcription and real-time quantitative PCR

Thirty stigmas were dissected from buds just before stage 13 (staging according to Smyth *et al.* 1990) and total RNA were extracted with the Arcturus® PicoPure® RNA isolation kit (Life Technologies). 265 ng of total RNA were reverse-transcribed with random hexanucleotides and RevertAid (200 U/µL ; Thermo scientific) and subjected to quantitative real-time PCR with *SRK14* or *ACTIN8* specific primers. Because *Arabidopsis lyrata* and two different accessions of *Arabidopsis thaliana* were compared, we designed primers that amplify a region of the *ACTIN8* cDNA conserved between each species (forward primer 5'-CGACGGACAAGTGATCACGATC-3' and reverse primer 5'-CATAGTTGTACCACCACTGAGCAC-3'). Amplification of *SRK14* was performed with two primers located within the first exon (forward primer 5'-GCCGCCAGACACATCCGGGGC-3' and reverse primer 5'-CAACCCTTCCCACCATCTTGG-3') Absence of contaminating genomic DNA was controlled with primers located within a non coding region close to the *ACTIN8* gene (forward primer 5'-GGCTGTGACAATGCGAAGCCCC-3' and reverse primer 5'-CCCCATTTTGGTATCTAGGG-3'). Quantitative analysis of real-time PCR results was performed using the $2^{-\Delta\Delta Ct}$ method (Schmittgen and Livak 2008).

20. Image acquisition

Stigmas were cut and mounted in water for live cell imaging using a Zeiss 710 confocal microscope, unless otherwise specified. Gain and offset were adjusted for near dark background (outside cells) and maximum signal intensity without saturation.

21. SDS-PAGE and protein gels blots

Total proteins from 50 stigmas were extracted in SDS-PAGE loading buffer (62.5 mM Tris, pH 6.8, 10 % vol/vol glycerol, 3 % mass/vol SDS, 2.5 % mass/vol dithiothreitol) as described (Giranton *et al.* 2000). Proteins were titrated (Lowry *et al.* 1951) and 15 µg of total proteins were loaded for SDS-PAGE. Antibodies were diluted as follows: mouse anti-SRK3 (mAb85-36-71, Ivanov and Gaude 2009) 1:1000, goat anti-mouse HRP (Promega) 1:7000, rabbit anti-phospho-threonine (Cell Signaling ref. 9381S) 1:1000, anti-rabbit AP (Promega ref. S373B) 1:5000. Protein gel blots using AP were revealed with NBT/BCIP ready-to-use tablets (Roche), HRP was revealed with Amersham ECL protein gel blotting detection reagents (GE Healthcare).

22. In vitro expression

In vitro expression was performed with the TnT® SP6 high yield wheat germ protein expression system (Promega) with 4 µg of plasmid.

BIBLIOGRAPHICAL REFERENCES

Abas, L., Benjamins, R., Malenica, N., Paciorek, T., Wišniewska, J., Moulinier–Anzola, J.C., Sieberer, T., Friml, J., and Luschnig, C. (2006). Intracellular trafficking and proteolysis of the Arabidopsis auxin-efflux facilitator PIN2 are involved in root gravitropism. Nature Cell Biology *8*, 249–256.

Andaya, C.B., and Ronald, P.C. (2003). A catalytically impaired mutant of the rice Xa21 receptor kinase confers partial resistance to Xanthomonas oryzae pv oryzae. Physiological and Molecular Plant Pathology *62*, 203–208.

Antolín-Llovera, M., Ried, M.K., Binder, A., and Parniske, M. (2012). Receptor Kinase Signaling Pathways in Plant-Microbe Interactions. Annual Review of Phytopathology *50*, 451–473.

Bache, K.G., Stuffers, S., Malerød, L., Slagsvold, T., Raiborg, C., Lechardeur, D., Wälchli, S., Lukacs, G.L., Brech, A., and Stenmark, H. (2006). The ESCRT-III Subunit hVps24 Is Required for Degradation but Not Silencing of the Epidermal Growth Factor Receptor. Mol. Biol. Cell *17*, 2513–2523.

Bai, Y., Vaddepalli, P., Fulton, L., Bhasin, H., Hülskamp, M., and Schneitz, K. (2013). ANGUSTIFOLIA is a central component of tissue morphogenesis mediated by the atypical receptor-like kinase STRUBBELIG. BMC Plant Biology *13*, 16.

Bandmann, V., and Homann, U. (2012). Clathrin-independent endocytosis contributes to uptake of glucose into BY-2 protoplasts. The Plant Journal *70*, 578–584.

Bar, M., and Avni, A. (2009). EHD2 inhibits ligand-induced endocytosis and signaling of the leucine-rich repeat receptor-like protein LeEix2. The Plant Journal *59*, 600–611.

Barberon, M., Zelazny, E., Robert, S., Conéjéro, G., Curie, C., Friml, J., and Vert, G. (2011). Monoubiquitin-dependent endocytosis of the IRON-REGULATED TRANSPORTER 1 (IRT1) transporter controls iron uptake in plants. PNAS *108*, E450–E458.

Bashline, L., Li, S., Anderson, C.T., Lei, L., and Gu, Y. (2013). The endocytosis of cellulose synthase in Arabidopsis is dependent on μ2, a clathrin mediated endocytosis adaptin. Plant Physiol.

Beck, M., Zhou, J., Faulkner, C., MacLean, D., and Robatzek, S. (2012). Spatio-Temporal Cellular Dynamics of the Arabidopsis Flagellin Receptor Reveal Activation Status-Dependent Endosomal Sorting. Plant Cell *24*, 4205–4219.

Bednarek, S.Y., and Backues, S.K. (2010). Plant dynamin-related protein families DRP1 and DRP2 in plant development. Biochemical Society Transactions *38*, 797.

Beguinot, L., Lyall, R.M., Willingham, M.C., and Pastan, I. (1984). Down-regulation of the epidermal growth factor receptor in KB cells is due to receptor internalization and subsequent degradation in lysosomes. PNAS *81*, 2384–2388.

Bliek, A.M., Redelmeier, T.E., Damke, H., Tisdale, E.J., Meyerowitz, E.M., and Schmid, S.L. (1993). Mutations in human dynamin block an intermediate stage in coated vesicle formation. J. Cell Biol. *122*, 553–563.

Bolte, S., Talbot, C., Boutte, Y., Catrice, O., Read, N.D., and Satiat-Jeunemaitre, B. (2004). FM-dyes as experimental probes for dissecting vesicle trafficking in living plant cells. Journal of Microscopy *214*, 159–173.

Braun, D.M., Stone, J.M., and Walker, J.C. (1997). Interaction of the maize and Arabidopsis kinase interaction domains with a subset of receptor-like protein kinases: implications for transmembrane signaling in plants. The Plant Journal *12*, 83–95.

Bücherl, C.A., Van Esse, G.W., Kruis, A., Luchtenberg, J., Westphal, A.H., Aker, J., Van Hoek, A., Albrecht, C., Borst, J.W., and De Vries, S.C. (2013). Visualization of BRI1 and BAK1(SERK3) membrane receptor hetero-oligomers during brassinosteroid signaling. Plant Physiol.

Butenko, M.A., Shi, C.-L., and Aalen, R.B. (2012). KNAT1, KNAT2 and KNAT6 Act Downstream in the IDA-HAE/HSL2 Signaling Pathway to Regulate Floral Organ Abscission. Plant Signaling & Behavior *7*, 135–138.

Cabrillac, D., Cock, J.M., Dumas, C., and Gaude, T. (2001). The S-locus receptor kinase is inhibited by thioredoxins and activated by pollen coat proteins. Nature *410*, 220–223.

Cao, X., Li, K., Suh, S.-G., Guo, T., and Becraft, P.W. (2005). Molecular analysis of the CRINKLY4 gene family in Arabidopsis thaliana. Planta *220*, 645–657.

Cao, Y., Aceti, D.J., Sabat, G., Song, J., Makino, S., Fox, B.G., and Bent, A.F. (2013). Mutations in FLS2 Ser-938 Dissect Signaling Activation in FLS2-Mediated Arabidopsis Immunity. PLoS Pathog *9*, e1003313.

Castells, E., and Casacuberta, J.M. (2007). Signalling through kinase-defective domains: the prevalence of atypical receptor-like kinases in plants. J. Exp. Bot. *58*, 3503–3511.

Castells, E., Puigdomènech, P., and Casacuberta, J.M. (2006). Regulation of the kinase activity of the MIK GCK-like MAP4K by alternative splicing. Plant Mol Biol *61*, 747–756.

Ceresa, B.P. (2005). rab7 Activity Affects Epidermal Growth Factor:Epidermal Growth Factor Receptor Degradation by Regulating Endocytic Trafficking from the Late Endosome. Journal of Biological Chemistry *281*, 1099–1106.

Chen, F., Gao, M.-J., Miao, Y.-S., Yuan, Y.-X., Wang, M.-Y., Li, Q., Mao, B.-Z., Jiang, L.-W., and He, Z.-H. (2010a). Plasma membrane localization and potential endocytosis of constitutively expressed XA21 proteins in transgenic rice. Mol Plant *3*, 917–926.

Chen, X., Chern, M., Canlas, P.E., Jiang, C., Ruan, D., Cao, P., and Ronald, P.C. (2010b). A Conserved Threonine Residue in the Juxtamembrane Domain of the XA21 Pattern Recognition Receptor Is Critical for Kinase Autophosphorylation and XA21-mediated Immunity. J. Biol. Chem. *285*, 10454–10463.

Chen, X., Irani, N.G., and Friml, J. (2011). Clathrin-mediated endocytosis: the gateway into plant cells. Current Opinion in Plant Biology *14*, 674–682.

Cheng, W., Munkvold, K.R., Gao, H., Mathieu, J., Schwizer, S., Wang, S., Yan, Y., Wang, J., Martin, G.B., and Chai, J. (2011). Structural Analysis of Pseudomonas syringae AvrPtoB Bound to Host BAK1 Reveals Two Similar Kinase-Interacting Domains in a Type III Effector. Cell Host & Microbe *10*, 616–626.

Cheung, A.Y., and Wu, H.-M. (2011). THESEUS 1, FERONIA and relatives: a family of cell wall-sensing receptor kinases? Current Opinion in Plant Biology *14*, 632–641.

Chinchilla, D., Boller, T., and Robatzek, S. (2007). Flagellin Signalling in Plant Immunity. In Current Topics in Innate Immunity, J.D. Lambris, ed. (Springer New York), pp. 358–371.

Chudakov, D.M., Matz, M.V., Lukyanov, S., and Lukyanov, K.A. (2010). Fluorescent Proteins and Their Applications in Imaging Living Cells and Tissues. Physiol Rev *90*, 1103–1163.

Clough, S.J., and Bent, A.F. (1998). Floral dip: a simplified method forAgrobacterium-mediated transformation ofArabidopsis thaliana. The Plant Journal *16*, 735–743.

Clouse, S.D. (2011). Brassinosteroid Signal Transduction: From Receptor Kinase Activation to Transcriptional Networks Regulating Plant Development. Plant Cell *23*, 1219–1230.

Cock, J.M., Vanoosthuyse, V., and Gaude, T. (2002). Receptor kinase signalling in plants and animals: distinct molecular systems with mechanistic similarities. Current Opinion in Cell Biology *14*, 230–236.

Collings, D.A., Gebbie, L.K., Howles, P.A., Hurley, U.A., Birch, R.J., Cork, A.H., Hocart, C.H., Arioli, T., and Williamson, R.E. (2008). Arabidopsis dynamin-like protein DRP1A: a null mutant with widespread defects in endocytosis, cellulose synthesis, cytokinesis, and cell expansion. J. Exp. Bot. *59*, 361–376.

Combet, C., Blanchet, C., Geourjon, C., and Deléage, G. (2000). NPS@: network protein sequence analysis. Trends Biochem. Sci. *25*, 147–150.

Contento, A.L., and Bassham, D.C. (2012). Structure and function of endosomes in plant cells. J Cell Sci *125*, 3511–3518.

Cymer, F., and Schneider, D. (2010). Transmembrane helix-helix interactions involved in ErbB receptor signaling. Cell Adh Migr *4*, 299–312.

Damke, H., Baba, T., Warnock, D.E., and Schmid, S.L. (1994). Induction of mutant dynamin specifically blocks endocytic coated vesicle formation. J. Cell Biol. *127*, 915–934.

Delorme, V., Giranton, J.-L., Hatzfeld, Y., Friry, A., Heizmann, P., Ariza, M.J., Dumas, C., Gaude, T., and Cock, J.M. (1995). Characterization of the S locus genes, SLG and SRK, of the Brassica S3 haplotype: identification of a membrane-localized protein encoded by the S locus receptor kinase gene. The Plant Journal *7*, 429–440.

Dettmer, J., Hong-Hermesdorf, A., Stierhof, Y.-D., and Schumacher, K. (2006). Vacuolar H+-ATPase Activity Is Required for Endocytic and Secretory Trafficking in Arabidopsis. Plant Cell *18*, 715–730.

Dhonukshe, P., Baluska, F., Schlicht, M., Hlavacka, A., Samaj, J., Friml, J., and Gadella, T.W.J., Jr (2006). Endocytosis of cell surface material mediates cell plate formation during plant cytokinesis. Dev. Cell *10*, 137–150.

Dhonukshe, P., Aniento, F., Hwang, I., Robinson, D.G., Mravec, J., Stierhof, Y.-D., and Friml, J. (2007). Clathrin-Mediated Constitutive Endocytosis of PIN Auxin Efflux Carriers in Arabidopsis. Current Biology *17*, 520–527.

Dhonukshe, P., Tanaka, H., Goh, T., Ebine, K., Mähönen, A.P., Prasad, K., Blilou, I., Geldner, N., Xu, J., Uemura, T., et al. (2008). Generation of cell polarity in plants links endocytosis, auxin distribution and cell fate decisions. Nature *456*, 962–966.

Ding, Z., Wang, H., Liang, X., Morris, E.R., Gallazzi, F., Pandit, S., Skolnick, J., Walker, J.C., and Van Doren, S.R. (2007). Phosphoprotein and Phosphopeptide Interactions with the FHA Domain from Arabidopsis Kinase-Associated Protein Phosphatase†. Biochemistry *46*, 2684–2696.

Dinkel, H., Michael, S., Weatheritt, R.J., Davey, N.E., Van Roey, K., Altenberg, B., Toedt, G., Uyar, B., Seiler, M., Budd, A., et al. (2012). ELM--the database of eukaryotic linear motifs. Nucleic Acids Res. *40*, D242–251.

Doherty, G.J., and McMahon, H.T. (2009). Mechanisms of Endocytosis. Annual Review of Biochemistry *78*, 857–902.

Dong, J., Xiao, F., Fan, F., Gu, L., Cang, H., Martin, G.B., and Chai, J. (2009). Crystal Structure of the Complex between Pseudomonas Effector AvrPtoB and the Tomato Pto Kinase Reveals Both a Shared and a Unique Interface Compared with AvrPto-Pto. Plant Cell *21*, 1846–1859.

Durocher, D., Taylor, I.A., Sarbassova, D., Haire, L.F., Westcott, S.L., Jackson, S.P., Smerdon, S.J., and Yaffe, M.B. (2000). The Molecular Basis of FHA Domain:Phosphopeptide Binding Specificity and Implications for Phospho-Dependent Signaling Mechanisms. Molecular Cell *6*, 1169–1182.

Ebine, K., Fujimoto, M., Okatani, Y., Nishiyama, T., Goh, T., Ito, E., Dainobu, T., Nishitani, A., Uemura, T., Sato, M.H., et al. (2011). A membrane trafficking pathway regulated by the plant-specific RAB GTPase ARA6. Nature Cell Biology *13*, 853–859.

Endres, N.F., Das, R., Smith, A.W., Arkhipov, A., Kovacs, E., Huang, Y., Pelton, J.G., Shan, Y., Shaw, D.E., Wemmer, D.E., et al. (2013). Conformational Coupling across the Plasma Membrane in Activation of the EGF Receptor. Cell *152*, 543–556.

Fan, L., Hao, H., Xue, Y., Zhang, L., Song, K., Ding, Z., Botella, M.A., Wang, H., and Lin, J. (2013). Dynamic analysis of Arabidopsis AP2 σ subunit reveals a key role in clathrin-mediated endocytosis and plant development. Development.

Fasano, J.M., Swanson, S.J., Blancaflor, E.B., Dowd, P.E., Kao, T., and Gilroy, S. (2001). Changes in Root Cap pH Are Required for the Gravity Response of the Arabidopsis Root. Plant Cell *13*, 907–921.

Finger, C., Escher, C., and Schneider, D. (2009). The Single Transmembrane Domains of Human Receptor Tyrosine Kinases Encode Self-Interactions. Science Signaling *2*, ra56–ra56.

Fisher, C.L., and Pei, G.K. (1997). Modification of a PCR-based site-directed mutagenesis method. BioTechniques *23*, 570–571, 574.

Fobis-Loisy, I., Chambrier, P., and Gaude, T. (2007). Genetic transformation of Arabidopsis lyrata: specific expression of the green fluorescent protein (GFP) in pistil tissues. Plant Cell Rep *26*, 745–753.

Friedrichsen, D.M., Joazeiro, C.A., Li, J., Hunter, T., and Chory, J. (2000). Brassinosteroid-insensitive-1 is a ubiquitously expressed leucine-rich repeat receptor serine/threonine kinase. Plant Physiol. *123*, 1247–1256.

Fujimoto, M., and Ueda, T. (2012). Conserved and Plant-Unique Mechanisms Regulating Plant Post-Golgi Traffic. Frontiers in Plant Science *3*.

Fujimoto, M., Arimura, S., Ueda, T., Takanashi, H., Hayashi, Y., Nakano, A., and Tsutsumi, N. (2010). Arabidopsis dynamin-related proteins DRP2B and DRP1A participate together in clathrin-coated vesicle formation during endocytosis. PNAS *107*, 6094–6099.

Galperin, E., and Sorkin, A. (2008). Endosomal Targeting of MEK2 Requires RAF, MEK Kinase Activity and Clathrin-Dependent Endocytosis. Traffic *9*, 1776–1790.

Gaude, T., Friry, A., Heizmann, P., Mariac, C., Rougier, M., Fobis, I., and Dumas, C. (1993). Expression of a self-incompatibility gene in a self-compatible line of Brassica oleracea. Plant Cell *5*, 75–86.

Gaude, T., Fobis-Loisy, I., and Miège, C. Control of fertilization by self-incompatibility mechanisms. In The Molecular Biology and Biotechnology of Flowering, B.R. Jordan, ed. (Wallingford: CABI), pp. 269–297.

Geldner, N., and Robatzek, S. (2008). Plant Receptors Go Endosomal: A Moving View on Signal Transduction. Plant Physiol. *147*, 1565–1574.

Geldner, N., Anders, N., Wolters, H., Keicher, J., Kornberger, W., Muller, P., Delbarre, A., Ueda, T., Nakano, A., and Jürgens, G. (2003). The Arabidopsis GNOM ARF-GEF Mediates Endosomal Recycling, Auxin Transport, and Auxin-Dependent Plant Growth. Cell *112*, 219–230.

Geldner, N., Hyman, D.L., Wang, X., Schumacher, K., and Chory, J. (2007). Endosomal signaling of plant steroid receptor kinase BRI1. Genes Dev. *21*, 1598–1602.

Geldner, N., Dénervaud-Tendon, V., Hyman, D.L., Mayer, U., Stierhof, Y.-D., and Chory, J. (2009). Rapid, combinatorial analysis of membrane compartments in intact plants with a multicolor marker set. The Plant Journal *59*, 169–178.

Gidalevitz, T., Stevens, F., and Argon, Y. (2013). Orchestration of secretory protein folding by ER chaperones. Biochim. Biophys. Acta *1833*, 2410–2424.

Gifford, M.L., Dean, S., and Ingram, G.C. (2003). The Arabidopsis ACR4 gene plays a role in cell layer organisation during ovule integument and sepal margin development. Development *130*, 4249–4258.

Gifford, M.L., Robertson, F.C., Soares, D.C., and Ingram, G.C. (2005). ARABIDOPSIS CRINKLY4 Function, Internalization, and Turnover Are Dependent on the Extracellular Crinkly Repeat Domain. Plant Cell *17*, 1154–1166.

Giranton, J.-L., Dumas, C., Cock, J.M., and Gaude, T. (2000). The integral membrane S-locus receptor kinase of Brassica has serine/threonine kinase activity in a membranous environment and spontaneously forms oligomers in planta. Proceedings of the National Academy of Sciences *97*, 3759–3764.

Gish, L.A., and Clark, S.E. (2011). The RLK/Pelle family of kinases. The Plant Journal *66*, 117–127.

Gómez-Gómez, L., Bauer, Z., and Boller, T. (2001). Both the Extracellular Leucine-Rich Repeat Domain and the Kinase Activity of FLS2 Are Required for Flagellin Binding and Signaling in Arabidopsis. Plant Cell *13*, 1155–1163.

Gonnord, P., Blouin, C.M., and Lamaze, C. (2012). Membrane trafficking and signaling: Two sides of the same coin. Seminars in Cell & Developmental Biology *23*, 154–164.

Greeff, C., Roux, M., Mundy, J., and Petersen, M. (2012). Receptor-like kinase complexes in plant innate immunity. Front. Plant Sci. *3*, 209.

Griesbeck, O., Baird, G.S., Campbell, R.E., Zacharias, D.A., and Tsien, R.Y. (2001). Reducing the environmental sensitivity of yellow fluorescent protein. Mechanism and applications. J. Biol. Chem. *276*, 29188–29194.

Gu, T., Mazzurco, M., Sulaman, W., Matias, D.D., and Goring, D.R. (1998). Binding of an arm repeat protein to the kinase domain of the S-locus receptor kinase. PNAS *95*, 382–387.

Guglielmo, G.M.D., Baass, P.C., Ou, W.J., Posner, B.I., and Bergeron, J.J. (1994). Compartmentalization of SHC, GRB2 and mSOS, and hyperphosphorylation of Raf-1 by EGF but not insulin in liver parenchyma. The EMBO Journal *13*, 4269.

Haas, T.J., Sliwinski, M.K., Martínez, D.E., Preuss, M., Ebine, K., Ueda, T., Nielsen, E., Odorizzi, G., and Otegui, M.S. (2007). The Arabidopsis AAA ATPase SKD1 Is Involved in Multivesicular Endosome Function and Interacts with Its Positive Regulator LYST-INTERACTING PROTEIN5. Plant Cell *19*, 1295–1312.

Hackett, R.M., Cadwallader, G., and Franklin, F.C. (1996). Functional analysis of a Brassica oleracea SLR1 gene promoter. Plant Physiol. *112*, 1601–1607.

Haglund, K., and Dikic, I. (2012). The role of ubiquitylation in receptor endocytosis and endosomal sorting. Journal of Cell Science *125*, 265–275.

Haugh, J.M., and Meyer, T. (2002). Active EGF receptors have limited access to PtdIns(4,5)P2 in endosomes: implications for phospholipase C and PI 3-kinase signaling. J Cell Sci *115*, 303–310.

Heese, A., Hann, D.R., Gimenez-Ibanez, S., Jones, A.M.E., He, K., Li, J., Schroeder, J.I., Peck, S.C., and Rathjen, J.P. (2007). The receptor-like kinase SERK3/BAK1 is a central regulator of innate immunity in plants. PNAS *104*, 12217–12222.

Hellens, R., Mullineaux, P., and Klee, H. (2000). Technical Focus:a guide to Agrobacterium binary Ti vectors. Trends Plant Sci. *5*, 446–451.

Herskovits, J.S., Burgess, C.C., Obar, R.A., and Vallee, R.B. (1993). Effects of mutant rat dynamin on endocytosis. J. Cell Biol. *122*, 565–578.

Heukers, R., Vermeulen, J.F., Fereidouni, F., Bader, A.N., Voortman, J., Roovers, R.C., Gerritsen, H.C., and Van Bergen En Henegouwen, P.M.P. (2013). EGFR endocytosis requires its kinase activity and N-terminal transmembrane dimerization motif. J. Cell. Sci.

Hink, M.A., Shah, K., Russinova, E., De Vries, S.C., and Visser, A.J.W.G. (2008). Fluorescence Fluctuation Analysis of Arabidopsis thaliana Somatic Embryogenesis Receptor-Like Kinase and Brassinosteroid Insensitive 1 Receptor Oligomerization. Biophysical Journal *94*, 1052–1062.

Hong, Z., Geisler-Lee, C.J., Zhang, Z., and Verma, D.P.S. (2003). Phragmoplastin dynamics: multiple forms, microtubule association and their roles in cell plate formation in plants. Plant Mol Biol *53*, 297–312.

Hothorn, M., Belkhadir, Y., Dreux, M., Dabi, T., Noel, J.P., Wilson, I.A., and Chory, J. (2011). Structural basis of steroid hormone perception by the receptor kinase BRI1. Nature *474*, 467–471.

Howe, C.L. (2005). Modeling the signaling endosome hypothesis: Why a drive to the nucleus is better than a (random) walk. Theoretical Biology and Medical Modelling *2*, 43.

Howe, C.L., Valletta, J.S., Rusnak, A.S., and Mobley, W.C. (2001). NGF Signaling from Clathrin-Coated Vesicles: Evidence that Signaling Endosomes Serve as a Platform for the Ras-MAPK Pathway. Neuron *32*, 801–814.

Huang, F., Goh, L.K., and Sorkin, A. (2007). EGF receptor ubiquitination is not necessary for its internalization. Proc. Natl. Acad. Sci. U.S.A. *104*, 16904–16909.

Huang, F., Zeng, X., Kim, W., Balasubramani, M., Fortian, A., Gygi, S.P., Yates, N.A., and Sorkin, A. (2013). Lysine 63-linked polyubiquitination is required for EGF receptor degradation. Proceedings of the National Academy of Sciences.

Hugly, S., and Somerville, C. (1992). A role for membrane lipid polyunsaturation in chloroplast biogenesis at low temperature. Plant Physiology *99*, 197–202.

Irani, N.G., and Russinova, E. (2009). Receptor endocytosis and signaling in plants. Current Opinion in Plant Biology *12*, 653–659.

Irani, N.G., Rubbo, S.D., Mylle, E., Begin, J.V. den, Schneider-Pizoń, J., Hniliková, J., Šíša, M., Buyst, D., Vilarrasa-Blasi, J., Szatmári, A.-M., et al. (2012). Fluorescent castasterone reveals BRI1 signaling from the plasma membrane. Nature Chemical Biology *8*, 583–589.

Ivanov, R., and Gaude, T. (2009). Endocytosis and Endosomal Regulation of the S-Receptor Kinase during the Self-Incompatibility Response in Brassica oleracea. Plant Cell *21*, 2107–2117.

Ivanov, R., Fobis-Loisy, I., and Gaude, T. (2010). When no means no: guide to Brassicaceae self-incompatibility. Trends in Plant Science *15*, 387–394.

Iwano, M., Shiba, H., Miwa, T., Che, F.-S., Takayama, S., Nagai, T., Miyawaki, A., and Isogai, A. (2004). Ca2+ Dynamics in a Pollen Grain and Papilla Cell during Pollination of Arabidopsis. Plant Physiol. *136*, 3562–3571.

Jaillais, Y., Fobis-Loisy, I., Miège, C., and Gaude, T. (2008). Evidence for a sorting endosome in Arabidopsis root cells. The Plant Journal *53*, 237–247.

Jaillais, Y., Hothorn, M., Belkhadir, Y., Dabi, T., Nimchuk, Z.L., Meyerowitz, E.M., and Chory, J. (2011). Tyrosine phosphorylation controls brassinosteroid receptor activation by triggering membrane release of its kinase inhibitor. Genes Dev. *25*, 232–237.

Jia, T., Gao, C., Cui, Y., Wang, J., Ding, Y., Cai, Y., Ueda, T., Nakano, A., and Jiang, L. (2013). ARA7(Q69L) expression in transgenic Arabidopsis cells induces the formation of enlarged multivesicular bodies. J. Exp. Bot.

Jiang, X., Huang, F., Marusyk, A., and Sorkin, A. (2003). Grb2 Regulates Internalization of EGF Receptors through Clathrin-coated Pits. Mol. Biol. Cell *14*, 858–870.

Johannessen, L.E., Ringerike, T., Molnes, J., and Madshus, I.H. (2000). Epidermal Growth Factor Receptor Efficiently Activates Mitogen-Activated Protein Kinase in HeLa Cells and Hep2 Cells Conditionally Defective in Clathrin-Dependent Endocytosis. Experimental Cell Research *260*, 136–145.

Johnson, L.N., Noble, M.E.., and Owen, D.J. (1996). Active and Inactive Protein Kinases: Structural Basis for Regulation. Cell *85*, 149–158.

Kakita, M., Murase, K., Iwano, M., Matsumoto, T., Watanabe, M., Shiba, H., Isogai, A., and Takayama, S. (2007a). Two Distinct Forms of M-Locus Protein Kinase Localize to the Plasma Membrane and Interact Directly with S-Locus Receptor Kinase to Transduce Self-Incompatibility Signaling in Brassica rapa. Plant Cell *19*, 3961–3973.

Kakita, M., Shimosato, H., Murase, K., Isogai, A., and Takayama, S. (2007b). Direct interaction between *S*-locus receptor kinase and *M*-locus protein kinase involved in *Brassica* self-incompatibility signaling. Plant Biotechnology *24*, 185–190.

Kang, B.-H., Busse, J.S., and Bednarek, S.Y. (2003). Members of the Arabidopsis Dynamin-Like Gene Family, ADL1, Are Essential for Plant Cytokinesis and Polarized Cell Growth. Plant Cell *15*, 899–913.

Karimi, M., Depicker, A., and Hilson, P. (2007). Recombinational Cloning with Plant Gateway Vectors. PLANT PHYSIOLOGY *145*, 1144–1154.

Kasai, K., Takano, J., Miwa, K., Toyoda, A., and Fujiwara, T. (2011). High Boron-induced Ubiquitination Regulates Vacuolar Sorting of the BOR1 Borate Transporter in Arabidopsis thaliana. J. Biol. Chem. *286*, 6175–6183.

Katsir, L., Davies, K.A., Bergmann, D.C., and Laux, T. (2011). Peptide Signaling in Plant Development. Current Biology *21*, R356–R364.

Kay, B.K., Williamson, M.P., and Sudol, M. (2000). The importance of being proline: the interaction of proline-rich motifs in signaling proteins with their cognate domains. FASEB J *14*, 231–241.

Kazazic, M., Bertelsen, V., Pedersen, K.W., Vuong, T.T., Grandal, M.V., Rødland, M.S., Traub, L.M., Stang, E., and Madshus, I.H. (2009). Epsin 1 is Involved in Recruitment of Ubiquitinated EGF Receptors into Clathrin-Coated Pits. Traffic *10*, 235–245.

Kim, H.H., Vijapurkar, U., Hellyer, N.J., Bravo, D., and Koland, J.G. (1998). Signal transduction by epidermal growth factor and heregulin via the kinase-deficient ErbB3 protein. Biochem. J. *334 (Pt 1)*, 189–195.

Kim, S.Y., Xu, Z.-Y., Song, K., Kim, D.H., Kang, H., Reichardt, I., Sohn, E.J., Friml, J., Juergens, G., and Hwang, I. (2013). Adaptor Protein Complex 2-Mediated Endocytosis Is Crucial for Male Reproductive Organ Development in Arabidopsis. The Plant Cell.

Kim, T.-W., Guan, S., Sun, Y., Deng, Z., Tang, W., Shang, J.-X., Sun, Y., Burlingame, A.L., and Wang, Z.-Y. (2009). Brassinosteroid signal transduction from cell-surface receptor kinases to nuclear transcription factors. Nature Cell Biology *11*, 1254–1260.

Kirchhausen, T., Macia, E., and Pelish, H.E. (2008). Use of Dynasore, the Small Molecule Inhibitor of Dynamin, in the Regulation of Endocytosis. In Methods in Enzymology, C.J.D. and A.H. William E. Balch, ed. (Academic Press), pp. 77–93.

Kitakura, S., Vanneste, S., Robert, S., Löfke, C., Teichmann, T., Tanaka, H., and Friml, J. (2011). Clathrin Mediates Endocytosis and Polar Distribution of PIN Auxin Transporters in Arabidopsis. Plant Cell *23*, 1920–1931.

Kitashiba, H., Liu, P., Nishio, T., Nasrallah, J.B., and Nasrallah, M.E. (2011). Functional test of Brassica self-incompatibility modifiers in Arabidopsis thaliana. Proc. Natl. Acad. Sci. U.S.A. *108*, 18173–18178.

Klaus-Heisen, D., Nurisso, A., Pietraszewska-Bogiel, A., Mbengue, M., Camut, S., Timmers, T., Pichereaux, C., Rossignol, M., Gadella, T.W.J., Imberty, A., et al. (2011). Structure-Function Similarities between a Plant Receptor-like Kinase and the Human Interleukin-1 Receptor-associated Kinase-4. J. Biol. Chem. *286*, 11202–11210.

Kleine-Vehn, J., Wabnik, K., Martinière, A., Łangowski, Ł., Willig, K., Naramoto, S., Leitner, J., Tanaka, H., Jakobs, S., Robert, S., et al. (2011). Recycling, clustering, and endocytosis jointly maintain PIN auxin carrier polarity at the plasma membrane. Molecular Systems Biology *7*.

Komander, D., and Rape, M. (2012). The ubiquitin code. Annu. Rev. Biochem. *81*, 203–229.

Konopka, C.A., and Bednarek, S.Y. (2008). Comparison of the Dynamics and Functional Redundancy of the Arabidopsis Dynamin-Related Isoforms DRP1A and DRP1C during Plant Development. Plant Physiol. *147*, 1590–1602.

Konopka, C.A., Backues, S.K., and Bednarek, S.Y. (2008). Dynamics of Arabidopsis Dynamin-Related Protein 1C and a Clathrin Light Chain at the Plasma Membrane. Plant Cell *20*, 1363–1380.

Kost, B., Lemichez, E., Spielhofer, P., Hong, Y., Tolias, K., Carpenter, C., and Chua, N.-H. (1999). Rac Homologues and Compartmentalized Phosphatidylinositol 4, 5-Bisphosphate Act in a Common Pathway to Regulate Polar Pollen Tube Growth. J Cell Biol *145*, 317–330.

Kotzer, A.M., Brandizzi, F., Neumann, U., Paris, N., Moore, I., and Hawes, C. (2004). AtRabF2b (Ara7) acts on the vacuolar trafficking pathway in tobacco leaf epidermal cells. J Cell Sci *117*, 6377–6389.

Kurten, R.C. (2003). Sorting motifs in receptor trafficking. Advanced Drug Delivery Reviews *55*, 1405–1419.

Kusaba, M., Dwyer, K., Hendershot, J., Vrebalov, J., Nasrallah, J.B., and Nasrallah, M.E. (2001). Self-Incompatibility in the Genus Arabidopsis: Characterization of the S Locus in the Outcrossing A. lyrata and Its Autogamous Relative A. thaliana. Plant Cell *13*, 627–643.

Lam, B.C.-H., Sage, T.L., Bianchi, F., and Blumwald, E. (2002). Regulation of ADL6 activity by its associated molecular network. The Plant Journal *31*, 565–576.

Lee, G.-J., Sohn, E.J., Lee, M.H., and Hwang, I. (2004). The Arabidopsis Rab5 Homologs Rha1 and Ara7 Localize to the Prevacuolar Compartment. Plant Cell Physiol *45*, 1211–1220.

Lee, Y., Bak, G., Choi, Y., Chuang, W.-I., Cho, H.-T., and Lee, Y. (2008). Roles of Phosphatidylinositol 3-Kinase in Root Hair Growth. Plant Physiol. *147*, 624–635.

Lefebvre, B., Klaus-Heisen, D., Pietraszewska-Bogiel, A., Herve, C., Camut, S., Auriac, M.-C., Gasciolli, V., Nurisso, A., Gadella, T.W.J., and Cullimore, J. (2012). Role of N-Glycosylation Sites and CXC Motifs in Trafficking of Medicago truncatula Nod Factor Perception Protein to Plasma Membrane. Journal of Biological Chemistry *287*, 10812–10823.

Lemmon, M.A., and Schlessinger, J. (2010). Cell Signaling by Receptor Tyrosine Kinases. Cell *141*, 1117–1134.

Li, J., Wen, J., Lease, K.A., Doke, J.T., Tax, F.E., and Walker, J.C. (2002). BAK1, an Arabidopsis LRR Receptor-like Protein Kinase, Interacts with BRI1 and Modulates Brassinosteroid Signaling. Cell *110*, 213–222.

Li, R., Liu, P., Wan, Y., Chen, T., Wang, Q., Mettbach, U., Baluška, F., Šamaj, J., Fang, X., Lucas, W.J., et al. (2012). A Membrane Microdomain-Associated Protein, Arabidopsis Flot1, Is Involved in a Clathrin-Independent Endocytic Pathway and Is Required for Seedling Development. Plant Cell *24*, 2105–2122.

Liu, G.-Z., Pi, L.-Y., Walker, J.C., Ronald, P.C., and Song, W.-Y. (2002). Biochemical Characterization of the Kinase Domain of the Rice Disease Resistance Receptor-like Kinase XA21. J. Biol. Chem. *277*, 20264–20269.

Liu, S.-H., Wong, M.L., Craik, C.S., and Brodsky, F.M. (1995). Regulation of clathrin assembly and trimerization defined using recombinant triskelion hubs. Cell *83*, 257–267.

Liu, S.-H., Marks, M.S., and Brodsky, F.M. (1998). A Dominant-negative Clathrin Mutant Differentially Affects Trafficking of Molecules with Distinct Sorting Motifs in the Class II Major Histocompatibility Complex (MHC) Pathway. J Cell Biol *140*, 1023–1037.

Llompart, B., Castells, E., Río, A., Roca, R., Ferrando, A., Stiefel, V., Puigdomènech, P., and Casacuberta, J.M. (2003). The Direct Activation of MIK, a Germinal Center Kinase (GCK)-like Kinase, by MARK, a Maize Atypical Receptor Kinase, Suggests a New Mechanism for Signaling through Kinase-dead Receptors. J. Biol. Chem. *278*, 48105–48111.

Lloyd, T.E., Atkinson, R., Wu, M.N., Zhou, Y., Pennetta, G., and Bellen, H.J. (2002). Hrs Regulates Endosome Membrane Invagination and Tyrosine Kinase Receptor Signaling in Drosophila. Cell *108*, 261–269.

Logemann, E., Birkenbihl, R.P., Ulker, B., and Somssich, I.E. (2006). An improved method for preparing Agrobacterium cells that simplifies the Arabidopsis transformation protocol. Plant Methods *2*, 16.

LOWRY, O.H., ROSEBROUGH, N.J., FARR, A.L., and RANDALL, R.J. (1951). Protein measurement with the Folin phenol reagent. J. Biol. Chem. *193*, 265–275.

Lu, D., Wu, S., Gao, X., Zhang, Y., Shan, L., and He, P. (2010). A receptor-like cytoplasmic kinase, BIK1, associates with a flagellin receptor complex to initiate plant innate immunity. PNAS *107*, 496–501.

Lu, D., Lin, W., Gao, X., Wu, S., Cheng, C., Avila, J., Heese, A., Devarenne, T.P., He, P., and Shan, L. (2011). Direct Ubiquitination of Pattern Recognition Receptor FLS2 Attenuates Plant Innate Immunity. Science *332*, 1439–1442.

Manabe, Y., Bressan, R.A., Wang, T., Li, F., Koiwa, H., Sokolchik, I., Li, X., and Maggio, A. (2008). The Arabidopsis Kinase-Associated Protein Phosphatase Regulates Adaptation to Na+ Stress. Plant Physiol. *146*, 612–622.

Manning, G., Whyte, D.B., Martinez, R., Hunter, T., and Sudarsanam, S. (2002). The Protein Kinase Complement of the Human Genome. Science *298*, 1912–1934.

Marks, B., Stowell, M.H.B., Vallis, Y., Mills, I.G., Gibson, A., Hopkins, C.R., and McMahon, H.T. (2001). GTPase activity of dynamin and resulting conformation change are essential for endocytosis. Nature *410*, 231–235.

McLaughlin, S. (2005). An Electrostatic Engine Model for Autoinhibition and Activation of the Epidermal Growth Factor Receptor (EGFR/ErbB) Family. The Journal of General Physiology *126*, 41–53.

McMahon, H.T., and Boucrot, E. (2011). Molecular mechanism and physiological functions of clathrin-mediated endocytosis. Nat Rev Mol Cell Biol *12*, 517–533.

Mooij, W.T.M., Mitsiki, E., and Perrakis, A. (2009). ProteinCCD: enabling the design of protein truncation constructs for expression and crystallization experiments. Nucleic Acids Res. *37*, W402–405.

Moscatelli, A., Ciampolini, F., Rodighiero, S., Onelli, E., Cresti, M., Santo, N., and Idilli, A. (2007). Distinct endocytic pathways identified in tobacco pollen tubes using charged nanogold. J Cell Sci *120*, 3804–3819.

Müller, R., Borghi, L., Kwiatkowska, D., Laufs, P., and Simon, R. (2006). Dynamic and Compensatory Responses of Arabidopsis Shoot and Floral Meristems to CLV3 Signaling. Plant Cell *18*, 1188–1198.

Murase, K., Shiba, H., Iwano, M., Che, F.-S., Watanabe, M., Isogai, A., and Takayama, S. (2004). A Membrane-Anchored Protein Kinase Involved in Brassica Self-Incompatibility Signaling. Science *303*, 1516–1519.

Murphy, J.E., Padilla, B.E., Hasdemir, B., Cottrell, G.S., and Bunnett, N.W. (2009). Endosomes: A legitimate platform for the signaling train. PNAS *106*, 17615–17622.

Naithani, S., Chookajorn, T., Ripoll, D.R., and Nasrallah, J.B. (2007). Structural modules for receptor dimerization in the S-locus receptor kinase extracellular domain. PNAS *104*, 12211–12216.

Naramoto, S., Kleine-Vehn, J., Robert, S., Fujimoto, M., Dainobu, T., Paciorek, T., Ueda, T., Nakano, A., Van Montagu, M.C.E., Fukuda, H., et al. (2010). ADP-ribosylation factor machinery mediates endocytosis in plant cells. Proceedings of the National Academy of Sciences *107*, 21890–21895.

Nasrallah, M.E., Liu, P., and Nasrallah, J.B. (2002). Generation of Self-Incompatible Arabidopsis thaliana by Transfer of Two S Locus Genes from A. lyrata. Science *297*, 247–249.

Nielsen, E., Cheung, A.Y., and Ueda, T. (2008). The Regulatory RAB and ARF GTPases for Vesicular Trafficking. Plant Physiol. *147*, 1516–1526.

Nimchuk, Z.L., Tarr, P.T., Ohno, C., Qu, X., and Meyerowitz, E.M. (2011). Plant Stem Cell Signaling Involves Ligand-Dependent Trafficking of the CLAVATA1 Receptor Kinase. Current Biology *21*, 345–352.

O'Malley, R.C., and Ecker, J.R. (2010). Linking genotype to phenotype using the Arabidopsis unimutant collection. The Plant Journal *61*, 928–940.

Oh, M.-H., Wang, X., Kota, U., Goshe, M.B., Clouse, S.D., and Huber, S.C. (2009). Tyrosine phosphorylation of the BRI1 receptor kinase emerges as a component of brassinosteroid signaling in Arabidopsis. PNAS *106*, 658–663.

Oh, M.-H., Wang, X., Wu, X., Zhao, Y., Clouse, S.D., and Huber, S.C. (2010). Autophosphorylation of Tyr-610 in the receptor kinase BAK1 plays a role in brassinosteroid signaling and basal defense gene expression. PNAS *107*, 17827–17832.

Onelli, E., Prescianotto-Baschong, C., Caccianiga, M., and Moscatelli, A. (2008). Clathrin-dependent and independent endocytic pathways in tobacco protoplasts revealed by labelling with charged nanogold. J. Exp. Bot. *59*, 3051–3068.

Ortiz-Zapater, E., Soriano-Ortega, E., Marcote, M.J., Ortiz-Masiá, D., and Aniento, F. (2006). Trafficking of the human transferrin receptor in plant cells: effects of tyrphostin A23 and brefeldin A. The Plant Journal *48*, 757–770.

Owen, D.J. (2004). Linking endocytic cargo to clathrin: structural and functional insights into coated vesicle formation. Biochem. Soc. Trans. *32*, 1–14.

Owen, D.M., Magenau, A., Williamson, D., and Gaus, K. (2012). The lipid raft hypothesis revisited - New insights on raft composition and function from super-resolution fluorescence microscopy. BioEssays *34*, 739–747.

Parton, R.G., and Del Pozo, M.A. (2013). Caveolae as plasma membrane sensors, protectors and organizers. Nature Reviews Molecular Cell Biology *14*, 98–112.

Parton, R.G., and Simons, K. (2007). The multiple faces of caveolae. Nature Reviews Molecular Cell Biology *8*, 185–194.

Pastuglia, M. (1997). Rapid Induction by Wounding and Bacterial Infection of an S Gene Family Receptor-like Kinase Gene in Brassica oleracea. THE PLANT CELL ONLINE *9*, 49–60.

Pillitteri, L.J., and Torii, K.U. (2012). Mechanisms of Stomatal Development. Annual Review of Plant Biology *63*, 591–614.

Polo, S., and Di Fiore, P.P. (2006). Endocytosis Conducts the Cell Signaling Orchestra. Cell *124*, 897–900.

Prigent, S.A., and Gullick, W.J. (1994). Identification of c-erbB-3 binding sites for phosphatidylinositol 3'-kinase and SHC using an EGF receptor/c-erbB-3 chimera. The EMBO Journal *13*, 2831.

Raffaele, S., Bayer, E., Lafarge, D., Cluzet, S., German Retana, S., Boubekeur, T., Leborgne-Castel, N., Carde, J.-P., Lherminier, J., Noirot, E., et al. (2009). Remorin, a Solanaceae Protein Resident in Membrane Rafts and Plasmodesmata, Impairs Potato virus X Movement. THE PLANT CELL ONLINE *21*, 1541–1555.

Reyes, F.C., Buono, R., and Otegui, M.S. (2011). Plant endosomal trafficking pathways. Current Opinion in Plant Biology *14*, 666–673.

Robatzek, S., and Wirthmueller, L. (2013). Mapping FLS2 function to structure: LRRs, kinase and its working bits. Protoplasma *250*, 671–681.

Robatzek, S., Chinchilla, D., and Boller, T. (2006). Ligand-induced endocytosis of the pattern recognition receptor FLS2 in Arabidopsis. Genes Dev. *20*, 537–542.

Robert, S., Chary, S.N., Drakakaki, G., Li, S., Yang, Z., Raikhel, N.V., and Hicks, G.R. (2008). Endosidin1 defines a compartment involved in endocytosis of the brassinosteroid receptor BRI1 and the auxin transporters PIN2 and AUX1. PNAS *105*, 8464–8469.

Robert, S., Kleine-Vehn, J., Barbez, E., Sauer, M., Paciorek, T., Baster, P., Vanneste, S., Zhang, J., Simon, S., Čovanová, M., et al. (2010). ABP1 Mediates Auxin Inhibition of Clathrin-Dependent Endocytosis in Arabidopsis. Cell *143*, 111–121.

Robinson, D.G., Jiang, L., and Schumacher, K. (2008). The Endosomal System of Plants: Charting New and Familiar Territories. Plant Physiol. *147*, 1482–1492.

Ron, M., and Avni, A. (2004). The Receptor for the Fungal Elicitor Ethylene-Inducing Xylanase Is a Member of a Resistance-Like Gene Family in Tomato. Plant Cell *16*, 1604–1615.

Rubbo, S., Irani, N.G., Kim, S.Y., Xu, Z.-Y., Gadeyne, A., Dejonghe, W., Vanhoutte, I., Persiau, G., Eeckhout, D., Simon, S., et al. (2013). The Clathrin Adaptor Complex AP-2 Mediates Endocytosis of BRASSINOSTEROID INSENSITIVE1 in Arabidopsis. Plant Cell.

Rush, J.S., and Ceresa, B.P. (2013). RAB7 and TSG101 are required for the constitutive recycling of unliganded EGFRs via distinct mechanisms. Mol. Cell. Endocrinol.

Russinova, E., Borst, J.-W., Kwaaitaal, M., Caño-Delgado, A., Yin, Y., Chory, J., and Vries, S.C. de (2004). Heterodimerization and Endocytosis of Arabidopsis Brassinosteroid Receptors BRI1 and AtSERK3 (BAK1). Plant Cell *16*, 3216–3229.

Samaddar, S., Dutta, A., Sinharoy, S., Paul, A., Bhattacharya, A., Saha, S., Chien, K., Goshe, M.B., and DasGupta, M. (2013). Autophosphorylation of gatekeeper tyrosine by symbiosis receptor kinase. FEBS Letters.

Šamaj, J., Baluška, F., Voigt, B., Schlicht, M., Volkmann, D., and Menzel, D. (2004). Endocytosis, Actin Cytoskeleton, and Signaling. Plant Physiol. *135*, 1150–1161.

Samuel, M.A., Chong, Y.T., Haasen, K.E., Aldea-Brydges, M.G., Stone, S.L., and Goring, D.R. (2009). Cellular Pathways Regulating Responses to Compatible and Self-Incompatible Pollen in Brassica and Arabidopsis Stigmas Intersect at Exo70A1, a Putative Component of the Exocyst Complex. Plant Cell *21*, 2655–2671.

Santiago, J., Henzler, C., and Hothorn, M. (2013). Molecular Mechanism for Plant Steroid Receptor Activation by Somatic Embryogenesis Co-Receptor Kinases. Science.

Sarker, R.H., Elleman, C.J., and Dickinson, H.G. (1988). Control of pollen hydration in Brassica requires continued protein synthesis, and glycosylation in necessary for intraspecific incompatibility. PNAS *85*, 4340–4344.

Sauer, M., Delgadillo, M.O., Zouhar, J., Reynolds, G.D., Pennington, J.G., Jiang, L., Liljegren, S.J., Stierhof, Y.-D., Jaeger, G.D., Otegui, M.S., et al. (2013). MTV1 and MTV4 Encode Plant-Specific ENTH and ARF GAP Proteins That Mediate Clathrin-Dependent Trafficking of Vacuolar Cargo from the Trans-Golgi Network. Plant Cell *25*, 2217–2235.

Sawa, S., Koizumi, K., Naramoto, S., Demura, T., Ueda, T., Nakano, A., and Fukuda, H. (2005). DRP1A Is Responsible for Vascular Continuity Synergistically Working with VAN3 in Arabidopsis. Plant Physiol. *138*, 819–826.

Scheuring, D., Viotti, C., Krüger, F., Künzl, F., Sturm, S., Bubeck, J., Hillmer, S., Frigerio, L., Robinson, D.G., Pimpl, P., et al. (2011). Multivesicular Bodies Mature from the Trans-Golgi Network/Early Endosome in Arabidopsis. Plant Cell *23*, 3463–3481.

Scheuring, D., Künzl, F., Viotti, C., Yan, M.S.W., Jiang, L., Schellmann, S., Robinson, D.G., and Pimpl, P. (2012). Ubiquitin initiates sorting of Golgi and plasma membrane proteins into the vacuolar degradation pathway. BMC Plant Biology *12*, 164.

Schmittgen, T.D., and Livak, K.J. (2008). Analyzing real-time PCR data by the comparative C(T) method. Nat Protoc *3*, 1101–1108.

Schulze, B., Mentzel, T., Jehle, A.K., Mueller, K., Beeler, S., Boller, T., Felix, G., and Chinchilla, D. (2010). Rapid Heteromerization and Phosphorylation of Ligand-activated Plant Transmembrane Receptors and Their Associated Kinase BAK1. J. Biol. Chem. *285*, 9444–9451.

Schwessinger, B., and Ronald, P.C. (2012). Plant Innate Immunity: Perception of Conserved Microbial Signatures. Annual Review of Plant Biology *63*, 451–482.

Serrano, M., Robatzek, S., Torres, M., Kombrink, E., Somssich, I.E., Robinson, M., and Schulze-Lefert, P. (2007). Chemical Interference of Pathogen-associated Molecular Pattern-triggered Immune Responses in Arabidopsis Reveals a Potential Role for Fatty-acid Synthase Type II Complex-derived Lipid Signals. J. Biol. Chem. *282*, 6803–6811.

Shah, K., Russinova, E., Gadella, T.W.J., Willemse, J., and Vries, S.C. de (2002). The Arabidopsis kinase-associated protein phosphatase controls internalization of the somatic embryogenesis receptor kinase 1. Genes Dev. *16*, 1707–1720.

Shaner, N.C., Campbell, R.E., Steinbach, P.A., Giepmans, B.N.G., Palmer, A.E., and Tsien, R.Y. (2004). Improved monomeric red, orange and yellow fluorescent proteins derived from Discosoma sp. red fluorescent protein. Nat. Biotechnol. *22*, 1567–1572.

Sharfman, M., Bar, M., Ehrlich, M., Schuster, S., Melech-Bonfil, S., Ezer, R., Sessa, G., and Avni, A. (2011). Endosomal signaling of the tomato leucine-rich repeat receptor-like protein LeEix2. The Plant Journal *68*, 413–423.

She, J., Han, Z., Kim, T.-W., Wang, J., Cheng, W., Chang, J., Shi, S., Wang, J., Yang, M., Wang, Z.-Y., et al. (2011). Structural insight into brassinosteroid perception by BRI1. Nature *474*, 472–476.

Shen, J., Zeng, Y., Zhuang, X., Sun, L., Yao, X., Pimpl, P., and Jiang, L. (2013). Organelle pH in the Arabidopsis Endomembrane System. Mol. Plant.

Shimosato, H., Yokota, N., Shiba, H., Iwano, M., Entani, T., Che, F.-S., Watanabe, M., Isogai, A., and Takayama, S. (2007). Characterization of the SP11/SCR High-Affinity

Binding Site Involved in Self/Nonself Recognition in Brassica Self-Incompatibility. Plant Cell *19*, 107–117.

Shiu, S.-H., and Bleecker, A.B. (2001a). Receptor-like kinases from Arabidopsis form a monophyletic gene family related to animal receptor kinases. PNAS *98*, 10763–10768.

Shiu, S.-H., and Bleecker, A.B. (2001b). Plant Receptor-Like Kinase Gene Family: Diversity, Function, and Signaling. Sci. STKE *2001*, re22.

Shiu, S.-H., Karlowski, W.M., Pan, R., Tzeng, Y.-H., Mayer, K.F.X., and Li, W.-H. (2004). Comparative Analysis of the Receptor-Like Kinase Family in Arabidopsis and Rice. Plant Cell *16*, 1220–1234.

Sigismund, S., Woelk, T., Puri, C., Maspero, E., Tacchetti, C., Transidico, P., Fiore, P.P.D., and Polo, S. (2005). Clathrin-independent endocytosis of ubiquitinated cargos. PNAS *102*, 2760–2765.

Sigismund, S., Argenzio, E., Tosoni, D., Cavallaro, E., Polo, S., and Di Fiore, P.P. (2008). Clathrin-Mediated Internalization Is Essential for Sustained EGFR Signaling but Dispensable for Degradation. Developmental Cell *15*, 209–219.

Simon-Plas, F., Perraki, A., Bayer, E., Gerbeau-Pissot, P., and Mongrand, S. (2011). An update on plant membrane rafts. Current Opinion in Plant Biology *14*, 642–649.

Slessareva, J.E., Routt, S.M., Temple, B., Bankaitis, V.A., and Dohlman, H.G. (2006). Activation of the Phosphatidylinositol 3-Kinase Vps34 by a G Protein α Subunit at the Endosome. Cell *126*, 191–203.

Smit, P., Limpens, E., Geurts, R., Fedorova, E., Dolgikh, E., Gough, C., and Bisseling, T. (2007). Medicago LYK3, an entry receptor in rhizobial nodulation factor signaling. Plant Physiol. *145*, 183–191.

Smyth, D.R., Bowman, J.L., and Meyerowitz, E.M. (1990). Early flower development in Arabidopsis. Plant Cell *2*, 755–767.

Snapp, E. (2001). Design and Use of Fluorescent Fusion Proteins in Cell Biology. In Current Protocols in Cell Biology, (John Wiley and Sons, Inc.),.

Sohn, E.J., Kim, E.S., Zhao, M., Kim, S.J., Kim, H., Kim, Y.-W., Lee, Y.J., Hillmer, S., Sohn, U., Jiang, L., et al. (2003). Rha1, an Arabidopsis Rab5 Homolog, Plays a Critical Role in the Vacuolar Trafficking of Soluble Cargo Proteins. Plant Cell *15*, 1057–1070.

Sorkin, A., and Zastrow, M. von (2009). Endocytosis and signalling: intertwining molecular networks. Nature Reviews Molecular Cell Biology *10*, 609–622.

Stahl, Arnoldo, Glavin, Goring, and Rothstein (1998). The self-incompatibility phenotype in brassica is altered by the transformation of a mutant S locus receptor kinase. Plant Cell *10*, 209–218.

Stein, J.C., Howlett, B., Boyes, D.C., Nasrallah, M.E., and Nasrallah, J.B. (1991). Molecular cloning of a putative receptor protein kinase gene encoded at the self-incompatibility locus of Brassica oleracea. PNAS *88*, 8816–8820.

Stone, J.M., Collinge, M.A., Smith, R.D., Horn, M.A., and Walker, J.C. (1994). Interaction of a protein phosphatase with an Arabidopsis serine-threonine receptor kinase. Science *266*, 793–795.

Stone, S.L., Anderson, E.M., Mullen, R.T., and Goring, D.R. (2003). ARC1 Is an E3 Ubiquitin Ligase and Promotes the Ubiquitination of Proteins during the Rejection of Self-Incompatible Brassica Pollen. Plant Cell *15*, 885–898.

Stoscheck, C.M., and Carpenter, G. (1984). Down regulation of epidermal growth factor receptors: direct demonstration of receptor degradation in human fibroblasts. J Cell Biol *98*, 1048–1053.

Subach, O.M., Cranfill, P.J., Davidson, M.W., and Verkhusha, V.V. (2011). An enhanced monomeric blue fluorescent protein with the high chemical stability of the chromophore. PLoS ONE *6*, e28674.

Sun, W., Cao, Y., Labby, K.J., Bittel, P., Boller, T., and Bent, A.F. (2012). Probing the Arabidopsis Flagellin Receptor: FLS2-FLS2 Association and the Contributions of Specific Domains to Signaling Function. Plant Cell *24*, 1096–1113.

Takano, J., Tanaka, M., Toyoda, A., Miwa, K., Kasai, K., Fuji, K., Onouchi, H., Naito, S., and Fujiwara, T. (2010). Polar localization and degradation of Arabidopsis boron transporters through distinct trafficking pathways. Proceedings of the National Academy of Sciences *107*, 5220–5225.

Tang, W., Kim, T.-W., Oses-Prieto, J.A., Sun, Y., Deng, Z., Zhu, S., Wang, R., Burlingame, A.L., and Wang, Z.-Y. (2008). BSKs Mediate Signal Transduction from the Receptor Kinase BRI1 in Arabidopsis. Science *321*, 557–560.

Teh, O., and Moore, I. (2007). An ARF-GEF acting at the Golgi and in selective endocytosis in polarized plant cells. Nature *448*, 493–496.

Tse, Y.C., Mo, B., Hillmer, S., Zhao, M., Lo, S.W., Robinson, D.G., and Jiang, L. (2004). Identification of Multivesicular Bodies as Prevacuolar Compartments in Nicotiana tabacum BY-2 Cells. Plant Cell *16*, 672–693.

Ueda, T., Uemura, T., Sato, M.H., and Nakano, A. (2004). Functional differentiation of endosomes in Arabidopsis cells. The Plant Journal *40*, 783–789.

Umebayashi, K., Stenmark, H., and Yoshimori, T. (2008). Ubc4/5 and c-Cbl Continue to Ubiquitinate EGF Receptor after Internalization to Facilitate Polyubiquitination and Degradation. Mol. Biol. Cell *19*, 3454–3462.

Vanoosthuyse, V., Tichtinsky, G., Dumas, C., Gaude, T., and Cock, J.M. (2003). Interaction of Calmodulin, a Sorting Nexin and Kinase-Associated Protein Phosphatase with the Brassica oleracea S Locus Receptor Kinase. Plant Physiol. *133*, 919–929.

Vermeer, J.E.M., Thole, J.M., Goedhart, J., Nielsen, E., Munnik, T., and Gadella Jr, T.W.J. (2009). Imaging phosphatidylinositol 4-phosphate dynamics in living plant cells. The Plant Journal *57*, 356–372.

Vert, G., and Chory, J. (2006). Downstream nuclear events in brassinosteroid signalling. Nature *441*, 96–100.

Vieira, A.V., Lamaze, C., and Schmid, S.L. (1996). Control of EGF receptor signaling by clathrin-mediated endocytosis. Science *274*, 2086–2089.

Viotti, C., Bubeck, J., Stierhof, Y.-D., Krebs, M., Langhans, M., Berg, W. van den, Dongen, W. van, Richter, S., Geldner, N., Takano, J., et al. (2010). Endocytic and Secretory Traffic in Arabidopsis Merge in the Trans-Golgi Network/Early Endosome, an Independent and Highly Dynamic Organelle. Plant Cell *22*, 1344–1357.

Walker, J.C. (1994). Structure and function of the receptor-like protein kinases of higher plants. Plant Mol Biol *26*, 1599–1609.

Wang, X., and Chory, J. (2006). Brassinosteroids Regulate Dissociation of BKI1, a Negative Regulator of BRI1 Signaling, from the Plasma Membrane. Science *313*, 1118–1122.

Wang, X., Goshe, M.B., Soderblom, E.J., Phinney, B.S., Kuchar, J.A., Li, J., Asami, T., Yoshida, S., Huber, S.C., and Clouse, S.D. (2005a). Identification and functional analysis of in vivo phosphorylation sites of the Arabidopsis BRASSINOSTEROID-INSENSITIVE1 receptor kinase. Plant Cell *17*, 1685–1703.

Wang, X., Li, X., Meisenhelder, J., Hunter, T., Yoshida, S., Asami, T., and Chory, J. (2005b). Autoregulation and Homodimerization Are Involved in the Activation of the Plant Steroid Receptor BRI1. Developmental Cell *8*, 855–865.

Wang, X., Kota, U., He, K., Blackburn, K., Li, J., Goshe, M.B., Huber, S.C., and Clouse, S.D. (2008). Sequential Transphosphorylation of the BRI1/BAK1 Receptor Kinase Complex Impacts Early Events in Brassinosteroid Signaling. Developmental Cell *15*, 220–235.

Wang, Z., Liu, J., Sudom, A., Ayres, M., Li, S., Wesche, H., Powers, J.P., and Walker, N.P.C. (2006). Crystal structures of IRAK-4 kinase in complex with inhibitors: a serine/threonine kinase with tyrosine as a gatekeeper. Structure *14*, 1835–1844.

Watson, F.L., Heerssen, H.M., Moheban, D.B., Lin, M.Z., Sauvageot, C.M., Bhattacharyya, A., Pomeroy, S.L., and Segal, R.A. (1999). Rapid nuclear responses to target-derived neurotrophins require retrograde transport of ligand-receptor complex. J. Neurosci. *19*, 7889–7900.

Wells, A., Welsh, J.B., Lazar, C.S., Wiley, H.S., Gill, G.N., and Rosenfeld, M.G. (1990). Ligand-induced transformation by a noninternalizing epidermal growth factor receptor. Science *247*, 962–964.

Williams, R.W., Wilson, J.M., and Meyerowitz, E.M. (1997). A possible role for kinase-associated protein phosphatase in the Arabidopsis CLAVATA1 signaling pathway. PNAS *94*, 10467–10472.

Woollard, A.A., and Moore, I. (2008). The functions of Rab GTPases in plant membrane traffic. Current Opinion in Plant Biology *11*, 610–619.

Wu, C., Ramirez, A., Cui, B., Ding, J., Delcroix, J.-D.M., Valletta, J.S., Liu, J.-J., Yang, Y., Chu, S., and Mobley, W.C. (2007). A Functional Dynein–Microtubule Network Is Required for NGF Signaling Through the Rap1/MAPK Pathway. Traffic *8*, 1503–1520.

Yamaoka, S., Shimono, Y., Shirakawa, M., Fukao, Y., Kawase, T., Hatsugai, N., Tamura, K., Shimada, T., and Hara-Nishimura, I. (2013). Identification and Dynamics of Arabidopsis Adaptor Protein-2 Complex and Its Involvement in Floral Organ Development. Plant Cell.

Yan, L., Ma, Y., Sun, Y., Gao, J., Chen, X., Liu, J., Wang, C., Rao, Z., and Lou, Z. (2011). Structural basis for mechanochemical role of Arabidopsis thaliana dynamin-related protein in membrane fission. J Mol Cell Biol *3*, 378–381.

Zhang, X., Facette, M., Humphries, J.A., Shen, Z., Park, Y., Sutimantanapi, D., Sylvester, A.W., Briggs, S.P., and Smith, L.G. (2012). Identification of PAN2 by Quantitative Proteomics as a Leucine-Rich Repeat–Receptor-Like Kinase Acting Upstream of PAN1 to Polarize Cell Division in Maize. Plant Cell *24*, 4577–4589.